

https://dspace.org/

The renormalisation group equation of the universal extra dimension models

Abdalgabar, Ammar Ibrahim

2015-05-07
http://hdl.handle.net/10539/17656

Downloaded from a DSpace repository. https://dspace.org/

The Renormalisation Group Equation of the Universal Extra Dimension Models

Ammar Ibrahim Abdalgabar



A dissertation submitted to the Faculty of Science, University of the Witwatersrand, Johannesburg, in fulfillment of the requirements for the degree of Doctor of Philosophy.

Supervisor: Prof. Alan S. Cornell

e-mail: ammar.abdalgabar@students.wits.ac.za

Johannesburg, December 2014

Declaration

I declare that all results presented in this thesis are original except where reference is made to the work of others. The following are the list of my original works discussed in this thesis.

1. **Ammar Abdalgabar** and A. S. Cornell. Published in J. Phys. Conf. Ser. **455**, 012050 (2013), arXiv:1305.3729 [hep-ph].

2. **Ammar Abdalgabar**, A. S. Cornell, A. Deandrea and A. Tarhini. Published in Phys. Rev. D **88**, 056006 (2013), arXiv:1306.4852 [hep-ph].

3. **Ammar Abdalgabar**, A. S. Cornell, A. Deandrea and A. Tarhini. Published in Eur.Phys.J. **C74** (2014) 2893, arXiv:1307.6401 [hep-ph].

4. **Ammar Abdalgabar**, A. S. Cornell, A. Deandrea and M. McGarrie. Published in JHEP **1407** (2014) 158, arXiv:1405.1038 [hep-ph].

5. **Ammar Abdalgabar**, A. S. Cornell. Submitted to SAIP Proceeding (2014), to be appear in J. Phys. Conference Series, arXiv:1410.2719 [hep-ph].

These papers are references [132], [133], [136], [134] and [135] in the bibliography and appear in chapters 5, 6, 7, 8, 9 respectively. This thesis is being submitted for the degree of Doctor of Philosophy to the University of the Witwatersrand, Johannesburg. It has not been submitted before for any degree or examination in any other University.



Ammar Abdalgabar

---12^{th}---day of ----------December-----2014---

Abstract

In this thesis the evolution equations of the Yukawa couplings and quark flavour mixings are derived for the one-loop renormalisation group equations in five and six-dimensional models, compactified in different possible ways to yield standard four space-time dimensions. Different possibilities for the matter fields are discussed, such as the case of bulk propagating or brane localized fields. We discuss in both cases the evolution of the Yukawa couplings, the Jarlskog parameter and the Cabibbo-Kobayashi-Maskawa matrix elements, finding that for both scenarios, as we run up to the unification scale, significant renormalisation group corrections are present. We also discuss the results of different observables of the five-dimensional universal extra dimension model in comparison with those of six-dimensional models and the model dependence of the results. We also studied the scaling of the mass ratios and the implications for the mixing angles in these six-dimensional model as well as the 5D Minimal Supersymmetric Standard Model on an S^1/Z_2 orbifold.

The renormalisation group equation evolutions for the Higgs sector and for the neutrino sector in six-dimensional models are also investigated. The recent experimental results of the Higgs boson from the LHC allow, in some scenarios, stronger constraints on the cutoff scale to be placed, from the requirement of the stability of the Higgs potential.

Furthermore, even if the unification and supersymmetry breaking scales are around 10^6 to 10^9 TeV, a large A_t coupling may be entirely generated at low energies through renormalisation group equation evolution in the 5D MSSM. Independent of the precise details of supersymmetry breaking, we take advantage of power law running in five dimensions and a compactification scale in the $10-10^3$ TeV range to show how the gluino mass may drive a large enough A_t to achieve the required 125.5 GeV Higgs mass. This also allows for sub-TeV stops, possibly observable at the LHC, and preserving GUT unification, thereby resulting in improved naturalness properties with respect to the four dimensional MSSM. The results may also be applied to models of split families in which the first and second generation matter fields are in the bulk and the third is on the boundary, which may assist in the generation of light stops whilst satisfying collider constraints on the first two generations of squarks.

Acknowledgements

I would like to express my sincere gratitude to my PhD supervisor, Alan S. Cornell. His constant encouragement and assistance at all times has been of immense value. I thank him for taking me on as his student and supporting me without hesitation throughout this work. It was a great pleasure to have been his student. I will forever remain indebted to him.

I would like to thank my overseas collaborators, Aldo Deandrea and Moritz McGarrie. Thanks to everyone for the hospitable and pleasant environments in the group of theoretical physics in Lyon-France.

My deep appreciation goes to the School of Physics for giving me a chance to demonstrate in physics laboratories, and for the opportunity to conduct in-depth physics research as a postgraduate student.

I would like to thank DAAD, the German Academic Exchange Service, for the financial support given to me for two years.

I would like to express my sincere thanks to all of my colleagues G. Kemp, Victor and W. Carlson for the nice discussions I had and for proof reading my thesis.

I am, of course, very grateful to all my family for their constant love and support, especially my wife and son, for being patient and their sacrifices. This thesis is dedicated to them.
I thank Allah who made all these possible.

Contents

1 Introduction **1**

2 The Standard Model **3**
2.1 SM Lagrangian . . . 3
2.1.1 Gauge Sector . . . 4
2.1.2 Fermion Sector . . . 4
2.2 The Higgs Mechanism . . . 5
2.2.1 Gauge Boson Masses . . . 7
2.2.2 Fermion Masses . . . 7
2.2.3 The Higgs Boson . . . 8
2.3 Gauge Fixing and Ghosts . . . 9
2.4 Why Do We Need New Physics . . . 9

3 Physics Beyond the Standard Model **12**
3.1 Supersymmetry . . . 12
3.1.1 SUSY Algebra . . . 13
3.1.2 Superspace and Superfields . . . 14
3.1.3 Minimal Supersymmetric Standard Model . . . 18
3.1.4 Soft SUSY breaking terms . . . 20
3.2 Universal Extra Dimensions . . . 22
3.2.1 Five-dimensional 1UED . . . 22
3.2.2 Six-dimensional 2UED . . . 26

4 Renormalisation Group Equations **28**
4.1 Dimensional Regularisation . . . 29
4.2 RGEs of CKM Matrix . . . 33
4.3 Evolution of X . . . 37
4.4 Evolution of Y . . . 39
4.5 Evolution of Z . . . 40
4.6 Evolution of J . . . 41

5 Evolution of Yukawa Couplings and Quark Flavour Mixings in 5D MSSM **43**
5.1 Introduction . . . 43
5.2 The 5D MSSM models . . . 44

5.3 Numerical Results and Discussions 46

6 Evolution of Yukawa Couplings and Quark Flavour Mixings in 2UED models 50
6.1 The 2UED SM 50
6.1.1 Fermions 51
6.1.2 Scalars 51
6.1.3 Gauge bosons 52
6.1.4 Yukawa interactions 52
6.1.5 Model dependence of the spectra 53
6.2 Gauge couplings evolution 53
6.3 Beta functions of the Yukawa couplings and CKM matrix elements in 1UED and 2UED models 56
6.3.1 Bulk 1UED case 57
6.3.2 Bulk 2UED case 57
6.3.3 Brane 1UED case 59
6.3.4 Brane 2UED case 59
6.4 Numerical results and discussions 60

7 Evolution of Quark Masses and Flavour Mixings in the 2UED 65
7.1 Mass Ratios, Mixings and Renormalisation invariance 65
7.2 Numerical Results and Discussions 66

8 Higgs Quartic Coupling, Neutrino Masses and Mixing Angles in 2UED Models 69
8.1 Introduction 69
8.2 The Quartic coupling RGEs 70
8.2.1 SM evolution equations 70
8.2.2 The 1UED and 2UED scenarios 71
8.2.3 The 2UED bulk and brane quartic results 73
8.3 Neutrino mixing and masses 74

9 Large A_t Without the Desert 78
9.1 Introduction 78
9.2 Generating large A_t in the 5D MSSM 79
9.2.1 The setup 79
9.3 Light Stops Without the Desert 84
9.4 Compatible models of SUSY breaking 85
9.4.1 Sequestered super-gravity mediation 86
9.4.2 Gauge mediation 87
9.5 RGEs for 5D MSSM 87
9.5.1 Gauge couplings 87
9.5.2 Yukawa couplings 88
9.5.3 Trilinear soft breaking parameters 89
9.5.4 Soft masses 90

9.5.5 Bilinear parameters μ and B_μ 93

10 Conclusions **94**

A One-loop correction for gauge coupling coefficients in the SM, MSSM, 5D MSSM, 1UED and 2UED **97**

B Calculation of the one-loop beta functions in the 2UED model **103**

C The number of KK states in 2UED models **111**

D The action and conventions of the 5D MSSM **113**

E Input parameters used in our numerical calculations **116**

List of Figures

2.1 *The Higgs potential $V(\Phi)$ with: in the left panel, the case $\mu^2 < 0$; and the right panel for the case $\mu^2 > 0$ as a function of $|\Phi| = \sqrt{\Phi^\dagger \Phi}$.* 6

2.2 *The one-loop Higgs self correction involving a fermion loop.* . . . 10

4.1 *The contour with: in the left panel, the k_0 integration plane; and the right panel for the contour used in the integration.* 32

5.1 *Gauge couplings (g_1 (red), g_2 (blue), g_3 (green) with: in the left panel, all matter fields in the bulk; and the right panel for all matter fields on the brane; for three different values of the compactification scales (1 TeV (solid line), 4 TeV (dot-dashed line), 15 TeV (dashed line))) as a function of the scale parameter t.* . 47

5.2 *Evolution of the mass ratio $\frac{m_d}{m_b}$, with: in the left panel, all matter fields in the bulk; and the right panel for all matter fields on the brane. Three different values of the compactification raduis have been used 1 TeV (dotted red line), 4 TeV (dot-dashed blue line), 15 TeV (dashed green line), all as a function of the scale parameter t.* 47

5.3 *Evolution of mass ratio $\frac{m_s}{m_b}$, with the same notations as Fig.5.2.* 48

5.4 *Evolution of mass ratio $\frac{m_d}{m_e}$, with the same notations as Fig.5.2.* 48

5.5 *Evolution of mass ratio $\frac{m_s}{m_\mu}$, with the same notations as Fig.5.2.* 48

5.6 *Evolution of mass ratio $\frac{m_b}{m_\tau}$, with the same notations as Fig.5.2.* 49

6.1 *The evolution of gauge couplings g_1 (red), g_2 (blue) and g_3 (green), with: in the left panel, all matter fields in the bulk; and the right panel for all matter fields on the brane; for three different values of the compactification scales 1 TeV (solid line), 2 TeV (dot-dashed line) and 10 TeV (dashed line), as a function of the scale parameter t.* 55

6.2 *Comparison of the gauge coupling evolutions g_1 (red), g_2 (blue), g_3 (green) between the 1UED case (dashed line) and the 2UED case (solid line) with: in the left panel, all matter fields in the bulk; and the right panel for all matter fields on the brane; for a compactification scale of 2 TeV as a function of the scale parameter t.* 55

6.3 *The evolution of the Weinberg angle ($sin^2\theta_W$) where the solid line represents the SM case with: in the left panel, all matter fields in the bulk; and the right panel for all matter fields on the brane; for three different values of the compactification scales 1 TeV (solid line) with the first KK threshold at $t = 2.394$, 2 TeV (dot-dashed line) with the first KK threshold at $t = 3.0879$ and 10 TeV (dashed line) with the first KK threshold at $t = 4.697$, as a function of the scale parameter t.* 56
6.4 *The evolution of top Yukawa coupling f_t where the solid line represents the SM case with: in the left panel all matter fields in the bulk; and the right panel for all matter fields on the brane; for three different values of the compactification scales 1 TeV (solid line) with the first KK threshold at $t = 2.394$, 2 TeV (dot-dashed line) with the first KK threshold at $t = 3.0879$ and 10 TeV (dashed line) with the first KK threshold at $t = 4.697$, as a function of the scale parameter t.* 61
6.5 *Comparison of the top Yukawa coupling evolution between the 1UED case (blue) and the 2UED case (red), where the solid line represent the SM case with: in the left panel all matter fields in the bulk; and the right panel for all matter fields on the brane; for a compactification scale of 2 TeV as a function of the scale parameter t.* 61
6.6 *The evolution of CKM element $|V_{ub}|$ where the solid line represents the SM case with: in the left panel all matter fields in the bulk; and the right panel for all matter fields on the brane; for three different values of the compactification scales 1 TeV (solid line), 2 TeV (dot-dashed line) and 10 TeV (dashed line), as a function of the scale parameter t.* 63
6.7 *Comparison of the $|V_{ub}|$ evolution between the 1UED case (blue) and the 2UED case (red), where the solid line represents the SM case with: in the left panel all matter fields in the bulk; and the right panel for all matter fields on the brane; for a compactification scale of 2 TeV as a function of the scale parameter t.* . . 63
6.8 *The evolution of the Jarlskog parameter J where the solid line represents the SM case with: in the left panel all matter fields in the bulk; and the right panel for all matter fields on the brane; for three different values of the compactification scales 1 TeV (solid line) with the first KK threshold at $t = 2.394$, 2 TeV (dot-dashed line) with the first KK threshold at $t = 3.0879$ and 10 TeV (dashed line) with the first KK threshold at $t = 4.697$, as a function of the scale parameter t.* 64

6.9 *Comparison of the Jarlskog parameter J evolution between the 1UED case (blue) and the 2UED case (red), where the solid line represent the SM case with: in the left panel all matter fields in the bulk; and the right panel for all matter fields on the brane; for a compactification scale of 2 TeV as a function of the scale parameter t.* 64

7.1 *Evolution of the mass ratio $\frac{m_u}{m_c}$ with: in the left panel all matter fields in the bulk; and the right panel for all matter fields on the brane. Three different values of the compactification radius have been used R^{-1} = 1 TeV (solid line) with the first KK threshold at $t = 2.394$, 2 TeV (dot-dashed line) with the first KK threshold at $t = 3.0879$, and 10 TeV (dashed line) with the first KK threshold at $t = 4.697$, all as a function of the scale parameter t.* 67
7.2 *Evolution of the mass ratio $\frac{m_b}{m_\tau}$, with the same notations as Fig.7.1* 67
7.3 *Evolution of the R_{13}, with the same notations as Fig.7.1* 68
7.4 *Evolution of* $\sin\beta$*, with the same notations as Fig.7.1* 68

8.1 *The evolution of the Higgs quartic coupling λ, where the solid line represents the SM case with: downward trajectories for all matter fields in the bulk; and upward for all matter fields on the brane; for three different values of the compactification scales 1 TeV (dotted line), 4 TeV (dot-dashed line) and 10 TeV (dashed line), as a function of the scale parameter t.* 74
8.2 *Comparison of the Higgs quartic coupling evolution between the 1UED case and the 2UED case, where the solid line represent the SM case; all matter fields are in the bulk; for a compactification scale of 1 TeV (dotted line), 4 TeV (dot-dashed line) and 10 TeV (dashed line), as a function of the scale parameter t. The 2UED line is always steeper than the corresponding 1UED one.* . 75
8.3 *The cut-off of the Higgs quartic coupling λ (dot-dashed line) and gauge couplings (dashed line) for all matter fields in the bulk; for different values of the compactification scales from 2 TeV to 14 TeV, as a function of the energy scale parameter t.* 76
8.4 *The evolution of Δm^2_{atm} where the solid line represents the SM case with: in the left panel all matter fields in the bulk; and the right panel for all matter fields on the brane; for three different values of the compactification scales 1 TeV (dotted line), 4 TeV (dot-dashed line) and 10 TeV (dashed line), as a function of the scale parameter t.* 76

9.1 *Running of the inverse fine structure constants $\alpha^{-1}(E)$, for three different values of the compactification scales 10 TeV (top left panel), 10^3 TeV (top right), 10^5 TeV (bottom left) and 10^{12} TeV (bottom right), with M_3 of 1.7 TeV, as a function of log(E/GeV).* 80

9.2 *Running of Yukawa couplings Y_i, for three different values of the compactification scales: 10 TeV (top left panel), 10^3 TeV (top right), 10^5 TeV (bottom left) and 10^{12} TeV (bottom right), with $M_3[10^3]$ of 1.7 TeV, as a function of log(E/GeV).* 81
9.3 *Running of trilinear soft terms $A_i(3,3)(E)$, for three different values of the compactification scales 10 TeV (top left panel), 10^3 TeV (top right), 10^5 TeV (bottom left) and 10^{12} TeV (bottom right), with $M_3[10^3]$ of 1.7 TeV, as a function of log(E/GeV).* . 82
9.4 *Running of trilinear soft terms $A_i(3,3)(E)$, for three different values of gluino masses, M_3: 1.7 TeV (top left panel), 3 TeV (top right panel) and 5 TeV (bottom panel), with R^{-1} of 10 TeV, as a function of log(E/GeV).* 83
9.5 *A plot of the one loop Higgs mass versus the lightest stop mass for representative values of $X_t = A_t - \mu \cot\beta$, corresponding to those of the 5D MSSM.* 85
9.6 *A plot of the one loop Higgs mass versus $\tan\beta$ for different values of the stop mass, for $X_t = A_t - \mu \cot\beta$ of -500 GeV (left panel) and -1.5 TeV (right panel).* 85
9.7 *The wavefunction renormalisation contribution for the five dimensional Yukawas.* 88
9.8 *The diagrams contributing to the five dimensional RGEs of the trilinear soft breaking parameters.* 90
9.9 *The diagrams for the five dimensional RGEs of the soft scalar masses at one loop.* 91

A.1 *The one-loop gauge field self correction involving the scalar A_5^n loop.* 101

B.1 *Diagrams contributing to Yukawa coupling RGEs in 2UED models in the Landau gauge. Solid (broken) lines correspond to fermions (SM scalars), while wavy lines (wavy+solid lines) represent ordinary gauge bosons (fifth components of gauge bosons).* 104
B.2 *Diagrams contributing to Higgs quartic coupling RGEs in the 2UED models in the Landau gauge. The notation is the same as in Fig. B.1.* 108

List of Tables

3.1 *MSSM chiral supermultiplets. The spin-0 fields correspond to the complex scalars, and the spin-1/2 fields correspond to left-handed two-component Weyl fermions [34].* 18

3.2 *MSSM gauge supermultiplets [34].* 19

5.1 *The terms present in the various Yukawa evolution equations, see Eq.(5.7).* 45

6.1 *The cut-offs in 5D and 6D for both bulk and brane cases for the three compactification radii R^{-1} =1, 2 and 10 TeV, where $t = \ln\left(\frac{\mu}{M_Z}\right)$.* 62

E.1 *Initial values at M_Z scale used in our numerical calculations. Data is taken from Refs. [53, 74].* 116

E.2 *Present limits on neutrino masses and mixing parameters. Data is taken from Ref. [90] for $sin^2(2\theta_{13})$, and from Ref. [96].* 117

Chapter 1

Introduction

The Standard Model (SM) of particle physics is a remarkably successful theory describing the interactions between elementary particles. Its predictions have been tested experimentally to a high level of accuracy, such as the structures of the neutral and charged current, which agree with experiment. The discoveries of the top quark in 1995 [1], the tau neutrino in 2000 [2], and the last missing piece in 2012 of the Higgs boson [3, 4] have furthered confirmed this model. However, there are some parameters that are unexplained within the SM context, which provide a likely new window for physics beyond the Standard Model (BSM). Examples include the hierarchy problem, the issue of fermion masses and their associated mixing angles, etc [5–7].

In order to solve the above mentioned issues with the SM, physicists implemented different independent models like Supersymmetry (SUSY), Extra Dimension etc. to extend the SM. SUSY is one of the most popular extensions to the SM, where its minimal version is called the Minimal Supersymmetric Standard Model (MSSM) and has been well developed theoretically. It solves the gauge hierarchy problem and gauge coupling unification at 10^{16} GeV. In addition, it also provides good dark matter candidates. It can also be tested in the Large Hadron Colidder (LHC) or future colliders.

Among other models, extra dimensional models in recent times have provided some exciting ideas for extensions to the SM, serving a number of purposes. Of these many possibilities much still remains unexplored, as the phenomenology of these models is quite sensitive to model details and assumptions. Therefore, a full exploration is needed, especially with the LHC now being operational and already exploring the TeV scale, where the possibility of Kaluza-Klein (KK) excitations to SM particles can be achieved.

The Universal Extra Dimension (UED) models at the TeV scale are discussed in various configurations, the simplest being the case of one flat extra dimension compactified on S^1/Z_2, which has been widely studied and constrained for more than a decade [8]. Electroweak precision measurements [9] combined with the LHC Higgs bounds impose a lower bound of $R^{-1} \geq 700$ GeV on the compactification scale [10]. On the other hand, the dark matter relic density observed by WMAP [11] sets an upper bound on the compactifi-

cation scale of 1.3 TeV $\leq R^{-1} \leq$ 1.5 TeV. In these UED models each SM field is accompanied by a tower of massive states, the KK particles. An extension of this scenario is to consider a type of model with two extra dimensions. This extension, however, is non-trivial and brings further insight to extra-dimensional scenarios. It is theoretically motivated by specific requirements, such as providing a dark matter candidate, suppressing the proton decay rate, as well as anomaly cancellations from the number of fermion generations being a multiples of three [12]. Different models with two extra dimensions have been proposed such as T^2/Z_2 [8], the chiral square T^2/Z_4 [13], $T^2/(Z_2 \times Z_2')$ [15], S^2/Z_2 [16], the flat real projective plane RP^2 [17], and the real projective plane starting from the sphere [18]. For simplicity, in this thesis we assume that the two extra space-like dimensions have the same size, that is $R_5 = R_6 = R$.

SUSY can be combined with extra dimension, where in this scenario the SM particles and superpartners (or subset) can access the extra dimension. From the 4D point of view, all the states that propagate in the bulk will have KK states, and the zero mode will be identified with the 4D MSSM particles.

The thesis is structured as follows: In chapter 2 we briefly review the SM of particle physics. Physics BSM are studied in chapter 3, specifically the SUSY and UED models which are discussed at length. We present the Renormalisation Group Equations (RGEs) in chapter 4. The evolution of the mass ratios in the 5D MSSM is introduced in chapter 5.

In chapter 6 we introduce the 2UED SM, followed by a presentation of the evolution equations for the gauge couplings and comparison between 5D and 6D UED models. We derive the RGEs for the Yukawa couplings and the Cabbibo Kobayshi Maskawa (CKM) matrix elements in the 2UED model for both cases, that is for matter fields propagating in the bulk and when they are restricted to the brane. We extend the discussion on the quark masses and flavour mixing in chapter 7.

In chapter 8 we derive the Higgs quartic coupling RGEs in six-dimensional models and compare the limits on the effective theory obtained by requiring the stability of the Higgs potential with other effective rules for the cutoff theory. These are obtained from other requirements, such as perturbativity of the interactions, gauge coupling unification and unitarity, we follow this study of the neutrino mixing and mass evolutions and compare them with the quark sector RGEs.

Chapter 9 explores the RGEs of a number of parameters in the 5D MSSM, from the unification scale to the electroweak scale, in particular focusing on achieving a large A_t parameter. We use the achieved values of A_t in our models to estimate the necessary size of the lightest stop mass, to obtain the currently observed Higgs mass, in particular emphasising that the 5D MSSM allows for sub-TeV stops due to the sizable A_t. Our conclusions will be given in chapter 10.

Chapter 2

The Standard Model

The SM is the theory that describes the interactions among elementary particles [19,20]. It combines the strong interaction known as Quantum Chromodynamics (QCD), based on the group $SU(3)_C$ [21], and the Glashow-Weinberg-Salam theory of the electroweak interaction (that unified the weak and electromagnetic interactions), based on the group $SU(2)_L \times U(1)_Y$ [22]. Therefore the SM is an $SU(3)_C \times SU(2)_L \times U(1)_Y$ gauge theory. We have the following fermionic assignment for the particle content

$$q_L = \begin{pmatrix} u \\ d \end{pmatrix}_L \; ; \;\; u_R, d_R, \tag{2.1}$$

$$\ell_L = \begin{pmatrix} \nu \\ e \end{pmatrix}_L \; ; \quad e_R, \tag{2.2}$$

where we have omitted the colour index for quarks and we present only one generation for simplicity.

The above assignment is the result of maximal parity violation by the weak interaction, since the left handed and right handed fermions transform differently. For instance, the doublet shown in Eq.(2.2) is assumed to transform in the fundamental representation of an $SU(2)_L$ group, whereas the right handed partners are taken to be a singlet under this group, and the neutrinos are assumed to be left handed only[1]. The neutrino will not acquire mass as its right handed partner does not exist in this theory [23–25].

2.1 SM Lagrangian

The SM Lagrangian can be written as:

$$\mathcal{L}_{SM} = \mathcal{L}_{Gauge} + \mathcal{L}_{Fermions} + \mathcal{L}_{Higgs} + \mathcal{L}_{Yukawa} + \mathcal{L}_{Gauge.fixing} + \mathcal{L}_{Ghost} \; . \tag{2.3}$$

We shall now briefly introduce each sector of this Lagrangian

[1]Because of maximal parity violation of the electroweak interactions, the neutrinos are massless in the SM. This can be generalised to study mixings in the lepton sector with V_{PMNS}, as we will see in chapter 8

2.1.1 Gauge Sector

The gauge sector is composed of 12 gauge fields which mediate the interactions among the fermion fields; the photon (γ, mediates the electromagnetic interactions), the three weak gauge bosons ($W^{\pm}$ and Z, mediate the weak interactions) and eight gluons (g_α, $\alpha = 1, 2, ..., 8$, mediate the strong interactions). The gauge field dynamics are embedded in the Lagrangian in terms of field strength tensors as

$$\mathcal{L}_{Gauge.Boson} = -\frac{1}{4} G^A_{\mu\nu} G^{A\mu\nu} - \frac{1}{4} W^a_{\mu\nu} W^{a\mu\nu} - \frac{1}{4} B_{\mu\nu} B^{\mu\nu} \ , \tag{2.4}$$

where repeated indices imply a summation over that index, and μ, ν takes 0,1,2,3, where the field strength tensors for non-Abelian theories are given by:

$$G^A_{\mu\nu} = \partial_\mu G^A_\nu - \partial_\nu G^A_\mu - i g_s f^{ABC} G^B_\mu G^C_\nu \ , \tag{2.5}$$

being the $SU(3)_C$ field strength, g_s is the coupling strength of the strong interaction, A, B, C run from 1 to 8 and f^{ABC} are the (antisymmetric) structure constants of $SU(3)$, which satisfies the Lie algebra for the group generator t^A

$$[t^A, t^B] = i f^{ABC} t^C \ . \tag{2.6}$$

$$W^a_{\mu\nu} = \partial_\mu W^a_\nu - \partial_\nu W^a_\mu - i g \epsilon^{abc} \ W^b_\mu W^c_\nu \tag{2.7}$$

is the $SU(2)_L$ field strength, a, b, c run from 1 to 3 and ϵ^{abc} is the totally antisymmetric three-index tensor with $\epsilon^{123} = 1$, g is the coupling strength of the weak interaction.

The field strength of the $U(1)_Y$ gauge boson which has the same form as electromagnetism is given by:

$$B_{\mu\nu} = \partial_\mu B_\nu - \partial_\nu B_\mu \ . \tag{2.8}$$

2.1.2 Fermion Sector

The SM contains three copies of chiral fermions (generations) with different gauge transformations. The fermionic Lagrangian has the usual covariant Dirac form

$$\mathcal{L}_{Fermions} = \sum_f i \bar{f} \gamma_\mu D^\mu f \ , \tag{2.9}$$

with

The covariant derivatives can be read as

$$D_\mu \begin{pmatrix} u \\ d \end{pmatrix}_L = \left(\partial_\mu - i g_s \frac{\lambda^a}{2} G^a_\mu - i g \frac{\sigma^a}{2} W^a_\mu - i g' \frac{1}{6} B_\mu \right) \begin{pmatrix} u \\ d \end{pmatrix}_L \ , \tag{2.10}$$

$$D_\mu u_R = \left(\partial_\mu - i g_s \frac{\lambda^a}{2} G^a_\mu - i g \frac{\sigma^a}{2} W^a_\mu - i g' \frac{2}{3} B_\mu \right) u_R \ , \tag{2.11}$$

$$D_\mu d_R = \left(\partial_\mu - ig_s\frac{\lambda^a}{2}G^a_\mu - ig\frac{\sigma^a}{2}W^a_\mu + ig'\frac{1}{3}B_\mu\right) d_R \ , \tag{2.12}$$

$$D_\mu \begin{pmatrix}\nu\\ e\end{pmatrix}_L = \left(\partial_\mu - ig\frac{\sigma^a}{2}W^a_\mu + ig'\frac{1}{2}B_\mu\right)\begin{pmatrix}\nu\\ e\end{pmatrix}_L \ , \tag{2.13}$$

and

$$D_\mu e_R = \left(\partial_\mu - ig\frac{\sigma^a}{2}W^a_\mu + ig'B_\mu\right) e_R \ . \tag{2.14}$$

Here γ_μ are the usual Dirac matrices, g' is the coupling strength of the hypercharge interaction, Y is the hypercharge, σ^a are the generators of $SU(2)_L$ (simply the Pauli matrices), and λ^a are the generators of $SU(3)_C$ (the Gell-Mann matrices).

Note that gauge symmetry forbids a mass term for fermions (quarks and leptons) and gauge bosons. A mass term would break the gauge invariance $SU(2)_L \times U(1)_Y$. However, we observe the mass of gauge bosons W and Z and the fermions experimentally [26], so we need to give mass to these particles. The masses in the SM are generated through a different mechanism, the Higgs mechanism, which will be discussed at length in section 2.2.

2.2 The Higgs Mechanism

As was presented in the previous section, a Dirac mass term will violate the gauge symmetry. As such we need a mechanism that gives mass to the SM particles and keeps the Lagrangian invariant under gauge symmetries. This can be done through the mechanism of spontaneous gauge symmetry breaking also known as the Higgs mechanism. This mechanism adds a new complex scalar field Φ which is a doublet under the $SU(2)_L$ group, a singlet with respect to $SU(3)_C$ and has hypercharge $Y_\Phi = 1$ [27–30].

$$\Phi = \begin{pmatrix}\phi^+\\ \phi^0\end{pmatrix} = \begin{pmatrix}\phi_1 + i\phi_2\\ \phi_3 + i\phi_4\end{pmatrix} \ , \tag{2.15}$$

where ϕ_1, ϕ_2, ϕ_3 and ϕ_4 are real scalars. This new scalar Φ adds extra terms to the SM Lagrangian:

$$\mathcal{L}_{Higgs} = (D_\mu\Phi)^\dagger(D^\mu\Phi) - V(\Phi) \ , \tag{2.16}$$

where the covariant derivative D_μ is defined as

$$D_\mu = \partial_\mu - i\frac{g'}{2}B_\mu - ig\frac{\sigma^a}{2}W^a_\mu \ . \tag{2.17}$$

The general gauge invariant renormalizable potential involving Φ is given by

$$V(\Phi) = -\frac{1}{2}\mu^2\Phi^\dagger\Phi + \frac{\lambda}{4}(\Phi^\dagger\Phi)^2 \ . \tag{2.18}$$

Eq.(2.18) describes the Higgs potential, which involves two new real parameters μ and λ. We demand $\lambda > 0$ for the potential to be bounded; otherwise the potential is unbounded from below and there will be no stable vacuum state. μ takes the following two values:

- $\mu^2 > 0$ then the vacuum corresponds to $\Phi = 0$, the potential has a minimum at the origin (see Fig.2.1 right panel).
- $\mu^2 < 0$ then the potential develops a non-zero Vacuum Expectation Value (VEV) and the minimum is along a circle of radius $\frac{\upsilon}{\sqrt{2}} = \frac{246}{\sqrt{2}}$ (see Fig.2.1 left panel). Minimizing the potential we get

$$\phi_1^2 + \phi_2^2 + \phi_3^2 + \phi_4^2 = -\frac{\mu^2}{\lambda} = \upsilon^2 \ . \tag{2.19}$$

As such, we need to choose one of these minima as the ground state ($\phi_3 = \upsilon$ and $\phi_1 = 0$, $\phi_2 = 0$ and $\phi_4 = 0$). Thus the vacuum does not have the original symmetry of the Lagrangian, and therefore spontaneously breaks the symmetry [30]. In other words, the Lagrangian is still invariant under the $SU(2)_L \times U(1)_Y$, while the ground state is not. We choose the VEV in the neutral direction as the photon is neutral, so Φ becomes

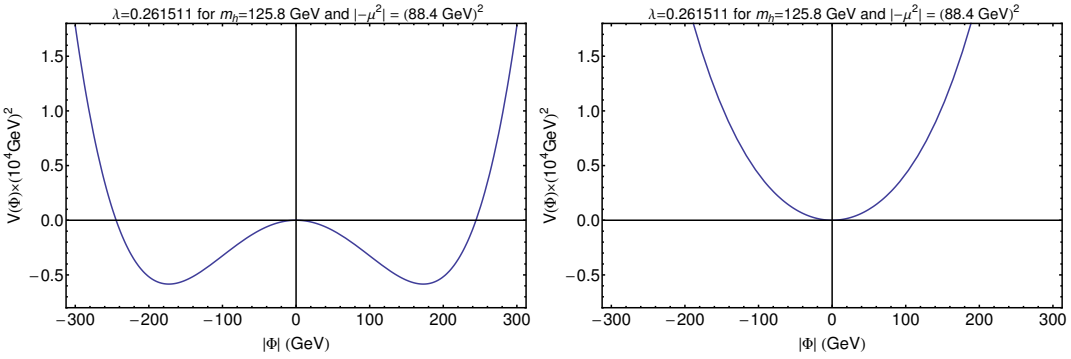


Figure 2.1: *The Higgs potential $V(\Phi)$ with: in the left panel, the case $\mu^2 < 0$; and the right panel for the case $\mu^2 > 0$ as a function of $|\Phi| = \sqrt{\Phi^\dagger \Phi}$.*

$$\langle\Phi\rangle = \frac{1}{\sqrt{2}}\begin{pmatrix}0\\ \upsilon\end{pmatrix} . \tag{2.20}$$

With this particular choice of the ground state, the electroweak gauge group $SU(2)_L \times U(1)_Y$ is broken to electromagnetism, $U(1)_{em}$,

$$SU(2)_L \times U(1)_Y \overset{\langle\Phi\rangle}{\rightarrow} U(1)_{em} . \tag{2.21}$$

2.2.1 Gauge Boson Masses

The gauge boson masses can be obtained from the kinetic term of the Higgs field [19]. Expanding the Lagrangian about the VEV yields:

$$\mathcal{L}_{Higgs} = \frac{1}{2}\begin{pmatrix}0 & \upsilon\end{pmatrix}(g\frac{\sigma^a}{2}W^a_\mu + \frac{1}{2}g'B_\mu)(g\frac{\sigma^b}{2}W^b_\mu + \frac{1}{2}g'B_\mu)\begin{pmatrix}0\\ \upsilon\end{pmatrix} . \tag{2.22}$$

From the definition of $W^\pm_\mu = \frac{1}{\sqrt{2}}(W^1_\mu \pm W^2_\mu)$, $Z_\mu = W^3_\mu \cos\theta_W - B_\mu \sin\theta_W$ and $A_\mu = W^3_\mu \sin\theta_W - B_\mu \cos\theta_W$, we get three massive gauge bosons

$$m^2_W = \frac{1}{4}g^2\upsilon^2 \ , \quad m^2_Z = \frac{1}{4}(g'^2 + g^2)\upsilon^2 , \tag{2.23}$$

and one massless gauge boson (identified as the photon)

$$m^2_A = 0 . \tag{2.24}$$

The Weinberg angle θ_W is defined by

$$\cos\theta_W = \frac{g}{\sqrt{g'^2 + g^2}} , \tag{2.25}$$

$$\sin\theta_W = \frac{g'}{\sqrt{g^2 + g'^2}} . \tag{2.26}$$

2.2.2 Fermion Masses

Fermion masses originate from Yukawa interactions, which are the couplings between the fermion doublets and the scalar field Φ [19]. These Yukawa couplings are uniquely fixed by gauge invariance and the Lagrangian, as given by:

$$\mathcal{L}_{Yukawa} = Y^d_{ij}\bar{q^i_L}\Phi d^j_R + Y^u_{ij}\bar{q^i_L}\tilde{\Phi}u^j_R + Y^e_{ij}\bar{l^i_L}\Phi e^j_R + \text{h.c.} , \tag{2.27}$$

where the Y's are 3×3 complex matrices, the so called Yukawa coupling constants, h.c. indicates the Hermitian conjugate and $\tilde{\phi}$ is defined by

$$\tilde{\Phi} = \begin{pmatrix}-\phi^*_2\\ \phi^*_1\end{pmatrix} . \tag{2.28}$$

When the Higgs doublet acquires a non vanishing VEV, Eq.(2.27) leads to the mass terms for the fermions as follows:

$$\mathcal{L}_{Yukawa} = m_u\, \bar{u}_L\, u_R + m_d\, \bar{d}_L\, d_R + m_e\, \bar{e}_L e_R\ , \tag{2.29}$$

with $m_u = \frac{1}{\sqrt{2}} y_u \upsilon;\ m_d = \frac{1}{\sqrt{2}} y_d \upsilon;\ \ m_e = \frac{1}{\sqrt{2}} y_e \upsilon$.

Note that neutrinos are massless and will never acquire mass, because its chiral partner ν_R does not exist in the theory. This shall be discussed further in chapter 8.

When we consider all the generations of quarks, there are possibilities for their mixing. This mixing is described by the CKM, which has four observable parameters, including three mixing angles and one phase [31]. It appears upon the diagonalisation of Yukawa matrices by using two unitary matrices U and V, where

$$U Y_u^\dagger Y_u U^\dagger = \mathrm{diag}(f_u^2, f_c^2, f_t^2); \qquad V Y_d^\dagger Y_d V^\dagger = \mathrm{diag}(h_d^2, h_s^2, h_b^2)\ . \tag{2.30}$$

The CKM matrix is given by

$$V_{CKM} = U V^\dagger\ . \tag{2.31}$$

The form of the CKM matrix that describes the quark sector mixing is parametrised as

$$V_{CKM} = \begin{pmatrix} V_{ud} & V_{us} & V_{ub} \\ V_{cd} & V_{cs} & V_{cb} \\ V_{td} & V_{ts} & V_{tb} \end{pmatrix}\ ,$$

and the standard parametrisation in terms of the three mixing angles and one phase can have the form

$$V_{CKM} = \begin{pmatrix} c_{12}c_{13} & s_{12}c_{13} & s_{13}e^{-i\delta} \\ -s_{12}c_{23} - c_{12}s_{23}s_{13}e^{i\delta} & c_{12}c_{23} - s_{12}s_{23}s_{13}e^{i\delta} & s_{23}c_{13} \\ s_{12}s_{23} - c_{12}c_{23}s_{13}e^{i\delta} & -c_{12}s_{23} - s_{12}c_{23}s_{13}e^{i\delta} & c_{23}c_{13} \end{pmatrix}\ , \tag{2.32}$$

where $s_{12} = \sin\theta_{12}$, $c_{12} = \cos\theta_{12}$ etc. are the sines and cosines of the three mixing angles θ_{12}, θ_{23} and θ_{13}, and δ is the CP violating phase. Note that this parametrisation of the matrix shall be used in the rest of the thesis, and its evolution will be derived in section 4.2.

2.2.3 The Higgs Boson

As was discussed in section 2.2, the spontaneous symmetry breaking predicted a new particle: the Higgs Boson, which must be a scalar and neutral. The Lagrangian for this new scalar comes from the kinetic term of Eq.(2.16) expanded around the VEV

$$\mathcal{L}_{Higgs.Boson} = \frac{1}{2}(\partial_\mu h)(\partial^\mu h) - \frac{1}{2}m_h^2 h^2 + \text{interactions} \,, \tag{2.33}$$

where $m_h^2 = \sqrt{\lambda}v$ is the Higgs boson mass. The interaction terms contain both Higgs self-interactions and interactions with gauge bosons and fermions. Note that as a consequence of the Higgs mechanism all the Higgs couplings are completely determined in terms of the coupling constants and masses. The Higgs boson, which was the last missing piece of the SM, has been confirmed by the ATLAS and CMS experiments, and this is compatible with the SM Higgs expectations with a mass of about 126 GeV [3, 4].

2.3 Gauge Fixing and Ghosts

Gauge fixing is necessary when the gauge fields are quantised. Quantisation means to develop a path integral formalism for the gauge theory. The path integral is diverging as one integrate over an infinite set of gauge-equivalent configuration, here the gauge fixing is used to pick up one arbitrary representative, therefore, giving meaning to the path integral. On other hands, the gauge invariance we look for in gauge theory, a naive path integral approach would spoiled it [19,32]. The solution is given by the what is called the Faddev-Popov procedure, where they introduced an identity expression consisting of a functional integral over a gauge fixing condition times a functional determinant over anticommuting fields in the path integral. The latter gives rise to what is known as ghost fields, which keep the gauge freedom within the theory, but are not physical particles (because ghost violate the spin-statistics relation).

As such, we need to add terms in the Lagrangian like

$$\mathcal{L}_{Gauge.fixing} = -\frac{\zeta}{2}(\partial_\mu A^\mu)^2 \,, \tag{2.34}$$

and

$$\mathcal{L}_{Ghost} = \bar{c}_b \partial^\mu D_\mu^{ab} c_a \,. \tag{2.35}$$

Thus, we are now in the right position to write the full SM Lagrangian

$$\mathcal{L}_{SM} = \mathcal{L}_{Gauge} + \mathcal{L}_{Fermions} + \mathcal{L}_{Yukawa} + \mathcal{L}_{Higgs} + \mathcal{L}_{Gauge.fixing} + \mathcal{L}_{Ghost}. \tag{2.36}$$

2.4 Why Do We Need New Physics

The SM is currently accepted and has been tested experimentally to a high level of accuracy. Despite the numerous successes of the SM theoretically and experimentally, it does not address the following problems:

The Hierarchy problem

The Hierarchy problem is the question of why there is such a huge difference between the electroweak scale $M_{EW} = \mathcal{O}(100)$ GeV and the Planck scale $M_{pl} = \mathcal{O}(10^{18})$ GeV. This is also known as the naturalness problem. To understand this, let us consider the quadratic divergence for the Higgs self energy correction due to the fermionic loop in Fig. 2.2

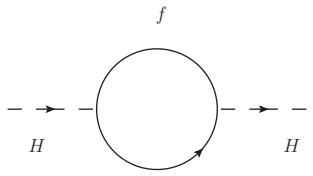


Figure 2.2: *The one-loop Higgs self correction involving a fermion loop.*

$$\Pi^f_{HH} = (-1)\int \frac{d^dp}{(2\pi)^d} Tr\left\{\frac{-i\lambda_f}{\sqrt{2}}\frac{i}{\not{p}-m_f} - \frac{-i\lambda_f}{\sqrt{2}}\frac{i}{\not{p}-m_f}\right\}. \tag{2.37}$$

Here λ_f is the coupling constant of the fermion-scalar-fermion and p is the momentum running inside the loop. The result of this integral is divergent, so we introduce a cut-off Λ to regulate this integral. Thus Eq. (2.4) becomes

$$\begin{aligned}\Pi^f_{HH} &= -2\lambda_f^2\int_0^\Lambda \frac{d^dp}{(2\pi)^d}\left\{\frac{1}{p^2-m_f^2} + \frac{2m_f^2}{(p^2-m_f^2)^2}\right\} \\ &= -\frac{\lambda_f^2}{8\pi^2}\Lambda^2 + \dots .\end{aligned} \tag{2.38}$$

Therefore, the correct Higgs mass is

$$m_H^2 = m_{H_0}^2 + \delta m_H^2 , \tag{2.39}$$

where δm_H^2 is proportional to Π^f_{HH} (since $\Lambda = 2\times 10^{16}$ GeV at the GUT scale, then fine tuning $\mathcal{O}(10^{26})$ is required to get $\lambda_f = 1$, so that the physical Higgs mass should be around 100 GeV). Note that this quadratic divergence can be renormalised away in exactly the same manner as for logarithmic divergences. Nothing is wrong with this fine tuning. However, most physicists consider this type of solution unattractive. We shall see in the next chapter naturally how this divergence is canceled.

Fermion mass hierarchy and mixing angles

A theory of fermion masses and the associated mixing angles is unexplained in the SM. Such as the origin of quark and lepton masses, or the apparent

hierarchy of family masses and quark mixing angles. Perhaps if we understand this we will also know the origin of CP violation and the matter-antimatter asymmetry in the universe better. Furthermore, the SM does not account for the neutrino oscillations and their non-zero masses as mentioned in section 2.2.

Gravity and Cosmology

Though the unification of the electromagnetic and weak interactions was achieved in the SM and the strong interaction appears to be part of the unification, the SM does not include the effects of gravity. Note that the effects of gravity become important at energies of the order of the Planck scale, $M_{pl} = 10^{18}$ GeV. The SM is treated as an effective theory at a natural cut-off scale Λ. The ultimate goal in particle physics is to unify all the fundamental forces in nature. Moreover, the SM does not have any dark matter candidates, as opposed to observational cosmology.

Chapter 3

Physics Beyond the Standard Model

As motivated in the previous chapter, a physical theory may exist beyond the SM. The experiments at current and future colliders, the LHC and International Linear Collider (ILC) etc. are expected to reveal its true nature. SUSY and extra dimensions have evolved into a new paradigm with many tools to solve the large number of outstanding issues that remain unanswered in the SM. This leads to other phenomenological implications which should be tested at colliders and elsewhere. As such, the present chapter will discuss Supersymmetric and UED models in details.

3.1 Supersymmetry

The progression of Quantum Field Theory (QFT) led to several no-go theorems. The Coleman-Mandula Theorem [33] states that any symmetry group of the S-Matrix has to be locally isomorphic to a direct product of an internal symmetry group and the Poincar'e group with respect to some very general QFT assumptions, and implicitly assumed that all generators of the symmetry groups form a commutator algebra. The consequence of the Coleman- Mandula theorem is that there are no symmetries in the QFT that will change the spin of any state. However, modifying or relaxing the assumption of the commutator algebra by introducing anticommutators, allows us to construct graded Lie algebras which are consistent with the other QFT assumptions [34–37]. In 1975 Haag, Lopuszanski and Sohnius generalised the results of Coleman-Mandula to include the symmetry operation which obeys Fermi statistics, and they derived the most general graded Lie algebra [38] for the SUSY QFT. Henceforth, SUSY has been studied intensively as a direct possible extension to the SM which we refer to as the MSSM. In its localised version (supergravity), SUSY naturally includes gravity, in the context of grand unification as well as in cosmology[1] and as a necessary ingredient of string theories that include fermions

[1]The lightest SUSY particle is a good candidate for dark matter, if stable.

(yielding superstring theory).

As such, SUSY is a generalisation of space-time transformations that relate fermions and bosons. In SUSY fermions transform into a boson and vice versa. It admits supermultiplets with fermionic and bosonic members. The couplings of those members are related to each other and their masses are split by SUSY breaking effects. For more details or further explanation, we direct the reader to Refs. [34–37].

Note that in this thesis we will study $\mathcal{N} = 1$ supersymmetry in four dimensions and $\mathcal{N} = 1$ supersymmetry in five dimensions, which can be represented by a four dimensional $\mathcal{N} = 2$ theory without central charges.

3.1.1 SUSY Algebra

As we mentioned in the previous section, the Coleman-Mandula theorm allows us to add anticommuting generators. In the minimal extension we can add one new fermionic generator $Q = (Q_\alpha, \bar{Q}^{\dot{\alpha}})^T$ of spin-1/2 (not 3/2 or higher)[2] [39]. These quantum operators will change the fermionic state into bosonic ones and vice versa,

$$Q_\alpha \left| fermion \right\rangle = \left| boson \right\rangle \ , \qquad \bar{Q}_{\dot{\alpha}} \left| boson \right\rangle = \left| fermion \right\rangle \ , \tag{3.1}$$

where α and $\dot{\alpha}$ are Weyl spinor indices and take the values 1 or 2. The bosonic generators P_μ, fermionic generators $Q's$ and the six Lorentz generators $M_{\mu\nu}$ form the most general SUSY algebra, and can be summarised in the following equations:

$$\begin{gathered}
[P_\mu, P_\nu] = 0, \qquad [P_\mu, M_{\nu\rho}] = i(g_{\mu\nu}P_\rho - g_{\mu\rho}P_\nu) \ , \\
[M_{\mu\nu}, M_{\rho\sigma}] = i(g_{\nu\rho}M_{\mu\sigma} - g_{\nu\sigma}M_{\mu\rho} - g_{\mu\rho}M_{\nu\sigma} + g_{\mu\sigma}M_{\nu\rho}) \ , \\
[Q_\alpha, M_{\mu\nu}] = (\sigma_{\mu\nu})_\alpha^\beta Q_\beta, \ \ [\bar{Q}_{\dot{\alpha}}, M_{\mu\nu}] = -\bar{Q}_{\dot{\beta}}(\sigma_{\mu\nu})_{\dot{\alpha}}^{\dot{\beta}}, \ \ [P_\mu, Q_\alpha] = 0 \ , \\
\{Q_\alpha, Q_\beta\} = 0 \ , \{\bar{Q}_{\dot{\alpha}}, \bar{Q}_{\dot{\beta}}\} = 0 \ , \{Q_\alpha, \bar{Q}_{\dot{\beta}}\} = 2\sigma^\mu_{\alpha\dot{\beta}} P_\mu \ .
\end{gathered} \tag{3.2}$$

Where $g_{\mu\nu}$ is the $Minkowski$ metric, $\sigma_\mu = (1, \sigma_i)$ and $\bar{\sigma}_\mu = (1, -\sigma_i)$ are Pauli's matrices, $\sigma_{\mu\nu} = \frac{1}{4}(\sigma_\mu\bar{\sigma}_\nu - (\mu \longleftrightarrow \nu))$, $\bar{\sigma}_{\mu\nu} = \frac{1}{4}(\bar{\sigma}_\mu\sigma_\nu - (\mu \longleftrightarrow \nu))$ and

$$P_\mu = i\partial_\mu, \ \ iQ_\alpha = \frac{\partial}{\partial\theta^\alpha} - i\sigma^\mu_{\alpha\dot{\alpha}}\bar{\theta}^{\dot{\alpha}}\partial_\mu \ , \ \ i\bar{Q}_{\dot{\alpha}} = -\frac{\partial}{\partial\bar{\theta}^{\dot{\alpha}}} + i\theta^\alpha\sigma^\mu_{\alpha\dot{\alpha}}\partial_\mu \ . \tag{3.3}$$

The covariant fermionic derivative can be defined as

$$D_\alpha = \frac{\partial}{\partial\theta^\alpha} + i\sigma^\mu_{\alpha\dot{\alpha}}\bar{\theta}^{\dot{\alpha}}\partial_\mu, \ \ \bar{D}_{\dot{\alpha}} = -\frac{\partial}{\partial\bar{\theta}^{\dot{\alpha}}} - i\theta^\alpha\sigma^\mu_{\alpha\dot{\alpha}}\partial_\mu \ . \tag{3.4}$$

These derivatives D_α and $\bar{D}_{\dot{\alpha}}$ anticommute with SUSY generators and they obey the algebra:

$$\{D_\alpha, \bar{D}_{\dot{\alpha}}\} = 2i\sigma^\mu_{\alpha\dot{\alpha}}\partial_\mu \ , \quad \{D_\alpha, D_\beta\} = \{\bar{D}_{\dot{\alpha}}, \bar{D}_{\dot{\beta}}\} = 0 \ . \tag{3.5}$$

The new coordinates θ_α and $\bar{\theta}_{\dot{\alpha}}$ are the two spinorial anticommuting coordinates, we will elaborate on these in the next section.

[2]Note that the spinor indices, meaning the dotted indices, are contracted from bottom to top, and undotted indices are contracted from top to bottom.

3.1.2 Superspace and Superfields

The SUSY algebra as summarised in the last section is a graded Lie algebra including commutators as well as anticommutators. Superspace combines our usual standard space-time and anticommuting spinorial 2-component parameters θ_α and $\bar{\theta}_{\dot{\alpha}}$ [40]. Superspace integration over the variables θ and $\bar{\theta}$ is similar to that of anticommuting Grassmann variables as

$$\int d^2\theta = 0, \quad \int d^2\bar{\theta} = 0, \quad \int d^2\theta\theta^2 = 1, \quad \int d^2\bar{\theta}\bar{\theta}^2 = 1 \; . \tag{3.6}$$

Furthermore

$$\delta(\theta) = \theta^2, \qquad \delta(\bar{\theta}) = \bar{\theta}^2 \; ,$$

where these delta functions act as delta Dirac distributions on functions of ordinary integrals with

$$\begin{aligned} d^2\theta &= -\frac{1}{4} d\theta^\alpha d\theta^\beta \epsilon_{\alpha\beta}, \quad d^4\theta = d^2\theta d^2\bar{\theta} \; , \\ d^2\bar{\theta} &= -\frac{1}{4} d\bar{\theta}_{\dot{\alpha}} d\bar{\theta}_{\dot{\beta}} \epsilon^{\dot{\alpha}\dot{\beta}}, \quad d^8 z = d^4 x d^4\theta \; . \end{aligned} \tag{3.7}$$

$\epsilon_{\alpha\beta}$ and $\epsilon^{\dot{\alpha}\dot{\beta}}$ are antisymmetric tensors and can be used to raise and lower indices (contract the indices). We choose $\epsilon^{12} = \epsilon_{21} = \epsilon^{\dot{1}\dot{2}} = \epsilon_{\dot{2}\dot{1}} = 1$. In Superspace the supertranslation of the coordinates x^μ, θ and $\bar{\theta}$ are

$$\begin{aligned} x_\mu &\longrightarrow x_\mu + a_\mu + i\theta\sigma_\mu\bar{\xi} - i\xi\sigma_\mu\bar{\theta} \; , \\ \theta &\longrightarrow \theta + \xi \; , \\ \bar{\theta} &\longrightarrow \bar{\theta} + \bar{\xi} \; , \end{aligned} \tag{3.8}$$

where ξ and $\bar{\xi}$ play the role of Grassmannian transformation parameters. The superfield formalism can simplify the calculations in supersymmetric field theories while keeping SUSY manifest. The superfields put the quantum fields, their superpartners, and the auxiliary fields in the same object, which are reducible representations of SUSY algebra. A superfield is a function of superspace, which is Minkowski space-time extended with additional fermionic coordinates θ and $\bar{\theta}$ [40]. Its expansion is finite because of the properties of anticommuting coordinates θ and $\bar{\theta}$. [3] This allows us to write down a finite expansion of any superfield as

$$\begin{aligned} F(x^\mu, \theta, \bar{\theta}) &= f(x) + \theta\chi(x) + \bar{\theta}\bar{\chi}(x) + \theta^2 m(x) + \bar{\theta}^2 n(x) + \theta\sigma^\mu\bar{\theta}\upsilon_\mu(x) \\ &\quad + \theta^2\bar{\theta}\bar{\lambda}(x) + \theta\bar{\theta}^2\lambda(x) + \theta^2\bar{\theta}^2 d(x) \; . \end{aligned} \tag{3.9}$$

Here f, m, n, and d are ordinary scalar fields; χ, $\bar{\chi}$, λ, and $\bar{\lambda}$ are two-component spinor fields; υ_μ is a vector field. The component fields of F will transform under SUSY transformations as

$$F(x^\mu, \theta, \bar{\theta}) \longrightarrow e^{i(-a^\nu P_\nu + \xi Q + \bar{\xi}\bar{Q})} F(x^\mu, \theta, \bar{\theta}) \; . \tag{3.10}$$

[3] Note that any expressions containing more than two powers of components of either θ and $\bar{\theta}$ vanish.

Chiral Superfield

A chiral superfield is defined to satisfy the following constraint

$$\bar{D}_{\dot{\alpha}}\Phi(x,\theta,\bar{\theta}) = 0 \,, \tag{3.11}$$

and has a component expansion as

$$\begin{aligned}\Phi(x,\theta,\bar{\theta}) &= \phi(x) + i\theta\sigma^{\mu}\bar{\theta}\partial_{\mu}\phi(x) + \frac{1}{4}\theta^2\bar{\theta}^2\partial^2\phi(x) \\ &\quad + \sqrt{2}\theta\psi(x) - \frac{i}{\sqrt{2}}\theta^2\partial_{\mu}\psi(x)\sigma^{\mu}\bar{\theta} + \theta^2 F(x) \,, \end{aligned} \tag{3.12}$$

where ϕ is complex scalar field, ψ is the two-component left handed Weyl spinor field and F is an auxiliary complex scalar field. The antichiral superfield $\Phi^{\dagger}(x,\theta,\bar{\theta})$ can be constructed as

$$\begin{aligned}\Phi^{\dagger}(x,\theta,\bar{\theta}) &= \phi^{\dagger}(x) - i\theta\sigma^{\mu}\bar{\theta}\partial_{\mu}\phi^{\dagger}(x) + \frac{1}{4}\theta^2\bar{\theta}^2\partial^2\phi^{\dagger}(x) \\ &\quad + \sqrt{2}\bar{\theta}\bar{\psi}(x) + \frac{i}{\sqrt{2}}\bar{\theta}^2\theta\sigma^{\mu}\partial_{\mu}\bar{\psi}(x) + \bar{\theta}^2 F^{\dagger}(x) \,, \end{aligned} \tag{3.13}$$

which obeys the following condition

$$D_{\alpha}\Phi^{\dagger}(x,\theta,\bar{\theta}) = 0 \,. \tag{3.14}$$

Note that the constraints obeyed by the chiral and anti-chiral superfields are needed to ensure that these fields capture an irreducible representation of SUSY.

Vector Superfield

A vector superfield, or real superfield, consists of a gauge field degree of freedom and its gaugino superpartner. It can be obtained by imposing the following constraint

$$V = V^{\dagger}. \tag{3.15}$$

the above constraint is needed to ensure that these fields capture an irreducible representation of SUSY. The transformation of a super-gauge field can be used to obtain its component field expansion as

$$\begin{aligned}V(x,\theta,\bar{\theta}) &= C(x) + i\theta\xi(x) - i\bar{\theta}\bar{\xi}(x) \\ &\quad + \frac{i}{2}\theta^2\left(M(x) + iN(x)\right) - \frac{i}{2}\bar{\theta}^2\left(M(x) - iN(x)\right) - \theta\sigma^{\mu}\bar{\theta}\upsilon_{\mu}(x) \\ &\quad + i\theta^2\bar{\theta}\left(\bar{\lambda}(x) + \frac{i}{2}\bar{\sigma^{\mu}}\partial_{\mu}\xi(x)\right) - i\bar{\theta}^2\theta\left(\lambda(x) + \frac{i}{2}\sigma^{\mu}\partial_{\mu}\bar{\xi}(x)\right) \\ &\quad + \frac{1}{2}\theta^2\bar{\theta}^2\left(D(x) + \frac{1}{2}\partial^2 C(x)\right) \,, \end{aligned} \tag{3.16}$$

where C, D, M and N are real scalar fields, ξ is a Weyl spinor and υ_μ is a vector field (gauge boson). A Wess-Zumino gauge can be obtained from the above expansion by eliminating the fields C, M, N and ξ [39]. Therefore

$$V(x,\theta,\bar{\theta}) = -\theta\sigma^\mu\bar{\theta}\upsilon_\mu(x) + i\theta^2\bar{\theta}\bar{\lambda}(x) - i\bar{\theta}^2\theta\lambda(x) + \frac{1}{2}\theta^2\bar{\theta}^2 D(x)\ . \tag{3.17}$$

Here υ_μ is the associated gauge boson (vector boson), λ is a Weyl fermion (the gaugino) and D is an auxiliary field.

The operators D and $\bar{D}$ of Eq.(3.4) for any V may be used to construct left and right chiral superfields[4]

$$W_\alpha = -\frac{1}{4}\bar{D}^2 D_\alpha V, \quad \bar{W}_{\dot{\alpha}} = -\frac{1}{4}D^2\bar{D}_{\dot{\alpha}}V\ . \tag{3.18}$$

SUSY Lagrangian

With chiral and real superfields discussed previously, we can easily write down the Lagrangian for SUSY. The most general renormalisable action for a chiral field theory is

$$\begin{aligned} S &= \int d^8z\Big(\bar{\Phi}_i\Phi_i + W(\Phi_i)\delta(\bar{\theta}) + W^\dagger(\Phi_i)\delta(\theta)\Big) \\ &= \int d^8z\Big(\bar{\Phi}_i\Phi_i + \Big(\frac{m_{ij}}{2}\Phi_i\Phi_j + \frac{\lambda_{ijk}}{3!}\Phi_i\Phi_j\Phi_k\Big)\delta(\bar{\theta})\Big) + \text{h.c.} \end{aligned} \tag{3.19}$$

The first term is the kinetic contribution of Φ, in the expansion of $\bar{\Phi}_i\Phi_i$. We will have a term proportional to $\theta^2\bar{\theta}^2$ which is the so called D term. The second term is the superpotential W, which corresponds to the mass and Yukawa coupling terms. The F term comes from the expansion components of θ^2. The kinetic term of free vector superfield is given by

$$\mathcal{L}_{gauge} = \frac{1}{4}W^\alpha W_\alpha|_{\theta^2} + \frac{1}{4}\bar{W}_{\dot{\alpha}}W^{\dot{\alpha}}|_{\bar{\theta}^2} \tag{3.20}$$

Abelian gauge group of SUSY case

For a $U(1)$ gauge field transformation the (anti) chiral superfields transform as

$$\Phi_i \longrightarrow e^{-iQ_i\Lambda}\Phi_i, \quad \bar{\Phi}_i \longrightarrow e^{iQ_i\bar{\Lambda}}\bar{\Phi}_i\ . \tag{3.21}$$

Λ is a scalar chiral superfield associated with the $U(1)$ gauge transformation and Q_i are the charges of matter superfields Φ_i. To make Eq.(3.19) gauge invariant we replace the $\bar{\Phi}\Phi$ terms with $\bar{\Phi}_i e^{2iQ_iV}\Phi_i$. Therefore, the most general renormalisable action in the Abelian gauge is:

[4]Not necessarily in the Wess-Zumino gauge.

$$S = \int d^8z \left(\bar{\Phi}_i e^{2iQ_iV} \Phi_i + \frac{1}{4} W^\alpha W_\alpha \delta(\bar{\theta}) + \frac{1}{4} \bar{W}_{\dot{\alpha}} \bar{W}^{\dot{\alpha}} \delta(\theta) \right) + \left(\frac{m_{ij}}{2} \Phi_i \Phi_j + \frac{\lambda_{ijk}}{3!} \Phi_i \Phi_j \Phi_k \right) \delta(\bar{\theta}) + \text{h.c.} \, . \tag{3.22}$$

Non-Abelian gauge group of SUSY case

The case of non-Abelian gauge groups can be easily generalised. The Lie algebra of the gauge group generators is

$$[T^a, T^b] = i f^{abc} T^c \, , \tag{3.23}$$

and the chiral superfields transformations are generalised to

$$\Phi_i \longrightarrow e^{-i\Lambda_{ij}} \Phi_j, \quad \bar{\Phi}_i \longrightarrow e^{i\bar{\Lambda}_{ij}} \bar{\Phi}_j \, , \tag{3.24}$$

where $\Lambda_{ij} = T^a_{ij} \Lambda_a$.

Gauge invariance insures that the vector superfield has to be transformed as

$$e^{2gV} \longrightarrow e^{-i\bar{\Lambda}} e^{2gV} e^{i\Lambda} \, , \tag{3.25}$$

where $V = T^a V^a$. The field-strength can be written as

$$W_\alpha = -\frac{1}{4} \bar{D}^2 e^{-2gV} D_\alpha e^{2gV} \, , \tag{3.26}$$

$$\bar{W}_{\dot{\alpha}} = -\frac{1}{4} D^2 e^{-2gV} \bar{D}_{\dot{\alpha}} e^{2gV} \, , \tag{3.27}$$

and it should be transformed as

$$W_\alpha \longrightarrow e^{-i\Lambda} W_\alpha e^{i\Lambda}, \quad \bar{W}_{\dot{\alpha}} \longrightarrow e^{i\bar{\Lambda}} \bar{W}_{\dot{\alpha}} e^{-i\bar{\Lambda}} \, . \tag{3.28}$$

Therefore the most general renormalisable action is

$$S_{SYM} = S_{gauge} + S_{matter} \, , \tag{3.29}$$

where

$$S_{gauge} = \int d^8z \frac{Tr}{16kg^2} \Big(W^\alpha W_\alpha \delta(\bar{\theta}) + \bar{W}_{\dot{\alpha}} \bar{W}^{\dot{\alpha}} \delta(\theta) \Big) \, , \tag{3.30}$$

and

$$S_{matter} = \int d^8z \left[\bar{\Phi}_i e^{2iQ_iV} \Phi_i + \left(\frac{m_{ij}}{2} \Phi_i \Phi_j + \frac{\lambda_{ijk}}{3!} \Phi_i \Phi_j \Phi_k \right) \delta(\bar{\theta}) \right] . \tag{3.31}$$

Note that the gauge fixing term, Faddeev-Popov ghost term, and the Feynman rules are not presented here. We refer interested readers to Refs. [34–37].

3.1.3 Minimal Supersymmetric Standard Model

The MSSM is an extension of the minimal SUSY to the SM. Since SUSY pairs fermions with bosons, every SM particle has a superpartner. The left-handed and right handed SM fermions will be associated with scalar degrees of freedom (sfermions). The model also contains the fermionic partners of the SM gauge bosons (gauginos) and Higgs boson (Higgsino). The MSSM particle content is listed in Table.3.1. Note that in Table.3.1 the MSSM demands two Higgs doublets for the following reasons: Firstly, the theory must be free from triangle gauge anomalies; secondly, to give the up-type quarks mass in the SM $\Phi^\dagger$ in Eq.(2.27) is used. However, analyticity of the superpotential forces a field of definite chirality only (because the analyticity of the superpotential is a consequence of SUSY), thus it does not involve any conjugate of the superfield $W(\Phi_i)$. As such we introduced a second Higgs doublet H_u with opposite hypercharge [34]. The gauge bosons and their superpartners (gauginos) are in one gauge supermultiplet as shown in Table.3.2.

As mentioned above, every SM particle is associated with a superpartner, give us positive contribution. This is due to the spin-statistics theorem, which means that fermions will have a negative contribution and bosons a positive contribution and as such, this solves the hierarchy problem discussed in section 2.4. We then have corrections to Eq. (2.4) from the scalar loop as:

$$\delta m_H^2 = 2\frac{\lambda_S}{16\pi^2}\Lambda^2 - \dots , \tag{3.32}$$

where λ_S is the coupling governing the interaction $\lambda^2 H^2 S^2$. If the following condition is imposed,

$$\lambda_S = |\lambda_f|^2 , \tag{3.33}$$

then the quadratic divergence will be canceled.

Table 3.1: *MSSM chiral supermultiplets. The spin-0 fields correspond to the complex scalars, and the spin-1/2 fields correspond to left-handed two-component Weyl fermions [34].*

Names		spin-0	spin-1/2	$SU(3)_C$, $SU(2)_L$, $U(1)_Y$
squarks, quarks	Q	$(\tilde{u}_L \;\; \tilde{d}_L)$	$(u_L \;\; d_L)$	$(\mathbf{3}, \mathbf{2}, \frac{1}{6})$
($\times$3 families)	$\bar{u}$	$\tilde{u}_R^*$	$u_R^\dagger$	$(\overline{\mathbf{3}}, \mathbf{1}, -\frac{2}{3})$
	$\bar{d}$	$\tilde{d}_R^*$	$d_R^\dagger$	$(\overline{\mathbf{3}}, \mathbf{1}, \frac{1}{3})$
sleptons, leptons	L	$(\tilde{\nu} \;\; \tilde{e}_L)$	$(\nu \;\; e_L)$	$(\mathbf{1}, \mathbf{2}, -\frac{1}{2})$
($\times$3 families)	$\bar{e}$	$\tilde{e}_R^*$	$e_R^\dagger$	$(\mathbf{1}, \mathbf{1}, 1)$
Higgs, higgsinos	H_u	$(H_u^+ \;\; H_u^0)$	$(\tilde{H}_u^+ \;\; \tilde{H}_u^0)$	$(\mathbf{1}, \mathbf{2}, +\frac{1}{2})$
	H_d	$(H_d^0 \;\; H_d^-)$	$(\tilde{H}_d^0 \;\; \tilde{H}_d^-)$	$(\mathbf{1}, \mathbf{2}, -\frac{1}{2})$

Table 3.2: *MSSM gauge supermultiplets [34].*

Names	spin-1/2	spin-1	$SU(3)_C$, $SU(2)_L$, $U(1)_Y$
bino, B boson	$\tilde{B}^0$	B^0	(**1**, **1** , 0)
winos, W bosons	$\tilde{W}^{\pm}$ $\tilde{W}^0$	$W^{\pm}$ W^0	(**1**, **3** , 0)
gluino, gluon	$\tilde{g}$	g	(**8**, **1** , 0)

The superpotential in the MSSM is the sum of the products of chiral superfields. We can write the most general renormalisable superpotential as

$$W_{\rm MSSM} = y^u_{ij}\bar{u}^c_i Q_j H_u + y^d_{ij}\bar{d}^c_i Q_j H_d + y^L_{ij}\bar{e}^c_i L_j H_d + \mu H_u H_d \ . \tag{3.34}$$

Here i and j are the fermion generation indices. The objects H_u, H_d, Q, L, $\bar{u}^c$, $\bar{d}^c$, $\bar{e}^c$ appearing in Eq.(3.34) are chiral superfields corresponding to the chiral supermultiplets in Table.3.1. The dimensionless Yukawa coupling parameters y_u, y_d, y_e are 3×3 matrices which determine the fermion masses as well as the CKM mixing angles mentioned in chapter 2. The μ term is the SUSY version of the Higgs boson mass in the SM. It is unique, because terms like $H^*_u H_u$ or $H^*_d H_d$ are disallowed in the superpotential and are responsible for the Higgsino mass [34–37]. After the two Higgs doublets H_u and H_d acquire non-zero VEVs (υ_u and υ_d), the ratio can be written as

$$\tan\beta = \frac{\upsilon_u}{\upsilon_d} \ . \tag{3.35}$$

The total number of Higgs scalar fields in the MSSM are eight real fields and the linear combination of these eight real fields form five scalar Higgs eigenstates in the mass eigenstate; two CP-even neutral scalars h^0 and H^0 ($m_h < m_H$), one CP-odd neutral scalar A^0 and two charged Higgses $H^{\pm}$. Three Nambu-Goldston bosons G^0 and $G^{\pm}$ will be "eaten" by the gauge bosons Z^0 and $W^{\pm}$. The neutral Higgsinos ($\tilde{H}^0_u$ and $\tilde{H}^0_d$) and the neutral gauginos ($\tilde{B}$ and $\tilde{W}$) form linear combinations for four neutral mass eigenstates called neutralinos $\tilde{N}_i$ ($i = 1, 2, 3, 4$). Similarly, the charged Higgsinos ($\tilde{H}^+_u$ and $\tilde{H}^-_{\bar{d}}$) and Winos ($\tilde{W}^+$ and $\tilde{W}^-$) mix to form two charged eigenstates called charginos $\tilde{C}_j$ ($j = 1, 2$).

Concerning the superpotential in Eq.(3.34), we can add the following term which violates either baryon and lepton number

$$W_{\not{B}\not{L}} = \lambda^1_{ijk} L_i L_j e_k + \lambda^2_{ijk} L_i Q_j d_k + \lambda^3_{ijk} u^c_i d^c_j d^c_k + \mu^1_i L_i H_u \ . \tag{3.36}$$

The above equation does not respect the baryon and lepton number[5] which leads to a rapid proton decay [34–37]. These terms can be eliminated by

[5]This would be disturbing since B and L violating processes have never been detected experimentally.

imposing the Z_2 symmetry called R-Parity (also known as matter parity) and defined as

$$R = (-1)^{3(B-L)+2S} \,. \tag{3.37}$$

Here S denotes the spin of the particle, $R = +1$ for all observed particles (even R-Parity) and $R = -1$ for all superpartners (odd R-Parity).

The phenomenological implications of R-Parity does not only prevent proton decay, but also ensures that SUSY particles are produced in pairs at colliders and that the lightest superpartner (LSP) is stable. Therefore it would be a dark matter candidate. For example, in most SUSY scenarios the lightest neutralino $\tilde{N}$ (which is a mixture of Binos, Winos and Higgsinos) is an attractive dark matter candidate if its mass is around the EW scale [34–37, 41].

3.1.4 Soft SUSY breaking terms

If SUSY is an exact symmetry, then we should be able to discover the selectron with the same mass as electron (0.511 MeV), photinos and gluinos. So far, none of the superpartners of the SM particles have been discovered in colliders. Therefore, from the theoretical perspective, analogous to the EW symmetry breaking, it is clear that SUSY is also a broken symmetry at some high scale M_{SUSY} known as the SUSY scale, and that all of the superpartners have to be heavy (order the scale $M_{SUSY} \sim 1$ TeV). On the other hand, the different couplings (such as Yukawa couplings of the particles and anti-particles) does change, so that the quadratic divergences of scalar mass corrections are preserved. The terms that fulfill the condition in Eq. (3.33) are called *soft* SUSY breaking terms[6], which means the coefficients of SUSY breaking couplings should have mass positive dimension in order to solve the gauge hierarchy problem mentioned in section 2.4. In order to constrain the number of allowed softly breaking terms, a hidden SUSY sector of particles is introduced which has no direct interaction with MSSM particles [41, 42]. In this hidden sector SUSY is broken spontaneously and communicated with the visible sector via a messenger sector which involves three types of mediation. We shall consider the most discussed in the literature; gravity-mediated (mSUGRA), gauge-mediated (GMSB), and anomaly-mediated (AMSB) SUSY breaking models [41, 42]. In these scenarios the large set of unknown SUSY parameters is minimised to about five parameters in a natural way. This can be done by imposing universality, known as constrained MSSM (CMMM)[7]. The spectrum of the soft terms can be obtained by the renormalisation group scaling of these parameters, and the phenomenological study of the MSSM becomes possible (see chapter 9).

[6]Soft terms induce large Flavour Changing Neutral Current (FCNC)

[7]Universality assumes that all gaugino mass terms, all the scalar mass terms, all the trilinear scalar interactions, and all bilinear scalar interactions are equal at a high scale.

Gravity mediation

In this scenarios, the SUSY breaking is mediated by gravitational interactions and the couplings are suppressed by the inverse of the Planck mass. To adjust the mass dimension in the visible sector we include a mass square.

$$\delta m = \frac{M^2_{\not{SUSY}}}{M_{Pl}} \ . \tag{3.38}$$

Since $M_{Pl} \sim 10^{18}$ GeV, and if we choose $\Delta m \sim 1$ TeV then $M_{\not{SUSY}} \sim 10^{11}$ GeV. Therefore the gravitino acquires a mass, $m_{3/2}$, of order Δm. And SUSY breaking is communicated at much lower energies.

Gauge mediation

SUSY breaking is mediated by the MSSM gauge fields [41,42] instead of gravity, and the matter fields are charged under

$$G = G_{SM} \times G_{\not{SUSY}} \ ,$$

where G provides $M_{\not{SUSY}}$ of order Δm in the TeV range; thus the gravitino mass $m_{3/2}$ is given by:

$$\frac{M^2_{\not{SUSY}}}{M_{Pl}} \sim 10^{-3} eV.$$

Anomaly mediation

Anomaly mediation is considered to be a special kind of gravity mediated SUSY breaking that results from the breaking mechanism being communicated to the visible sector through the conformal anomaly.

The most general MSSM Lagrangian for all observable sectors is

$$\mathcal{L} = \mathcal{L}_{SUSY} + \mathcal{L}_{\not{SUSY}} \ ,$$

where $\mathcal{L}_{SUSY}$ is the sum of Eq.(3.30) and Eq.(3.31), and

$$\mathcal{L}_{\not{SUSY}} = m_0^2 \phi^* \phi + (M_\lambda \lambda\lambda + c.c) + (a\phi^3 + c.c) \ . \tag{3.39}$$

Here, the first term is the mass term for the scalar, the second term corresponds to the gaugino masses, and the last term is representing the trilinear couplings. The most general soft SUSY breaking part of the Lagrangian in the MSSM can be written as follows:

$$\begin{aligned}
\mathcal{L}^{MSSM}_{soft} &= \frac{1}{2}\Big(M_3 \tilde{g}\tilde{g} + M_2 \tilde{W}\tilde{W} + M_1 \tilde{B}\tilde{B} + c.c\Big) \\
&+\Big(\tilde{\bar{u}} a_u \tilde{Q} H_u - \tilde{\bar{d}} a_d \tilde{Q} H_d - \tilde{\bar{e}} a_e \tilde{L} H_d + c.c\Big) \\
&+\tilde{Q}^\dagger m_Q^2 \tilde{Q} + \tilde{L}^\dagger m_L^2 \tilde{L} + \tilde{\bar{u}} m_{\bar{u}}^2 \tilde{\bar{u}}^\dagger + \tilde{\bar{d}} m_{\bar{d}}^2 \tilde{\bar{d}}^\dagger + \tilde{\bar{e}} m_{\bar{e}}^2 \tilde{\bar{e}}^\dagger \\
&+m_{H_u}^2 H_u^* H_u + m_{H_d}^2 H_d^* H_d + \Big(b H_u H_d + c.c\Big) \ ,
\end{aligned} \tag{3.40}$$

where b is a complex scalar, which stands for the bilinear interactions for the Higgs doublets.

3.2 Universal Extra Dimensions

Whilst our universe seems to consist of four space-time dimensions, the possibility of including extra spatial dimensions is an idea which dates back quite some time. In fact, as early as the 1920's Kaluza and Klein proposed the existence of an additional spatial dimension compactified in such a way as to make it too small to have as yet been observed [43,44]. There are several versions of this model, the simplest being the case of one flat extra dimension compactified on an S^1/Z_2 orbifold which has a size $1/R \sim 1$ TeV. This compactification lead to a tower of new particle states in the effective four dimensional theory [45].

As such, in the four dimensional effective theory there appears an infinite tower of massive KK states, Φ^n, with a mass contribution inversely proportional to the radius of the extra-dimension. Due to the orbifolding mechanism, the momentum is no longer conserved along the fifth dimension, and the symmetry is reduced to a KK-parity, $P = (-1)^n$, which is now an exact symmetry.

The Universal Extra Dimension (UED) model is an effective theory in four dimensions with a cutoff Λ, with the consequence that the tree level spectrum is highly degenerate and where loop corrections to masses become quite significant. The phenomenology of these UED models will arise when their flat extra dimensions allow all (or a subset) of the SM fields to propagate in the full space-time [46]. There are many reasons to study such models (see section 2.4), primarily as they provide a way to address the hierarchy problem, i.e., the question of why the Planck scale $M_{pl} \sim 10^{18}$ GeV is so much smaller than the electroweak scale ~ 1 TeV. It also provides a means of breaking the electroweak symmetry, the generation of fermion mass hierarchies, and new sources of CP violation. Furthermore, TeV scale grand unification and sources of dark matter are also possible in these theories [47,48]. To date UED models have been an interesting source of BSM study at the TeV-scale.

In this section we will discuss the model building of five and six extra dimensions in the universal extra dimensional (1UED and 2UED) models.

3.2.1 Five-dimensional 1UED

We shall consider first one flat extra dimension, which allows all (or a subset) of the SM fields to propagate in the full space-time. The space-time coordinate $x_\mu(\mu = 1, 2, 3, 4)$ denotes the usual Minkowski space, and the one extra spatial dimension coordinate x_5 is compactified on the orbifold S^1/Z_2 with radius R. For simplicity we will use the flat extra dimensional notation.

Scalar fields

The Lagrangian for a scalar field Φ is

$$\mathcal{L}_{Scalars} = \int dx_5 \Big\{ D_M \Phi^\dagger D^M \Phi - M^2 \Phi^\dagger \Phi - \lambda_5 (\Phi^\dagger \Phi)^2 \Big\}, \quad (3.41)$$

where $M = 1, 2, \ldots, 5$ and by applying the variational principle to the above equation yields the corresponding equation of motion.

$$\left(\partial_5^2 + p^2 - M^2\right) \Phi = 0\,, \quad (3.42)$$

where $p^2 = -\partial_\mu \partial^\mu$. Note that as we are ignoring the interaction term then λ_5 does not appear in the equation of motion After making use of Fourier decomposition along the fifth coordinate, the field can be written as a sum of KK modes. The wave function satisfies the above equation with p^2 replaced by the mass squared of the mode. The solution of this equation is the usual combination of sines and cosines (with frequencies determined by the periodicity). The masses are given by the formula:

$$m_n^2 = M^2 + \frac{n^2}{R^2}\,, \quad (3.43)$$

where R is the compactification radius, and the mass eigenstates can be labeled by their parity assignment with respect to the generators of the symmetry group of the orbifold and by the KK numbers (n).

We assign an even parity to the five dimensional (scalar) Higgs doublet, so that its corresponding KK mode expansion is:

$$\Phi(x^\mu, x_5) = \frac{1}{\sqrt{2\pi R}} \Phi^{(0)}(x^\mu) + \sum_{n=1}^{\infty} \frac{1}{\sqrt{\pi R}} \Phi^{(n)}(x^\mu) \cos\left(\frac{n x_5}{R}\right). \quad (3.44)$$

Expanding the covariant objects $D_M \Phi$ and $D_5 \Phi$ in KK towers, and integrating out the fifth dimension, the effective 4 dimensional kinetic term in Eq. (3.41) can be written as

$$\begin{aligned} \mathcal{L}_{4D} &= (D_\mu \Phi)^{(0)\dagger}(x)(D^\mu \Phi)^{(0)}(x) + (D_\mu \Phi)^{(n)\dagger}(x)(D^\mu \Phi)^{(n)}(x) \\ &\quad + (D_5 \Phi)^{(n)\dagger}(x)(D^5 \Phi)^{(n)}(x), \end{aligned} \quad (3.45)$$

where repeated indices mean summation. The four dimensional covariant derivatives $(D_\mu \Phi)^{(0)}$, $(D_\mu \Phi)^{(n)}$ and $(D_5 \Phi)^{(n)}$ appearing in Eq. (3.45) are given by

$$\begin{aligned} (D_\mu \Phi)^{(0)} &= D_\mu^{(0)} \Phi^{(0)} - \left(i g \frac{\sigma^i}{2} W_\mu^{(n)i} + i g' \frac{Y}{2} B_\mu^{(n)} \right) \Phi^{(n)}\,, \\ (D_\mu \Phi)^{(n)} &= D_\mu^{(ns)} \Phi^{(s)} - \left(i g \frac{\sigma^i}{2} W_\mu^{(n)i} + i g' \frac{Y}{2} B_\mu^{(n)} \right) \Phi^{(0)}\,, \\ (D_5 \Phi)^{(n)} &= D_5^{(ns)} \Phi^{(s)} - \left(i g \frac{\sigma^i}{2} W_5^{(n)i} + i g' \frac{Y}{2} B_5^{(n)} \right) \Phi^{(n)}\,, \end{aligned} \quad (3.46)$$

where

$$
\begin{aligned}
D_\mu^{(0)} &= \partial_\mu - \Big(ig\frac{\sigma^i}{2} W_\mu^{(0)i} + ig'\frac{Y}{2} B_\mu^{(0)} \Big) \,, \\
D_\mu^{(ns)} &= \delta^{ns} D_\mu^{(0)} - \Delta^{nsr} \Big(ig\frac{\sigma^i}{2} W_\mu^{(r)i} + ig'\frac{Y}{2} B_\mu^{(r)} \Big) \,, \\
D_5^{(ns)} &= -\delta^{ns}\frac{n}{R} - \Delta'^{nsr} \Big(ig\frac{\sigma^i}{2} W_5^{(r)i} + ig'\frac{Y}{2} B_5^{(r)} \Big) \,,
\end{aligned} \tag{3.47}
$$

with

$$
\begin{aligned}
\Delta^{nsr} &= \frac{1}{\sqrt{2}} \Big(\delta^{s,n+r} + \delta^{n,s+r} + \delta^{r,n+s} \Big) \,, \\
\Delta'^{nsr} &= \frac{1}{\sqrt{2}} \Big(\delta^{s,n+r} + \delta^{n,s+r} - \delta^{r,n+s} \Big) \,.
\end{aligned} \tag{3.48}
$$

On the other hand the Higgs potential is given by

$$
V = \int dx_5 \Big(M^2 \Phi^\dagger \Phi + \lambda_5 (\Phi^\dagger \Phi)^2 \Big) \,. \tag{3.49}
$$

Once the fifth coordinate is integrated out, we obtain

$$
\begin{aligned}
V_{4D} &= M^2 \Big(\Phi^{(0)\dagger}(x^\mu)\Phi^{(0)}(x^\mu) \Big) + \lambda \Big(\Phi^{(0)\dagger}(x^\mu)\Phi^{(0)}(x^\mu) \Big)^2 \\
&+ \Big(M^2 + \lambda \Phi^{(0)\dagger}(x^\mu)\Phi^{(0)}(x^\mu) \Big) \Phi^{(n)\dagger}(x^\mu)\Phi^{(n)}(x^\mu) \\
&+ \lambda \Big(\Phi^{(0)\dagger}(x^\mu)\Phi^{(n)}(x^\mu) + \Phi^{(n)\dagger}(x^\mu)\Phi^{(0)}(x^\mu) \Big)^2 \\
&+ 2\Delta^{nsr} \lambda \Big(\Phi^{(0)\dagger}(x^\mu)\Phi^{(n)}(x^\mu) + \Phi^{(n)\dagger}(x^\mu)\Phi^{(0)}(x^\mu) \Big) \Phi^{(s)\dagger}(x^\mu)\Phi^{(r)}(x^\mu) \\
&+ \Delta^{nsrp} \lambda \Phi^{(n)\dagger}(x^\mu)\Phi^{(s)}(x^\mu)\Phi^{(r)\dagger}(x^\mu)\Phi^{(p)}(x^\mu) \,,
\end{aligned} \tag{3.50}
$$

with $\lambda = \frac{\lambda_5}{\pi R}$, and Δ^{nsrp} is given by

$$
\Delta^{nsrp} = \frac{1}{2} \Big(\delta^{n,s+r+p} + \delta^{s,n+r+p} + \delta^{r,n+s+p} + \delta^{p,n+s+r} + \delta^{n+s,r+p} + \delta^{n+r,s+p} + \delta^{n+p,s+r} \Big) \,. \tag{3.51}
$$

Gauge fields

The Lagrangian for an Abelian gauge field (also for non-Abelian gauge symmetries at quadratic level) is

$$
\mathcal{L}_{Gauge+GF} = \int dx_5 \, \left(-\frac{1}{4} F^{MN} F_{MN} - \frac{1}{2\xi} \left(\partial_\mu A^\mu - \xi(\partial_5 A_5) \right)^2 \right) \,, \tag{3.52}
$$

where ξ is the gauge fixing parameter and $F_{MN} = \partial_M A_N - \partial_N A_M$. The gauge fixing term eliminates the mixing between A_μ and the extra polarization A_5. Once the parities are assigned, the spectra and the wave functions will be the same as for the scalar field (but without a mass term):

$$m_n^2 = \frac{n^2}{R^2} \,. \tag{3.53}$$

In the Feynman-'t Hooft gauge $\xi = 1$, the equations of motion for A_5 can be obtained:

$$(\partial_5^2 - \partial_\mu^2) A_5 = 0 \,. \tag{3.54}$$

The spectra and the wave functions are similar to the scalar case, with some additional constraints. Therefore, the gauge fields decompose into towers of 4D spin-1 fields $A_\mu^{(n)}$ and a tower of real scalars $A_5^{(n)}$ belonging to the adjoint representation.

We write $A_\mu^a(x^\mu, x^5)$, with $A = (G, W, B)$ being the $5D$ gauge fields of even parity, $x_5 \longrightarrow -x_5$, with KK decomposition given by:

$$A_\mu^a(x^\mu, x_5) = \frac{1}{\sqrt{2\pi R}} A_\mu^{(0)a}(x^\mu) + \sum_{n=1}^{\infty} \frac{1}{\sqrt{\pi R}} A_\mu^{(n)a}(x^\mu) \cos\left(\frac{n x_5}{R}\right) . \tag{3.55}$$

On the other hand an odd parity is assigned to the fifth component A_5^a, its expansion series is:

$$A_5^a(x^\mu, x_5) = \sum_{n=1}^{\infty} \frac{1}{\sqrt{\pi R}} A_5^{(n)a}(x^\mu) \sin\left(\frac{n x_5}{R}\right) . \tag{3.56}$$

These decompositions lead to an effective 4D Lagrangian by integration of the fifth coordinate, yielding:

$$\begin{aligned} \mathcal{L}_{4D} \;=\; & -\frac{1}{4}\Big(G_{\mu\nu}^{(0)a} G^{(0)a\mu\nu} + G_{\mu\nu}^{(n)a} G^{(n)a\mu\nu} + 2G_{\mu 5}^{(n)a} G^{(n)a\mu 5}\Big) \\ & -\frac{1}{4}\Big(W_{\mu\nu}^{(0)a} W^{(0)a\mu\nu} + W_{\mu\nu}^{(n)a} W^{(n)a\mu\nu} + 2W_{\mu 5}^{(n)a} W^{(n)a\mu 5}\Big) \\ & -\frac{1}{4}\Big(B_{\mu\nu}^{(0)} B^{(0)\mu\nu} + B_{\mu\nu}^{(n)} B^{(n)\mu\nu} + 2B_{\mu 5}^{(n)} B^{(n)\mu 5}\Big) \,. \end{aligned} \tag{3.57}$$

Again, repeated indices are sums, including those for KK modes.

Fermion fields

By analogy with Dirac algebra in Minkowski space, the standard Dirac matrices in five dimensions can be generalised to satisfy the Clifford algebra

$$\left\{\Gamma^M, \Gamma^N\right\} = 2g^{MN} \,, \tag{3.58}$$

where $\Gamma^M = (\gamma^\mu, i\gamma^5)$, $\gamma^5 = i\gamma^0\gamma^1\gamma^2\gamma^3$ and $g^{MN} = diag(+----)$ is the five dimensional metric tensor.

Obviously the fermions in 5D theory are not chiral, this is due to the fact that it is not possible to construct a Γ^5 matrix that anticommutes with all Γ^M. The chirality can be recovered from the parity operation, which can be used to obtain the left handed doublet fermions and the right handed singlet fermions.

The Lagrangian for the Dirac field is given by:

$$\mathcal{L}_{Fermion} = \bar{\psi}\left(i\Gamma^M D_M - m\right)\psi\ . \tag{3.59}$$

Under parity operations the 5D Dirac spinors transform as

$$\psi \longrightarrow \gamma_5\psi(x^\mu, -x_5).$$

Therefore, even and odd parity are assigned to 5D representations of this group, ψ_+ and ψ_-, to yield:

$$\psi_+(x^\mu, x_5) = \frac{1}{\sqrt{2\pi R}}\psi^{(0)}_{+R} + \frac{1}{\sqrt{\pi R}}\sum_{n=1}^{\infty}\left(\psi^{(n)}_{+R}(x^\mu)\cos\left(\frac{nx_5}{R}\right) + \psi^{(n)}_{+L}(x^\mu)\sin\left(\frac{nx_5}{R}\right)\right), \tag{3.60}$$

$$\psi_-(x^\mu, x_5) = \frac{1}{\sqrt{2\pi R}}\psi^{(0)}_{-L} + \frac{1}{\sqrt{\pi R}}\sum_{n=1}^{\infty}\left(\psi^{(n)}_{-L}(x^\mu)\cos\left(\frac{nx_5}{R}\right) + \psi^{(n)}_{-R}(x^\mu)\sin\left(\frac{nx_5}{R}\right)\right). \tag{3.61}$$

Here $\psi^{(0)}_{+R}$ is the zero mode, which can be identified with the SM right handed singlets, the zero mode $\psi^{(0)}_{-L}$ represents the SM left handed doublets, with the KK modes $\psi^{(n)}_{+R}$ and $\psi^{(n)}_{+L}$ being the right handed and the left handed singlets respectively, and $\psi^{(n)}_{-R}$ and $\psi^{(n)}_{-L}$ are the right handed and the left handed doublets respectively.

The effective 4D Lagrangian can be obtained from expansions of these fields in Fourier series and integration of the fifth coordinate x_5 as follows:

$$\begin{aligned}
\mathcal{L}_{4D} \;=\; & i\bar{\psi}^{(0)}_{-L}\gamma^\mu D_\mu\psi^{(0)}_{-L} + i\bar{\psi}^{(n)}_{-L}\gamma^\mu D_\mu\psi^{(n)}_{-L} + i\bar{\psi}^{(0)}_{-R}\gamma^\mu D_\mu\psi^{(0)}_{-R} \\
& -\bar{\psi}^{(0)}_{-L}D_5\psi^{(0)}_{-L} - \bar{\psi}^{(n)}_{-L}D_5\psi^{(n)}_{-L} + \bar{\psi}^{(n)}_{-R}D_5\psi^{(n)}_{-R} \\
& +i\bar{\psi}^{(0)}_{+R}\gamma^\mu D_\mu\psi^{(0)}_{+R} + i\bar{\psi}^{(n)}_{+R}\gamma^\mu D_\mu\psi^{(n)}_{+R} + i\bar{\psi}^{(0)}_{+L}\gamma^\mu D_\mu\psi^{(0)}_{+L} \\
& -\bar{\psi}^{(0)}_{+R}D_5\psi^{(0)}_{+R} - \bar{\psi}^{(n)}_{+R}D_5\psi^{(n)}_{+R} + \bar{\psi}^{(n)}_{+L}D_5\psi^{(n)}_{+L}\ .
\end{aligned} \tag{3.62}$$

3.2.2 Six-dimensional 2UED

We shall also study a model with two universal extra dimensions, where all the SM fields propagate universally in six-dimensional space-time (or a subset). The space-time coordinate $x^\mu(\mu = 0, 1, 2, 3)$ forms the usual Minkowski space. Two spatial dimension coordinates x_5 and x_6 are flat and compactified with

$0 \leq x_5, x_6 \leq L$ on a chiral square of side length L, where the adjacent sides are identified with each other. The compactification radius R is related to the size L of the compactified space as:

$$L = \pi R.$$

Any 6D field $\Phi(x^\mu, x_5, x_6)$ (fermion/gauge or scalar) can be decomposed as:

$$\Phi(x^\mu, x_5, x_6) = \frac{1}{L} \sum_{j,k} f^{(j,k)}(x_5, x_6) \phi^{(j,k)}(x^\mu) \ , \tag{3.63}$$

where

$$\begin{aligned} f^{(j,k)}(x_5, x_6) &= \frac{1}{1 + \delta_{0,j}\delta_{0,k}} \left[e^{-\frac{in\pi}{2}} \cos\left(\frac{jx_5 + kx_6}{R} + \frac{n\pi}{2} \right) \right. \\ &\qquad \left. + \cos\left(\frac{kx_5 - jx_6}{R} + \frac{n\pi}{2} \right) \right] \ . \end{aligned} \tag{3.64}$$

The 4D fields $\phi^{(j,k)}(x^\mu)$ are the (j,k)-th KK modes of the 6D fields $\Phi(x^M)$, and n is an integer whose value is restricted to $0, 1, 2$ or 3 by the boundary conditions. The zero mode $(j, k = 0)$ is allowed only for $n = 0$ in the 4D effective theory.

In 6D, the weak fermion doublet has opposite chirality with respect to the weak-singlet fermions, and as such, the quarks of one generation are given by $Q_+ = (U_+, D_+), U_-, D_-$. The 6D doublet fermions decompose into a tower of heavy vector-like 4D fermion doublets with left-handed zero mode doublets. Similarly, each 6D singlet fermion decomposes into a towers of heavy 4D vector-like singlet fermions along with a zero mode right-handed singlet. These zero mode fields are identified with the SM fermions. In 6D each of the gauge fields, has six components. Upon compactification they decompose into towers of 4D spin-1 fields and two towers of real scalars belonging to the adjoint representation, called spinless adjoints [49]. We will explain and discuss this model in more detail in chapter 6.

Chapter 4

Renormalisation Group Equations

This chapter shall discuss the RGEs and dimensional regularisation method. Basically the renormalisation theory is implemented to remove all the divergences in loop integrals from the physical measurable quantities. These loop diagrams are supposed to give finite results to the physical quantities but they give infinities instead [50, 51]. This tells us that our theory has missed some information. One might ask where do these infinities come from? These infinities arise from the integration over all momentum. In other words, the infinities occur because we let our theory go to arbitrary high energy (UV). However, it is possible to compute physical measurable that do not depend on UV modes by the renormalisation techniques. These techniques will divide the divergent integrals into two portions; one piece contains the finite term while the other contains the divergent piece. There are many techniques which split the divergent integrals, the methods of splitting up the integrals are called regulators. The method of dimensional regularisation is widely used, which will be discussed in details in the next section [32].

As discussed in the previous chapter, loop contributions are important when studying UED models. These will require tools usually reserved for probing higher energies, these tools being the RGEs [55]. Recall that RGEs provide a way by which partial explorations of the physics implications at a high energy scale are possible, as the theories at asymptotic energies may reveal new symmetries or other interesting properties that may lead to deeper insights into the physical content of the universe. In order to understand and study some of the issues in the SM listed in chapter 2, such as the mixing angles and fermion masses hierarchies, a great deal of work has gone into analysing the RGEs of UEDs and their possible extensions (see Refs. [56, 57] and references therein). As an example, the evolution of a generic Yukawa coupling (which describes the fermion-boson interactions) is given by a beta function. The proper Yukawa vertex renormalisation depends on the corresponding beta functions, and include contributions from the anomalous dimensions of the field

operators

$$\mu\frac{\partial \ln Y^R}{\partial \mu} = \frac{1}{2}\mu\frac{\partial \ln Z_{\psi_L}}{\partial \mu} + \frac{1}{2}\mu\frac{\partial \ln Z_{\psi_R}}{\partial \mu} + \frac{1}{2}\mu\frac{\partial \ln Z_{\phi}}{\partial \mu} - \mu\frac{\partial \ln Z_{coupling}}{\partial \mu}\ , \quad (4.1)$$

for some scale parameter μ and renormalised Yukawa coupling Y^R. The renormalisation constants Z_i in general have the form

$$Z = 1 - \frac{\gamma}{2\pi}\ln\frac{\mu}{\mu_0}, \quad (4.2)$$

where γ is the anomalous dimension [32].

Similarly the RGEs of Higgs quartic couplings can be written as

$$\mu\frac{\partial \ln \lambda^R}{\partial \mu} = \mu\frac{\partial \ln Z_{\phi}^2}{\partial \mu} - \mu\frac{\partial \ln Z_{vertex}}{\partial \mu}\ . \quad (4.3)$$

To date RGE technology has proven an important tool when studying the properties of quark masses and the CKM matrix elements at different energy scales, the evolution of the Higgs quartic coupling etc. [59]. Recently this has been expanded to supersymmetric versions of the UED. However, much remains undone [60, 61, 63].

The gauge g_i, Yukawa couplings Y_i, Higgs quartic couplings λ and neutrino running parameter k RGEs at one-loop in the 2UED model will be calculated by utilizing the technique of dimensional regularisation, which discussed at length in Appendices A and B. Note that extra dimension models are effective theories, so the renormalisation will be applied in a different way to these non-renormalisable theories, as dimensional regularisation will hide quadratic divergences from our calculation. Therefore, we shall explain only the technique of dimensional regularisation in detail in the next section and other renoramlisation techniques can be found in Refs. [64–66].

4.1 Dimensional Regularisation

This section shall discuss in detail the method of dimensional regularisation, which will be important to our calculations in this thesis. Divergent integrals result from the Feynman diagrams which involve loops [32, 51]. Such integrals can be tackled simply by introducing a cut off, giving them finite upper bounds. However, this method of regularising infinite integrals is inconvenient when working with theories which have local symmetries, as the procedure does not respect the gauge invariance. Ideally one would prefer to choose a regularisation scheme which preserves all of the symmetries of the classical action. Generally this is not possible. But, there are many regularisation schemes that preserve the local symmetries. Amongst these dimensional regularisation is found to be the most convenient [51].

Yang-Mills theories can be formulated in any number of space-time dimensions. However, the degree of divergence of loop integrals depends strongly

on the space-time dimension. The main idea of dimensional regularisation is to evaluate the integrals in a space-time in which the integrals converge. As a consequence the result will be an analytic function of space-time dimension D for sufficiently small D and the final result should be a well-defined limit as $D \longrightarrow 4$. To understand the method of dimensional regularisation, let us consider the following integral

$$J_\Lambda(p^2, m^2) = -i \int \frac{d^4k}{(2\pi)^4} \frac{1}{(k^2 - m^2 + i\epsilon)((p-k)^2 - m^2 + i\epsilon)} . \tag{4.4}$$

The above integral diverges logarithmically in $4D$ space-time. However, it will converge if the space-time dimension is smaller than 4. We therefore, consider a D-dimensional integral

$$J_D(p^2, m^2) = -i \int \frac{d^Dk}{(2\pi)^D} \frac{1}{(k^2 - m^2 + i\epsilon)((p-k)^2 - m^2 + i\epsilon)} , \tag{4.5}$$

where now k^2 reads

$$k^2 = k_0^2 - k_1^2 - ..... - k_{D-1}^2 . \tag{4.6}$$

To proceed, we use the Feynman parametrisation

$$\frac{1}{ab} = \int_0^1 d\ z \frac{1}{(az + (1-z)b)^2} , \tag{4.7}$$

and insert the above into Eq. (4.5),

$$J_D(p^2, m^2) = -i \int_0^1 d\ z \int \frac{d^D\ k}{(2\pi)^D} \frac{1}{(k^2 + z(1-z)p^2 - m^2 + i\epsilon)^2} , \tag{4.8}$$

where we have changed the integration variable as $k \longrightarrow k + zp$.

We can perform the k_0 integration by making use of the Cauchys residue theorem. The poles in the complex k_0-plane are located at

$$k_0 = \pm\sqrt{-z(1-z)p^2 + \vec{k}^2 + m^2} \mp i\epsilon . \tag{4.9}$$

If p is space-like i.e. $p^2 < 0$, then the square root is real. The singularities of the k_0 integration are located as shown in Fig. 4.1

In this case, the k integration can be evaluated easily. Assuming now $p^2 < 0$ and using the identity

$$0 = \int_C \frac{d\ k_0}{2\pi} \frac{1}{(k_0^2 - \vec{k}^2 + z(1-z)p^2 - m^2 + i\epsilon)^2} , \tag{4.10}$$

where C is described right panel of Fig. 4.1. Note that it does not enclose any of the poles.

Eventually, we shall let the radii of C_1 and C_2 go to infinity, where in this limit one gets

$$\int_{-\infty}^{+\infty} \frac{dk_0}{2\pi} \frac{1}{(k_0^2 - \vec{k}^2 + z(1-z)p^2 - m^2 + i\epsilon)^2} = i \int_{-\infty}^{+\infty} \frac{dk_D}{2\pi} \frac{1}{(k_D^2 + \vec{k}^2 - z(1-z)p^2 + m^2 + i\epsilon)^2} ,$$

where in the last step we change the integration variable $k_0 \longrightarrow k_D = -ik_0$. With this formula we can rewrite J_D in the form of a Euclidean integral

$$J_D(p^2, m^2) = -i \int_0^1 d\ z \int \frac{d^D\ k}{(2\pi)^D} \frac{1}{(k^2 - z(1-z)p^2 - m^2)^2} , \tag{4.11}$$

where $k^2 = k_1^2 + k_2^2 - ..... + k_{D-1}^2 + k_D^2$ is the length square of a D-dimensional Euclidean vector. Note that the integral has a rotational symmetry, thus the angular integration can be performed as

$$J_D(p^2, m^2) = \frac{S_{D-1}}{(2\pi)^D} \int_0^1 d\ z \int_0^\infty d\ k\ \frac{k^{D-1}}{(k^2 - z(1-z)p^2 - m^2)^2} , \tag{4.12}$$

where S_{D-1} corresponds to the surface area of a unit sphere in D-dimensional Euclidean space R^D, and is given by

$$S_{D-1} = \frac{2\pi^{\frac{D}{2}}}{\Gamma(\frac{D}{2})} . \tag{4.13}$$

The *Gamma*-function is defined by

$$\Gamma(\epsilon) = \int_0^\infty d\ x\ x^{\epsilon-1}\ e^{-x} \qquad \Re\epsilon > 0 . \tag{4.14}$$

The radial integral in Eq. (4.12) can be evaluated with help of the standard integral

$$\int_0^\infty d\ u\ \frac{u^\alpha}{(u+a)^\beta} = a^{\alpha+1-\beta} \frac{\Gamma(\alpha+1)\Gamma(\beta-\alpha-1)}{\Gamma(\beta)} . \tag{4.15}$$

Therefore Eq. (4.12) becomes

$$J_D(p^2, m^2) = \frac{S_{D-1}}{2(2\pi)^D} \Gamma\left(\frac{D}{2}\right) \Gamma\left(\frac{4-D}{2}\right) \int_0^1 d\ z\ (-z(1-z)p^2 + m^2)^2 . \tag{4.16}$$

This result implies that J_D is a meromorphic function of D with well defined singularities residing at the position of the poles of the Γ-functions.

The pole structure of $\Gamma(\epsilon)$ follows from the basic property

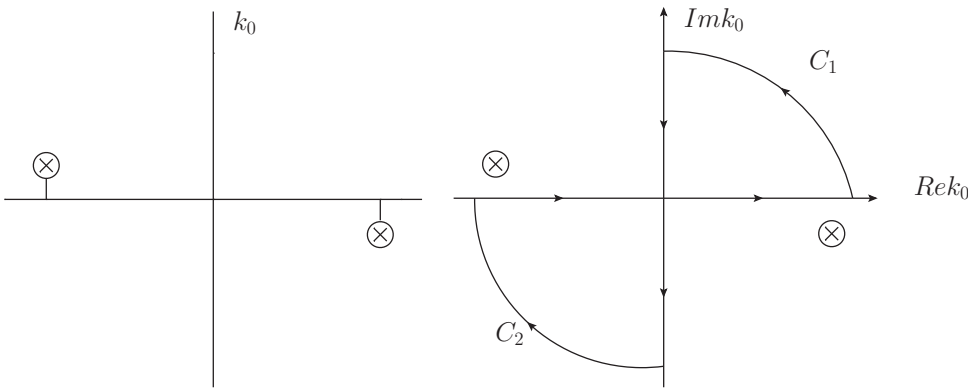


Figure 4.1: *The contour with: in the left panel, the k_0 integration plane; and the right panel for the contour used in the integration.*

$$\Gamma(\epsilon+1) = \epsilon\Gamma(\epsilon) \ , \tag{4.17}$$

which follows from an integration by parts of Eq. (4.14). From this relation we see that

$$\Gamma(\epsilon)|_{\epsilon\longrightarrow 0} = \frac{1}{\epsilon} - \gamma + \mathcal{O}(\epsilon) \ . \tag{4.18}$$

Eq. (4.18) indicate a constant plus terms of the first and higher order in ϵ, where $\gamma = 0.5772...$ is the Euler number.

If we let $\epsilon = 4 - D$, it should be clear that as $D \longrightarrow 4$, i.e. as $\epsilon \longrightarrow 0$, Eq. (4.16) reduces to

$$J_\epsilon(p^2, m^2) = \frac{1}{8\pi^2}\frac{1}{\epsilon} - \frac{1}{16\pi^2}\int_0^1 d\ z\ \ln\left(-z(1-z)\frac{p^2}{m^2}\right) + \text{const} + \mathcal{O}(\epsilon) \ . \tag{4.19}$$

Note that we had assumed $p^2 < 0$ to derive Eq. (4.19), and it can been clearly seen that the argument of the ln is positive for $p^2 < 4m^2$. One can evaluate $J_\epsilon(0, m^2)$

$$J_\epsilon(0, m^2) = \frac{1}{8\pi^2}\frac{1}{\epsilon} + \text{const} \ . \tag{4.20}$$

Thus

$$J_\epsilon(p^2, m^2) - J_\epsilon(0, m^2) = -\frac{1}{16\pi^2}\int_0^1 d\ z\ \ln(-z(1-z)\frac{p^2}{m^2}) \ . \tag{4.21}$$

Therefore Eq. (4.21) is finite, but this procedure is not unique. For instance, we could just subtract the $\frac{1}{8\pi^2}\frac{1}{\epsilon}$ from Eq. (4.19) and still get a finite result. But this result would be independent of p, what was subtracted is called a scheme. The renormalisation scheme in which we subtract only the pole parts in ϵ is known as the minimal subtraction scheme.

4.2 RGEs of CKM Matrix

In this section we will derive the RGEs for the quark mixing matrix in the SM as well as its SUSY extension. Note that this section rely heavily on Ref. [73]. As we mentioned in chapter 2, the (non Hermitian) Yukawa coupling matrices Y_u, Y_d and Y_e, can be diagonalised by the bi-unitary transformations

$$U_R Y_u U_L^\dagger = D = diag\,(f_u, f_c, f_t)\ , \tag{4.22}$$

$$U'_R Y_d U'^\dagger_L = D' = diag\,(h_d, h_s, h_b)\ , \tag{4.23}$$

and

$$U''_R Y_e U''^\dagger_L = D'' = diag\,(l_e, l_\mu, l_\tau)\ . \tag{4.24}$$

For example U_L could be determined by noting that $U_L Y_u^\dagger Y_u U_R^\dagger = D^2$.

The CKM matrix $V = U_L U_L'^\dagger$ results from the diagonalisation of the Yukawa matrices. Note that the matrices U_R, U'_R are irrelevant, since the charged current involves only left-handed quark fields [73]. The Yukawa coupling matrices Y_u, Y_d and Y_e run with momentum in the SM according to

$$16\pi^2 \frac{dY_u}{dt} = Y_u \left(T - G_u + \frac{3}{2}\left(Y_u^\dagger Y_u - Y_d^\dagger Y_d \right) \right)\ , \tag{4.25}$$

$$16\pi^2 \frac{dY_d}{dt} = Y_d \left(T - G_d + \frac{3}{2}\left(Y_d^\dagger Y_d - Y_u^\dagger Y_u \right) \right)\ , \tag{4.26}$$

and

$$16\pi^2 \frac{dY_e}{dt} = Y_e \left(T - G_e + \frac{3}{2} Y_e^\dagger Y_e \right)\ , \tag{4.27}$$

where

$$T = \mathrm{Tr}\left(3Y_u^\dagger Y_u + 3Y_d^\dagger Y_d + Y_e^\dagger Y_e \right)\ , \tag{4.28}$$

$$G_u = \frac{17}{20} g_1^2 + \frac{9}{4} g_2^2 + 8 g_3^2\ , \tag{4.29}$$

$$G_d = \frac{1}{4} g_1^2 + \frac{9}{4} g_2^2 + 8 g_3^2\ , \tag{4.30}$$

$$G_e = \frac{9}{4} g_1^2 + \frac{9}{4} g_2^2\ . \tag{4.31}$$

Here $t = \ln \frac{\mu}{M_Z}$. Defining $M = Y_u^\dagger Y_u$, $M' = Y_d^\dagger Y_d$, $M'' = Y_e^\dagger Y_e$, and multiplying $Y_u^\dagger$ from the right on both side of the Eq. (4.25), we obtain

$$16\pi^2 Y_u^\dagger \frac{dY_u}{dt} = Y_u^\dagger Y_u \left(T - G_u + \frac{3}{2}\left(Y_u^\dagger Y_u - Y_d^\dagger Y_d \right) \right)\ . \tag{4.32}$$

Taking the Hermitian conjugate of Eq. (4.25) and multiplying on both sides from the left by Y_u we obtain

$$16\pi^2 \frac{dY_u^\dagger}{dt} Y_u = \left(T - G_u + \frac{3}{2} \left(Y_u^\dagger Y_u - Y_d^\dagger Y_d \right) \right) Y_u^\dagger Y_u \ . \tag{4.33}$$

Adding Eq. (4.32) to Eq. (4.33) yields

$$16\pi^2 \frac{dY_u^\dagger Y_u}{dt} = 2 Y_u^\dagger Y_u \left(T - G_u + 3 Y_u^\dagger Y_u \right) - \frac{3}{2} \{ Y_u^\dagger Y_u, Y_d^\dagger Y_d \} \ , \tag{4.34}$$

thus

$$16\pi^2 \frac{dM}{dt} = 2 \left(T - G_u \right) M + 3 M^2 - \frac{3}{2} \{ M, M' \} \ . \tag{4.35}$$

Similarly for M' and M'',

$$16\pi^2 \frac{dM'}{dt} = 2 \left(T - G_d \right) M' + 3 M'^2 - \frac{3}{2} \{ M', M \} \ , \tag{4.36}$$

$$16\pi^2 \frac{dM''}{dt} = 2 \left(T - G_e \right) M'' + 3 M''^2 \ . \tag{4.37}$$

M and M' can be diagonalised by two unitary matrices U_L and U'_L at some momentum scale μ

$$U_L M U_L^\dagger = D^2 = diag \left(f_u^2, f_c^2, f_t^2 \right) \ , \tag{4.38}$$

$$U'_L M' U_L'^\dagger = D'^2 = diag \left(h_d^2, h_s^2, h_b^2 \right) \ . \tag{4.39}$$

Therefore the CKM matrix at the scale μ will be given by

$$V = U_L U_L'^\dagger \ . \tag{4.40}$$

The changing in μ lead to the new mass matrices $M + \Delta M$ and $M' + \Delta M'$ which can not be diagonalised by U_L and U'_L, because of the occurrence of the term $\{M, M'\}$ in Eqs. (4.35)-(4.36). Note that a change in the diagonal couplings can be obtained by using Eqs.(4.35, 4.36, 4.38, 4.39, 4.40)

$$\begin{aligned} U_L \Delta M U_L^\dagger &= \frac{1}{16\pi^2} \Bigg(2 \left(T - G_u \right) D^2 + 3 D^4 - \frac{3}{2} \left(D^2 V D'^2 V^\dagger \right. \\ &\quad \left. + \ V D'^2 V^\dagger D^2 \right) \Bigg) \Delta t \ , \end{aligned} \tag{4.41}$$

$$\begin{aligned} U'_L \Delta M' U_L'^\dagger &= \frac{1}{16\pi^2} \Bigg(2 \left(T - G_e \right) D'^2 + 3 D'^4 - \frac{3}{2} \left(D^2 V D'^2 V^\dagger \right. \\ &\quad \left. + \ V D'^2 V^\dagger D^2 \right) \Bigg) \Delta t \ . \end{aligned} \tag{4.42}$$

The eigenvalues of ΔM and $\Delta M'$ are the diagonal entries to the lowest order. Thus Eqs. (4.41, 4.42) lead to the variation of the diagonal couplings as

$$16\pi^2 \frac{df_i^2}{dt} = f_i^2 \left(2\left(T - G_u\right) + 3f_i^2 - 3\sum_\alpha h_\alpha^2 |V_{i\alpha}|^2 \right) \ , \tag{4.43}$$

$$16\pi^2 \frac{dh_\alpha^2}{dt} = h_\alpha^2 \left(2\left(T - G_d\right) + 3h_\alpha^2 - 3\sum_i f_i^2 |V_{i\alpha}|^2 \right) \ , \tag{4.44}$$

here $i = (u, c, t)$ and $\alpha = (d, s, b)$

In a similar manner the variation of the lepton Yukawa couplings $l_a^2 (a = e, \mu, \tau)$ can be obtained

$$16\pi^2 \frac{dl_a^2}{dt} = l_a^2 \left(2\left(T - G_e\right) + 3l_a^2 \right) \ . \tag{4.45}$$

Now we turn our attention to the variation of the mixing angles.

The following matrix

$$\begin{aligned} U_L \left(M + \Delta M\right) U_L^\dagger \ &= \ D^2 + \frac{1}{16\pi^2} \left(2\left(T - G_u\right) D^2 + 3D^4 - \frac{3}{2} \left(D^2 V D'^2 V^\dagger \right.\right. \\ &\left.\left. + \ V D'^2 V^\dagger D^2 \right) \right) \Delta t \end{aligned} \tag{4.46}$$

can be diagonalised by a unitary transformation $(1 + \epsilon)$, with unitarity conditions $\epsilon^\dagger = -\epsilon$ and $\epsilon_{ii} = 0$. As such,

$$\left(1 + \epsilon\right) \left(D^2 + U_L \Delta M U_L^\dagger \right) \left(1 - \epsilon\right) = D^2 + \Delta D^2 \ , \tag{4.47}$$

and together with Eq. (4.41), the non vanishing elements of ϵ can be derived

$$\left(D^2 + U_L \Delta M U_L^\dagger \right) + \epsilon \left(D^2 + U_L \Delta M U_L^\dagger \right) - \left(D^2 + U_L \Delta M U_L^\dagger \right) \epsilon = D^2 + \Delta D^2. \tag{4.48}$$

After some algebra we get

$$D^2 \epsilon - \epsilon D^2 = -\frac{3}{2} \frac{1}{16\pi^2} \left(D^2 V D'^2 V^\dagger + V D'^2 V^\dagger D^2 \right) \Delta t \ , \tag{4.49}$$

then for $i \neq j$ we will have

$$f_i^2 \epsilon_{ij} - \epsilon_{ij} f_j^2 = -\frac{3}{2} \frac{1}{16\pi^2} \left(\left(f_i^2 + f_j^2 \right) \sum_\alpha h_\alpha^2 V_{i\alpha} V_{j\alpha}^* \right) \Delta t \ . \tag{4.50}$$

The nonzero elements of ϵ are

$$\epsilon_{ij} = -\frac{3}{2} \frac{1}{16\pi^2} \left(\frac{f_i^2 + f_j^2}{f_i^2 - f_j^2} \sum_\alpha h_\alpha^2 V_{i\alpha} V_{j\alpha}^* \right) \Delta t \ . \tag{4.51}$$

Similarly if $(1+\epsilon')$ is assumed to diagonalise $U'_L\left(M'+\Delta M'\right)U'^{\dagger}_L$ then,

$$\epsilon'_{\alpha\beta}=-\frac{3}{2}\frac{1}{16\pi^2}\left(\frac{h_\alpha^2+h_\beta^2}{h_\alpha^2-h_\beta^2}\sum_i f_i^2 V_{i\alpha}^* V_{i\beta}\right)\Delta t\ . \tag{4.52}$$

Finally the variation of the CKM matrix in the SM is given by

$$\Delta V=\epsilon V-V\epsilon'\ , \tag{4.53}$$

which implies

$$16\pi^2\frac{dV_{i\alpha}}{dt}=-\frac{3}{2}\left(\sum_{\beta,j\neq i}\frac{f_i^2+f_j^2}{f_i^2-f_j^2}h_\beta^2 V_{i\beta}V_{j\beta}^*V_{j\alpha}+\sum_{j,\beta\neq\alpha}\frac{h_\alpha^2+h_\beta^2}{h_\alpha^2-h_\beta^2}f_j^2V_{j\beta}^*V_{j\alpha}V_{i\beta}\right) \tag{4.54}$$

It is useful to describe the evolution of CKM matrix in term of four independent parameters of V [73]. By defining $X=|V_{ud}|^2$, $Y=|V_{us}|^2$, $Z=|V_{cd}|^2$ and $J=\mathrm{Im}(V_{ud}V_{cs}V_{us}^*V_{cd}^*)$ with the help of unitarity conditions of the CKM matrix, $|V_{i\alpha}|^2$ takes part in Eqs. (4.35) and (4.36) and can be expressed as

$$|V_{ub}|^2=1-X-Y\ , \tag{4.55}$$

$$|V_{td}|^2=1-X-Z\ , \tag{4.56}$$

$$|V_{cs}|^2=\frac{XYZ+(1-X-Y)(1-X-Z)-2K}{(1-X)^2}\ , \tag{4.57}$$

$$|V_{cb}|^2=\frac{XZ(1-X-Y)+Y(1-X-Z)+2K}{(1-X)^2}\ , \tag{4.58}$$

$$|V_{ts}|^2=\frac{XY(1-X-Z)+Z(1-X-Y)+2K}{(1-X)^2}\ , \tag{4.59}$$

$$|V_{tb}|^2=\frac{YZ+X(1-X-Y)(1-X-Z)-2K}{(1-X)^2}\ , \tag{4.60}$$

where

$$K=\sqrt{XYZ(1-X-Y)(1-X-Z)-J^2(1-X)^2}\ . \tag{4.61}$$

The evolution of X, Y, Z and J follow from Eq. (4.54). Multiplying Eq. (4.54) by $V_{i\alpha}^*$ on both sides from the left

$$\begin{aligned}16\pi^2V_{i\alpha}^*\frac{dV_{i\alpha}}{dt} &= -\frac{3}{2}\left(\sum_{\beta,j\neq i}\frac{f_i^2+f_j^2}{f_i^2-f_j^2}h_\beta^2V_{i\alpha}^*V_{i\beta}V_{j\beta}^*V_{j\alpha}\right.\\ &\left.+\sum_{j,\beta\neq\alpha}\frac{h_\alpha^2+h_\beta^2}{h_\alpha^2-h_\beta^2}f_j^2V_{i\alpha}^*V_{j\beta}^*V_{j\alpha}V_{i\beta}\right)\ ,\end{aligned} \tag{4.62}$$

and taking the complex conjugate of the Eq. (4.54) and then multiplying both sides from the right by $V_{i\alpha}$, we obtain

$$16\pi^2 \frac{dV^*_{i\alpha}}{dt} V_{i\alpha} = -\frac{3}{2}\left(\sum_{\beta, j\neq i} \frac{f_i^2 + f_j^2}{f_i^2 - f_j^2} h_\beta^2 V^*_{i\beta} V_{j\beta} V^*_{j\alpha} V_{i\alpha} + \sum_{j,\beta\neq\alpha} \frac{h_\alpha^2 + h_\beta^2}{h_\alpha^2 - h_\beta^2} f_j^2 V_{j\beta} V^*_{j\alpha} V^*_{i\beta} V_{i\alpha} \right) . \tag{4.63}$$

Adding Eq. (4.62) to Eq. (4.63) we get

$$16\pi^2 \frac{d|V_{i\alpha}|^2}{dt} = -\frac{3}{2}\left(\sum_{\beta, j\neq i} \frac{f_i^2 + f_j^2}{f_i^2 - f_j^2} h_\beta^2 \Big(V^*_{i\alpha} V_{i\beta} V^*_{j\beta} V_{j\alpha} + V^*_{i\beta} V_{j\beta} V^*_{j\alpha} V_{i\alpha} \Big) - \sum_{j,\beta\neq\alpha} \frac{h_\alpha^2 + h_\beta^2}{h_\alpha^2 - h_\beta^2} f_j^2 \Big(V^*_{i\alpha} V^*_{j\beta} V_{j\alpha} V_{i\beta} + V_{j\beta} V^*_{j\alpha} V^*_{i\beta} V_{i\alpha} \Big) \right) . \tag{4.64}$$

4.3 Evolution of X

Let $i = u, j = (c, t)$ and $\alpha = d, \beta = (d, s, b)$ in the first sum and $i = u, j = (u, c, t)$ and $\alpha = d, \beta = (s, b)$ in the last summation. In which case Eq. (4.64)

becomes

$$
\begin{aligned}
16\pi^2\frac{d|V_{ud}|^2}{dt} &= -\frac{3}{2}\Bigg(\frac{f_u^2+f_c^2}{f_u^2-f_c^2}\Big(h_d^2\Big(V_{ud}^*V_{ud}V_{cd}^*V_{cd}+V_{ud}^*V_{cd}V_{cd}^*V_{ud}\Big)\\
&+ h_s^2\Big(V_{ud}^*V_{us}V_{cs}^*V_{cd}+V_{us}^*V_{cs}V_{cd}^*V_{ud}\Big)\Big)\\
&- \frac{f_u^2+f_c^2}{f_u^2-f_c^2}h_b^2\Big(V_{ud}^*V_{ub}V_{cb}^*V_{cd}+V_{ub}^*V_{cb}V_{cd}^*V_{ud}\Big)\\
&- \frac{f_u^2+f_t^2}{f_u^2-f_t^2}h_d^2\Big(V_{ud}^*V_{ud}V_{td}^*V_{td}+V_{ud}^*V_{td}V_{td}^*V_{ud}\Big)\\
&- \frac{f_u^2+f_t^2}{f_u^2-f_t^2}\Big(h_s^2\Big(V_{ud}^*V_{us}V_{ts}^*V_{td}+V_{us}^*V_{ts}V_{td}^*V_{ud}\Big)\\
&+ h_b^2\Big(V_{ud}^*V_{ub}V_{tb}^*V_{td}+V_{ub}^*V_{tb}V_{td}^*V_{ud}\Big)\Big)\\
&- \frac{h_d^2+h_s^2}{h_d^2-h_s^2}\Big(f_u^2\Big(V_{ud}^*V_{us}^*V_{ud}V_{us}+V_{us}V_{ud}^*V_{us}^*V_{ud}\Big)\\
&+ f_c^2\Big(V_{ud}^*V_{cs}^*V_{cd}V_{us}+V_{cs}V_{cd}^*V_{us}^*V_{ud}\Big)\Big)\\
&- \frac{h_d^2+h_s^2}{h_d^2-h_s^2}f_t^2\Big(V_{ud}^*V_{ts}^*V_{td}V_{us}+V_{ts}V_{td}^*V_{us}^*V_{ud}\Big)\\
&- \frac{h_d^2+h_b^2}{h_d^2-h_b^2}f_u^2\Big(V_{ud}^*V_{ub}^*V_{ud}V_{ub}+V_{ub}V_{ud}^*V_{ub}^*V_{ud}\Big)\\
&- \frac{h_d^2+h_s^2}{h_d^2-h_s^2}\Big(f_c^2\Big(V_{ud}^*V_{cb}^*V_{cd}V_{ub}+V_{cb}V_{cd}^*V_{ub}^*V_{ud}\Big)\\
&+ f_t^2\Big(V_{ud}^*V_{tb}^*V_{td}V_{ub}+V_{tb}V_{td}^*V_{ub}^*V_{ud}\Big)\Big)\Bigg)\ . \qquad (4.65)
\end{aligned}
$$

Plugging all ingredients in the above equation yields:

$$
\begin{aligned}
16\pi^2\frac{dX}{dt} &= -3\Bigg(\frac{f_u^2+f_t^2}{f_u^2-f_t^2}\Big(\Big(h_d^2-h_b^2\Big)X\Big(1-X-Z\Big)\\
&+ \frac{h_b^2-h_s^2}{1-X}\Big(XY\,(1-X-Z)+K\Big)\Big)\\
&- \frac{h_d^2+h_b^2}{h_d^2-h_b^2}\Big(\Big(f_u^2-f_t^2\Big)X\Big(1-X-Y\Big)\\
&+ \frac{f_t^2-f_c^2}{1-X}\Big(XZ(1-X-Y)+K\Big)\Big)\\
&- \frac{f_u^2+f_c^2}{f_u^2-f_c^2}\Big(\Big(h_d^2-h_b^2\Big)XZ+\frac{h_b^2-h_s^2}{1-X}\Big(XYZ-K\Big)\Big)\\
&- \frac{h_d^2+h_s^2}{h_d^2-h_s^2}\Big(\Big(f_u^2-f_t^2\Big)XY+\frac{f_t^2-f_c^2}{1-X}\Big(XYZ-K\Big)\Big)\Bigg) \qquad (4.66)
\end{aligned}
$$

4.4 Evolution of Y

Let $i = u, j = (c, t)$ and $\alpha = s, \beta = (d, s, b)$ in the first sum and $i = u, j = (u, c, t)$ and $\alpha = s, \beta = (d, b)$ in the last sum of Eq. (4.64), we obtain

$$\begin{aligned}
16\pi^2\frac{d|V_{us}|^2}{dt} &= -\frac{3}{2}\frac{f_u^2+f_c^2}{f_u^2-f_c^2}\Big(h_d^2\Big(V_{us}^*V_{ud}V_{cd}^*V_{cs}+V_{ud}^*V_{cd}V_{cs}^*V_{us}\Big)\\
&+h_s^2\Big(V_{us}^*V_{us}V_{cs}^*V_{cs}+V_{us}^*V_{cs}V_{cs}^*V_{us}\Big)\\
&+h_b^2\Big(V_{us}^*V_{ub}V_{cb}^*V_{cs}+V_{ub}^*V_{cb}V_{cs}^*V_{us}\Big)\Big)\\
&-\frac{3}{2}\frac{f_u^2+f_t^2}{f_u^2-f_t^2}\Big(h_d^2\Big(V_{us}^*V_{ud}V_{td}^*V_{ts}+V_{ud}^*V_{td}V_{ts}^*V_{us}\Big)\\
&+h_s^2\Big(V_{us}^*V_{us}V_{ts}^*V_{ts}+V_{us}^*V_{ts}V_{ts}^*V_{us}\Big)\\
&+h_b^2\Big(V_{us}^*V_{ub}V_{tb}^*V_{ts}+V_{ub}^*V_{tb}V_{ts}^*V_{us}\Big)\Big)\\
&-\frac{3}{2}\frac{h_d^2+h_s^2}{h_d^2-h_s^2}\Big(f_u^2\Big(V_{us}^*V_{ud}^*V_{ud}V_{us}+V_{ud}V_{us}^*V_{ud}^*V_{us}\Big)\\
&+f_c^2\Big(V_{us}^*V_{cd}^*V_{cs}V_{ud}+V_{cd}V_{cs}^*V_{ud}^*V_{us}\Big)\\
&-f_t^2\Big(V_{us}^*V_{td}^*V_{ts}V_{ud}+V_{td}V_{ts}^*V_{ud}^*V_{us}\Big)\Big)\\
&-\frac{3}{2}\frac{h_d^2+h_b^2}{h_d^2-h_b^2}\Big(f_u^2\Big(V_{us}^*V_{ub}^*V_{us}V_{ub}+V_{us}V_{ub}^*V_{us}^*V_{ub}\Big)\\
&-f_c^2\Big(V_{us}^*V_{cb}^*V_{cs}V_{ub}+V_{cb}V_{cs}^*V_{ub}^*V_{us}\Big)\\
&+f_t^2\Big(V_{us}^*V_{tb}^*V_{ts}V_{ub}+V_{tb}V_{ts}^*V_{ub}^*V_{us}\Big)\Big)\ . \qquad (4.67)
\end{aligned}$$

Substituting all ingredients in the above equation, gives the simple form:

$$\begin{aligned}
16\pi^2\frac{dY}{dt} &= -3\frac{f_u^2+f_c^2}{f_u^2-f_c^2}\left(\frac{h_s^2-h_b^2}{(1-X)^2}Y\Big(XZY+(1-X-Y)(1-X-Z)-2K\Big)\right.\\
&\left.+\frac{h_b^2-h_d^2}{1-X}\Big(XYZ-K\Big)\right)\\
&-3\frac{f_u^2+f_t^2}{f_u^2-f_t^2}\left(\frac{h_s^2-h_b^2}{(1-X)^2}Y\Big(XY(1-X-Z)+Z(1-X-Y)+2K\Big)\right.\\
&\left.+\frac{h_d^2-h_b^2}{(1-X)}\Big(XY(1-X-Z)+K\Big)\right)\\
&-3\frac{h_s^2+h_d^2}{h_s^2-h_d^2}\left(\Big(f_u^2-f_t^2\Big)XY+\frac{f_t^2-f_c^2}{1-X}\Big(XYZ-K\Big)\right)\\
&-3\frac{h_s^2+h_b^2}{h_s^2-h_b^2}\left(\frac{f_c^2-f_t^2}{(1-X)^2}\Big(\Big(1-X-Y\Big)\Big(XYZ-Y\Big(1-X-Z\Big)\Big)\right.\\
&\left.-K\Big(1-X-2Y\Big)\Big)+\Big(f_u^2-f_t^2\Big)Y\Big(1-X-Y\Big)\right)\ . \qquad (4.68)
\end{aligned}$$

4.5 Evolution of Z

Let $i = c, j = (u, t)$ and $\alpha = d, \beta = (d, s, b)$ in the first sum and $i = c, j = (u, c, t)$ and $\alpha = d, \beta = (s, b)$ in the last sum of Eq. (4.64), we get

$$\begin{aligned}
16\pi^2\frac{d|V_{cd}|^2}{dt} &= -\frac{3}{2}\frac{f_c^2+f_u^2}{f_c^2-f_u^2}\Big(h_d^2\Big(V_{cd}^*V_{cd}V_{ud}^*V_{us}+V_{cd}^*V_{ud}V_{ud}^*V_{cd}\Big)\\
&\quad + h_s^2\Big(V_{cd}^*V_{cs}V_{us}^*V_{ud}+V_{cs}^*V_{us}V_{ud}^*V_{cd}\Big)\\
&\quad + h_b^2\Big(V_{cd}^*V_{cb}V_{ub}^*V_{ud}+V_{cb}^*V_{ub}V_{ud}^*V_{cd}\Big)\Big)\\
&\quad -\frac{3}{2}\frac{f_c^2+f_t^2}{f_c^2-f_t^2}\Big(h_d^2\Big(V_{cd}^*V_{cd}V_{td}^*V_{td}+V_{cd}^*V_{td}V_{td}^*V_{cd}\Big)\\
&\quad + h_s^2\Big(V_{cd}^*V_{cs}V_{ts}^*V_{td}+V_{cs}^*V_{ts}V_{td}^*V_{cd}\Big)\\
&\quad + h_b^2\Big(V_{cd}^*V_{cb}V_{tb}^*V_{td}+V_{cb}^*V_{tb}V_{td}^*V_{cd}\Big)\Big)\\
&\quad -\frac{3}{2}\frac{h_d^2+h_s^2}{h_d^2-h_s^2}\Big(f_u^2\Big(V_{cd}^*V_{us}^*V_{ud}V_{cs}+V_{us}V_{ud}^*V_{cs}^*V_{cd}\Big)\\
&\quad + f_c^2\Big(V_{cd}^*V_{cs}^*V_{cd}V_{cs}+V_{cs}V_{cd}^*V_{cs}^*V_{cd}\Big)\\
&\quad + f_t^2\Big(V_{cd}^*V_{ts}^*V_{td}V_{cs}+V_{ts}V_{td}^*V_{cs}^*V_{cd}\Big)\Big)\\
&\quad -\frac{3}{2}\frac{h_d^2+h_b^2}{h_d^2-h_b^2}\Big(f_u^2\Big(V_{cd}^*V_{ub}^*V_{ud}V_{cb}+V_{ub}V_{ud}^*V_{cb}^*V_{cd}\Big)\\
&\quad + f_c^2\Big(V_{cd}^*V_{cb}^*V_{cd}V_{cb}+V_{cb}V_{cd}^*V_{cb}^*V_{cd}\Big)\\
&\quad + f_t^2\Big(V_{cd}^*V_{tb}^*V_{td}V_{cb}+V_{tb}V_{td}^*V_{cb}^*V_{cd}\Big)\Big)\ . \qquad (4.69)
\end{aligned}$$

Plugging all ingredients into the above equation, we obtain

$$\begin{aligned}
16\pi^2\frac{dZ}{dt} &= -3\frac{f_c^2+f_u^2}{f_c^2-f_u^2}\Big(\Big(h_d^2-h_b^2\Big)XZ+\frac{h_b^2-h_s^2}{1-X}\Big(XYZ-K\Big)\Big)\\
&\quad -3\frac{f_c^2+f_t^2}{f_c^2-f_t^2}\Big(\frac{h_s^2-h_b^2}{(1-X)^2}\Big(1-X-Z\Big)\Big(XYZ-Z(1-X-Y)\Big)\\
&\quad - K\Big(1-X-2Z\Big)+\Big(h_d^2-h_b^2\Big)Z\Big(1-X-Z\Big)\Big)\\
&\quad -3\frac{h_d^2+h_s^2}{h_d^2-h_s^2}\Big(\frac{f_c^2-f_t^2}{(1-X)^2}Z\Big(XYZ+(1-X-Y)(1-X-Z)-2K\Big)\\
&\quad + \frac{f_u^2-f_t^2}{1-X}\Big(K-XYZ\Big)\Big)\\
&\quad -3\frac{h_d^2+h_b^2}{h_d^2-h_b^2}\Big(\frac{f_c^2-f_t^2}{(1-X)^2}Z\Big(XZ(1-X-Y)+Y(1-X-Z)+2K\Big)\\
&\quad + \frac{f_t^2-f_u^2}{1-X}\Big(XZ(1-X-Y)+K\Big)\Big)\ . \qquad (4.70)
\end{aligned}$$

4.6 Evolution of J

The quantity J is the basis-independent measure of CP violation [68, 73]. Its evolution in the SM is given by

$$16\pi^2 \frac{dJ}{dt} = \frac{3}{4} J \left(\sum_{\alpha, i \neq j} \frac{f_i^2 + f_j^2}{f_i^2 - f_j^2} h_\alpha^2 \left(|V_{i\alpha}|^2 - |V_{j\alpha}|^2 \right) + \sum_{i, \alpha \neq \beta} \frac{h_\alpha^2 + h_\beta^2}{h_\alpha^2 - h_\beta^2} f_i^2 \left(|V_{i\alpha}|^2 - |V_{i\beta}|^2 \right) \right) . \tag{4.71}$$

In SUSY extensions of the SM at least two Higgs doublets are needed, one being coupled to the up quarks and the other one is coupled to down quarks and leptons [73].

The Yukawa couplings run as [67]

$$16\pi^2 \frac{dY_u}{dt} = Y_u \left(T_u - G_u + 3Y_u^\dagger Y_u + Y_d^\dagger Y_d \right) , \tag{4.72}$$

$$16\pi^2 \frac{dY_d}{dt} = Y_d \left(T_d - G_d + 3Y_d^\dagger Y_d + Y_u^\dagger Y_u \right) , \tag{4.73}$$

and

$$16\pi^2 \frac{dY_e}{dt} = Y_e \left(T_e - G_e + 3Y_e^\dagger Y_e \right) , \tag{4.74}$$

where

$$T_u = \mathrm{Tr} \left(3Y_u^\dagger Y_u \right) , \tag{4.75}$$

$$T_d = T_e = \mathrm{Tr} \left(3Y_d^\dagger Y_d + Y_e^\dagger Y_e \right) , \tag{4.76}$$

$$G_u = \frac{13}{15} g_1^2 + 3g_2^2 + \frac{16}{3} g_3^2 , \tag{4.77}$$

$$G_d = \frac{7}{15} g_1^2 + 3g_2^2 + \frac{16}{3} g_3^2 , \tag{4.78}$$

$$G_e = \frac{9}{5} g_1^2 + 3g_2^2 . \tag{4.79}$$

The evolution of physical Yukawa couplings [70, 73] can be written as

$$16\pi^2 \frac{df_i^2}{dt} = f_i^2 \left(2 \left(T_u - G_u \right) + 6f_i^2 + 2 \sum_\alpha h_\alpha^2 |V_{i\alpha}|^2 \right) , \tag{4.80}$$

$$16\pi^2 \frac{dh_\alpha^2}{dt} = h_\alpha^2 \left(2 \left(T_d - G_d \right) + 6h_\alpha^2 + 2 \sum_i f_i^2 |V_{i\alpha}|^2 \right) , \tag{4.81}$$

$$16\pi^2 \frac{dl_a^2}{dt} = l_a^2 \left(2\left(T_e - G_e\right) + 6l_a^2\right) \ . \tag{4.82}$$

The CKM matrix evolution in the MSSM is the same as in the SM except that the coefficients -3 on Eqs.(4.66,4.68, 4.70) are changed to $+2$, and $+\frac{3}{4}$ of Eq. (4.71) is replaced by $-\frac{1}{2}$ [73].

Chapter 5

Evolution of Yukawa Couplings and Quark Flavour Mixings in 5D MSSM

In this chapter we will study the evolution of quark masses and flavour mixings in the 5D MSSM, we derive the RGEs of all observables related to up and down quarks and quark flavour mixings at one-loop level. We qualitatively analyse these quantities in the 5D MSSM with small, intermediate, and large $\tan\beta$.

5.1 Introduction

A theory of fermion masses and the associated mixing angles provide an interesting puzzle and a likely window to physics BSM, where one of the main issues in particle physics is to understand the fermion mass hierarchy and mixings as stated in section 2.4. A clear feature of the fermion mass spectrum is [71]

$$m_u \ll m_c \ll m_t \ , \ m_d \ll m_s \ll m_b \ , \ m_e \ll m_\mu \ll m_\tau \ . \tag{5.1}$$

There have been many attempts to understand the fermion mass hierarchies and their mixings by making use of RGEs especially for UED models and their possible extensions (see Refs. [53, 56] and references therein).

Recall that in extra-dimensional scenarios we are lead to a power law running of the gauge couplings due to the large number of KK states. These KK modes contribute the same way as the zeroth mode does, which we identify as the usual 4D MSSM particles. In 5-dimensions, though, only Dirac fermions are allowed by the Lorentz algebra. As such there are eight supercharges which correspond to the 4D view point of an $\mathcal{N} = 2$ supersymmetry, where the S^1/Z_2 orbifolding present in our UED models [53] will break the $\mathcal{N} = 1$ SUSY, for more details see Refs. [52, 54]. We briefly discuss the 5D MSSM in the next section and more details can be found in Appendix D.

5.2 The 5D MSSM models

In the 5D MSSM, the Higgs superfields and gauge superfields always propagate in the fifth dimension. However, different possibilities of localisation for the matter superfields can be studied. We shall consider the two limiting cases of superfields with SM matter fields all in the bulk or all superfields containing SM matter fields restricted to the brane. When all fields propagate in the bulk, the action for the matter fields Φ_i is [52, 53]:

$$\begin{aligned} S_{matter} &= \int d^8z dx_5 \left[\bar{\Phi}_i\Phi_i + \Phi_i^c\bar{\Phi}_i^c + \Phi_i^c\partial_5\Phi_i\delta(\bar{\theta}) - \bar{\Phi}_i\partial_5\bar{\Phi}_i^c\delta(\theta)\right. \\ &\quad \left. +\tilde{g}(2\bar{\Phi}_iV\Phi_i - 2\Phi_i^cV\bar{\Phi}_i^c + \Phi_i^c\chi\Phi_i\delta(\bar{\theta}) + \bar{\Phi}_i\bar{\chi}\bar{\Phi}_i^c\delta(\theta))\right] \end{aligned} \quad (5.2)$$

Similarly, when all superfields containing SM fermions are restricted to the brane, the part of the action involving only gauge and Higgs fields is not modified, whereas the action for the superfields containing the SM fermions becomes:

$$S_{matter} = \int d^8z dx_5\delta(y)\left[\bar{\Phi}_i\Phi_i + 2\tilde{g}\bar{\Phi}_iV\Phi_i\right] . \quad (5.3)$$

For $\mathcal{N} = 1$ 4D SUSY, the superfield formalism is well established: superfields describe quantum fields and their superpartners, as well as auxiliary fields as a single object. This simplifies the notation and the calculation considerably. A similar formulation for a 5D vector superfield and the superfield formulation for matter supermultiplets has been developed in Ref. [54]. Note that in our model the Yukawa couplings in the bulk are forbidden by the 5D $\mathcal{N} = 1$ SUSY. However, they can be introduced on the branes, which are 4D subspaces with reduced SUSY. We will write the following interaction terms, called brane interactions, containing Yukawa-type couplings:

$$S_{brane} = \int d^8z dx_5\delta(x^5)\left(\frac{1}{6}\tilde{\lambda}_{ijk}\Phi_i\Phi_j\Phi_k\right)\delta(\bar{\theta}) + h.c. . \quad (5.4)$$

In 4D MSSM, the one-loop correction to the gauge couplings [70] are given by

$$16\pi^2\frac{dg_i}{dt} = b_ig_i^3 , \quad (5.5)$$

where $b_i = (\frac{33}{5}, 1, -3)$, $t = \ln(\mu/M_Z)$, and M_Z is the Z boson mass [72].

In 5D MSSM, the one-loop corrections to gauge couplings are given by [53, 60]

$$16\pi^2\frac{dg_i}{dt} = (b_i + (S(t) - 1)\tilde{b_i})g_i^3 , \quad (5.6)$$

where $S(t) = e^tM_ZR$ is the number of KK states, $\tilde{b_i} = (\frac{66}{5}, 10, 6)$ for matter fields in the bulk and $\tilde{b_i} = (\frac{6}{5}, -2, -6)$ for matter fields localised to the brane (for more details about the calculations of b_i and $\tilde{b_i}$ see appendix A). As can be seen in Fig. 5.1 (and Eq. (5.6)), the one-loop running of the gauge

Table 5.1: *The terms present in the various Yukawa evolution equations, see Eq.(5.7).*

Scenarios	G_u	G_d	G_e
Bulk	$\frac{13}{15}g_1^2 + 3g_2^2 + \frac{16}{3}g_3^2$	$\frac{7}{15}g_1^2 + 3g_2^2 + \frac{16}{3}g_3^2$	$\frac{9}{5}g_1^2 + 3g_2^2$
Brane	$\frac{43}{30}g_1^2 + \frac{9}{2}g_2^2 + \frac{32}{3}g_3^2$	$\frac{19}{30}g_1^2 + \frac{9}{2}g_2^2 + \frac{32}{3}g_3^2$	$\frac{33}{10}g_1^2 + \frac{9}{2}g_2^2$
Scenarios	$T_d = T_e$	T_u	
Bulk	$(3Tr(Y_d^\dagger Y_d) + Tr(Y_e^\dagger Y_e))\pi S^2(t)$	$3Tr(Y_u^\dagger Y_u)\pi S^2(t)$	
Brane	$3Tr(Y_d^\dagger Y_d) + Tr(Y_e^\dagger Y_e)$	$3Tr(Y_u^\dagger Y_u)$	
Scenarios	F_u	F_d	F_e
Bulk	$(3Y_u^\dagger Y_u + Y_d^\dagger Y_d)\pi S^2(t)$	$(3Y_d^\dagger Y_d + Y_u^\dagger Y_u)\pi S^2(t)$	$(3Y_e^\dagger Y_e)\pi S^2(t)$
Brane	$(6Y_u^\dagger Y_u + 2Y_d^\dagger Y_d)S(t)$	$(6Y_d^\dagger Y_d + 2Y_u^\dagger Y_u)S(t)$	$6Y_e^\dagger Y_e S(t)$

couplings changes with energy scale drastically and lowers the unification scale considerably. Specifically for the compactification radii $R^{-1} = 1$, 4, 15 TeV respectively. As such, the Yukawa couplings also receive finite corrections at each KK level, whose magnitudes depend on the cutoff energy scale. The evolution of the Yukawa couplings were derived using the standard techniques of Refs. [52, 53]. As such, the one-loop RGEs for Yukawa couplings in the 5D MSSM are:

$$16\pi^2 \frac{dY_i}{dt} = Y_i \left[T_i - G_i S(t) + F_i\right] \ , \tag{5.7}$$

where $i = u, d, e$ and the values of G_i, F_i and T_i are given in table 5.1. That is, when the energy scale $\mu > \frac{1}{R}$, or when the energy scale parameter $t > \ln(\frac{1}{M_Z R})$ (where we have set M_Z as the renormalization point) we shall use Eq.(5.7). However, when the energy scale $M_Z < \mu < \frac{1}{R}$, the Yukawa evolution equations are dictated by the usual MSSM ones [70, 72].

We shall follow the same procedure presented in section 4.2. Recall that the Yukawa coupling matrices can be diagonalised by using two unitary matrices U and V, where

$$UY_u^\dagger Y_u U^\dagger = diag(f_u^2, f_c^2, f_t^2) \ , \ VY_d^\dagger Y_d V^\dagger = diag(h_d^2, h_s^2, h_b^2) \ .$$

The CKM matrix appears as a result (upon this diagonalisation of quark mass matrices) of $V_{CKM} = UV^\dagger$. The variation of the CKM matrix and its evolution

equation for all matter fields in the bulk is [56, 63, 73]:

$$16\pi^2 \frac{dV_{i\alpha}}{dt} = \pi S^2 \left[\sum_{\beta, j\neq i} \frac{f_i^2 + f_j^2}{f_i^2 - f_j^2} h_\beta^2 V_{i\beta} V_{j\beta}^* V_{j\alpha} + \sum_{j,\beta\neq\alpha} \frac{h_\alpha^2 + h_\beta^2}{h_\alpha^2 - h_\beta^2} f_j^2 V_{j\beta}^* V_{j\alpha} V_{i\beta} \right] . \tag{5.8}$$

For all matter fields on the brane, the CKM evolution is the same as Eq.(5.8) but πS^2 is replaced by 2 S.

In making use of these equations for this current work, we recall that in the 4D MSSM the particle spectrum contains two Higgs doublets and the supersymmetric partners to the SM fields. After the spontaneous symmetry breaking of the electroweak symmetry, five physical Higgs particles are left in the spectrum. The two Higgs doublets H_u and H_d, with opposite hypercharges, are responsible for the generation of the up-type and down-type quark masses respectively. The VEVs of the neutral components of the two Higgs fields satisfy the relation $v_u^2 + v_d^2 = (\frac{246}{\sqrt{2}})^2 = (174GeV)^2$. The fermion mass matrices appear after the spontaneous symmetry breaking from the fermion-Higgs-Yukawa couplings. As a result, the initial Yukawa couplings are given by the ratios of the fermion masses to the appropriate Higgs VEV as follows:

$$f_{u,c,t} = \frac{m_{u,c,t}}{v_u} \ , \ h_{d,s,b} = \frac{m_{d,s,b}}{v_d} \ , \ y_{e,\mu,\tau} = \frac{m_{e,\mu,\tau}}{v_d} \ , \tag{5.9}$$

where we define $\tan\beta = \frac{v_u}{v_d}$, which is the ratio of VEVss of the two Higgs fields H_u and H_d.

5.3 Numerical Results and Discussions

For our numerical calculations we assume the fundamental scale is not far from the range of the LHC and set the compatification radii to be $R^{-1} = 1$ TeV, 4 TeV and 15 TeV. Only some selected plots will be shown and we will comment on the other similar cases not explicitly presented. We quantitatively analyse these quantities in the 5D MSSM with small, intermediate, and large $\tan\beta$, though we observed similar behaviours for all values of $\tan\beta$; the initial values we shall adopt at the M_Z scale are presented in Table E.1

As illustrated in Figs. 5.2 and 5.3 the mass ratios evolve in the usual logarithmic fashion when the energies are below 1 TeV, 4 TeV and 15 TeV respectively. However, once the first KK threshold is reached the contributions from the KK states become increasingly significant and the effective 4D MSSM couplings begin to deviate from their normal trajectories. They evolve faster and faster after that point, their evolution diverging due to the faster running of the gauge couplings, where in approaching our cutoff for the effective theory, Λ, any new physics would then come into play, see Fig.5.1. As such, we have chosen cutoffs for our effective theory; for the bulk case, where g_3 becomes large (and perturbation theory breaks down), and for the brane case, where $g_2 = g_3$ (and an expected mechanism for unification would take over). Therefore, the one-loop running of the gauge couplings changes with energy scale

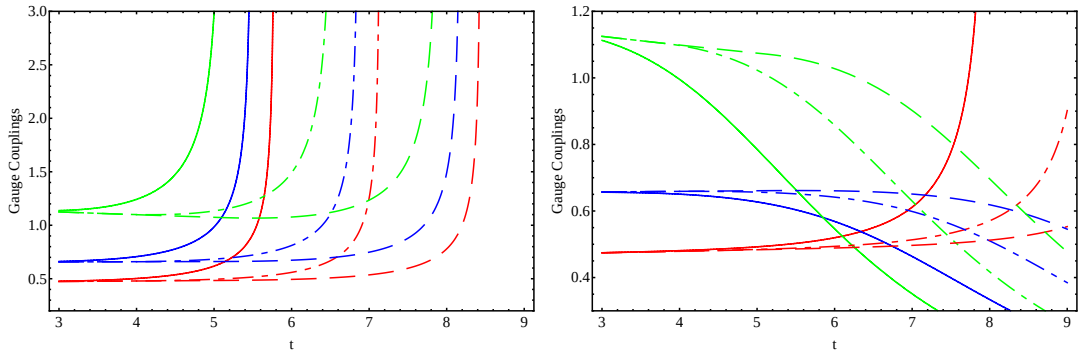


Figure 5.1: *Gauge couplings (g_1 (red), g_2 (blue), g_3 (green) with: in the left panel, all matter fields in the bulk; and the right panel for all matter fields on the brane; for three different values of the compactification scales (1 TeV (solid line), 4 TeV (dot-dashed line), 15 TeV (dashed line))) as a function of the scale parameter t.*

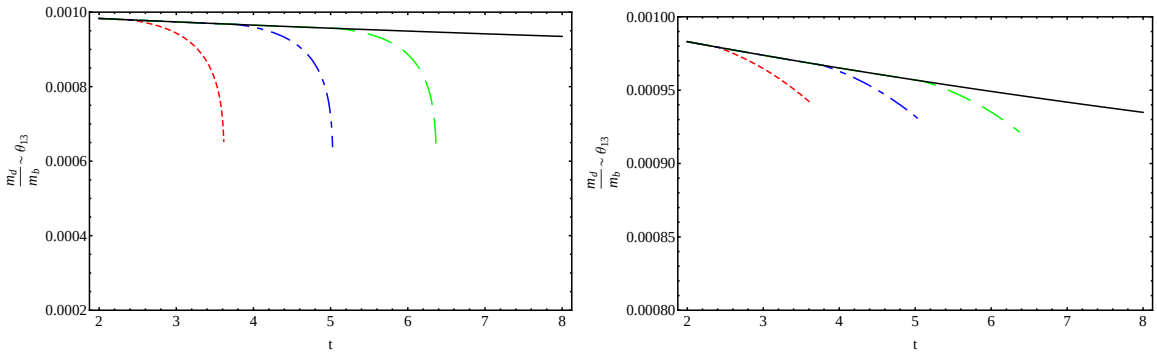


Figure 5.2: *Evolution of the mass ratio $\frac{m_d}{m_b}$, with: in the left panel, all matter fields in the bulk; and the right panel for all matter fields on the brane. Three different values of the compactification raduis have been used 1 TeV (dotted red line), 4 TeV (dot-dashed blue line), 15 TeV (dashed green line), all as a function of the scale parameter t.*

drastically and lowers the unification scale considerably. Specifically, for the compactification radii $R^{-1} = 1$, 4, 15 TeV, we find that for the brane localised matter fields case the cut-off $\Lambda \approx 30$, 120, 430 TeV respectively. For the bulk case the cut-off is around $\Lambda \approx 6$, 30, 70 TeV respectively.

On the other hand, in $SU(5)$ theory we have $m_d = m_e$, $m_s = m_\mu$ and $m_b = m_\tau$ at the unification scale, where in the 5D MSSM, due to power law running of the Yukawa couplings, the renormalization effects on these relations can be large for m_d/m_e and m_s/m_μ, for both scenarios see Figs. 5.4 and 5.5. We have shown, by numerical analysis of the one loop calculation, that the mass ratios m_d/m_e, m_s/m_μ and m_b/m_τ decrease as energy increases. However, m_b/m_τ for matter fields in the bulk increases as energy increases, see Fig. 5.6

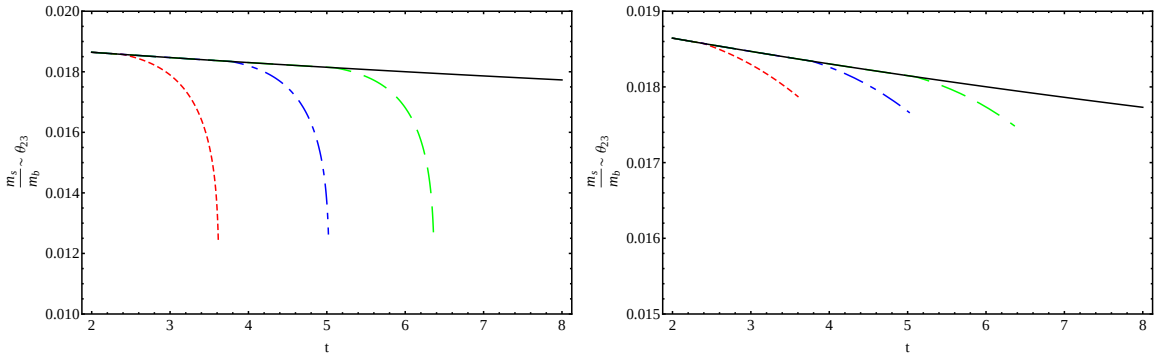


Figure 5.3: *Evolution of mass ratio* $\frac{m_s}{m_b}$*, with the same notations as Fig.5.2.*

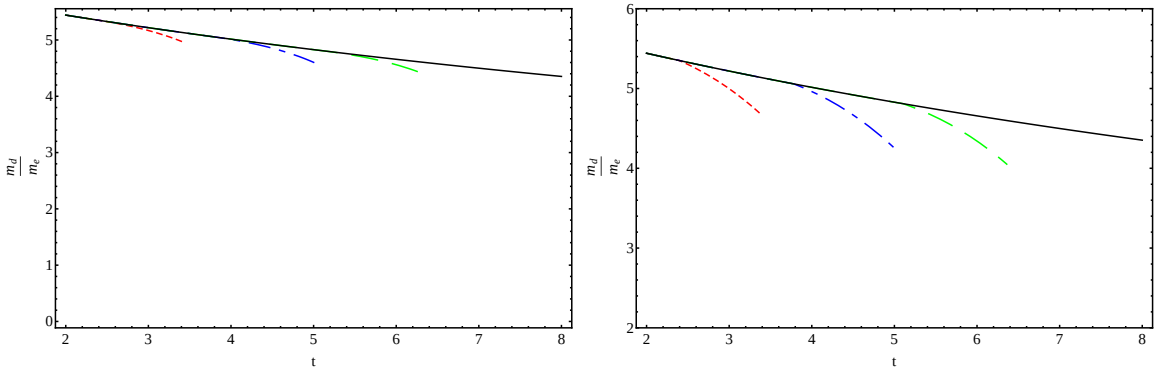


Figure 5.4: *Evolution of mass ratio* $\frac{m_d}{m_e}$*, with the same notations as Fig.5.2.*

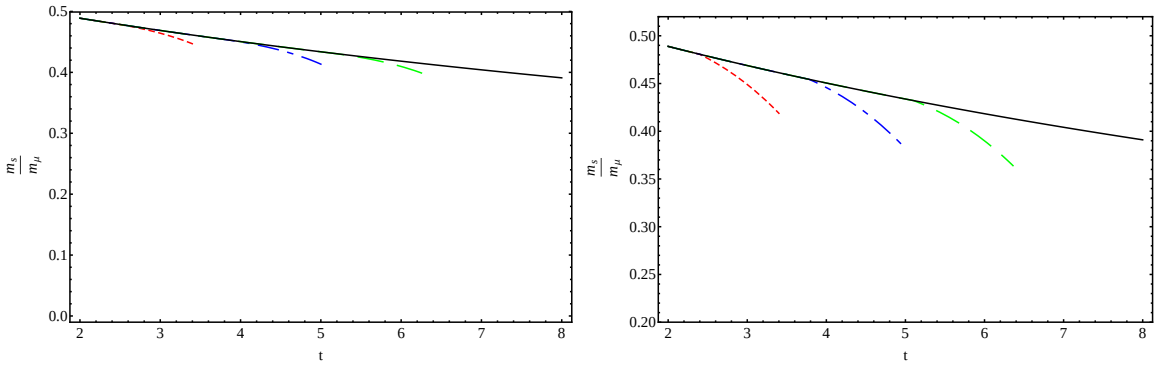


Figure 5.5: *Evolution of mass ratio* $\frac{m_s}{m_\mu}$*, with the same notations as Fig.5.2.*

left panel.

As depicted in Fig. 5.6, for the third generation the mass ratios increase rapidly as one crosses the KK threshold at $\mu = R^{-1}$ for the bulk case, resulting in a rapid approach to a singularity before the unification scale is reached. For

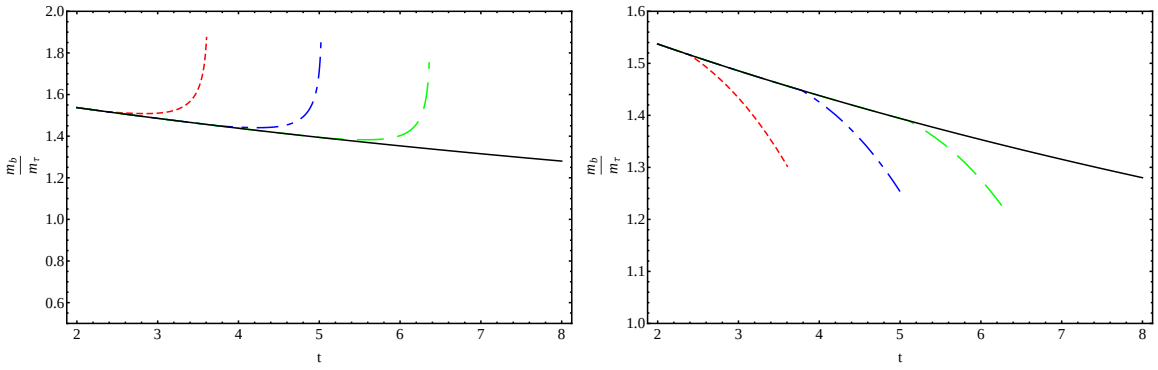


Figure 5.6: *Evolution of mass ratio* $\frac{m_b}{m_\tau}$*, with the same notations as Fig.5.2.*

the brane localised case the contribution from the gauge couplings may become significant, therefore the trajectory might change direction, and the mass ratios decrease instead of increasing.

Chapter 6

Evolution of Yukawa Couplings and Quark Flavour Mixings in 2UED models

In this chapter we qualitatively explore the complete set of RGEs for the Yukawa couplings and quark flavour mixings in six-dimensional models. In these UED models we examine the contribution of KK particle states to the RGEs, i.e, gauge couplings, Yukawa couplings and CKM matrix elements. In particular we look at the one-loop corrections of the gauge and Yukawa couplings for the quark sector, as well as various flavour observables, by considering different possibilities for the matter fields (either they are propagating in the bulk or localized to the brane). We then investigate the consequences of the UED models and perform a qualitative study of the behaviour of different observables. We also compare the one-loop correction to the observables in the 1UED with 2UED cases. From the phenomenological point of view, in the 2UED case, the KK mass spectrum is not equally-spaced as in 1UED, up to radiative corrections, this would have impacts on collider physics signatures.

6.1 The 2UED SM

In generic models with two universal extra dimensions, where all the SM fields (or some subset) propagate universally in 6D space-time, the space-time coordinate $x_\mu(\mu = 1, 2, 3, 4)$ denotes the usual Minkowski space, and the two extra spatial dimension coordinates x_5 and x_6 are compactified. For simplicity we will refer here to the flat extra dimensional notation, however, for the purpose of computing renormalisation evolution equations, we will later consider also the case of a curved orbifold (the sphere S^2 and related orbifolds). We shall follow the setup given in section 3.2.

6.1.1 Fermions

The spinor dimension of a fermion Ψ in 6 dimensions is minimally 8 (contrary to 4 minimal components in 4 and 5 dimensions): the Clifford algebra contains six 8×8 gamma matrices $\Gamma^1 \dots \Gamma^6$. Moreover, one can define

$$\Gamma^7 = \Gamma^1\Gamma^2\Gamma^3\Gamma^4\Gamma^5\Gamma^6 \,, \tag{6.1}$$

and it is possible to define two 6D chiralities

$$P_\pm = \frac{1}{2}\left(1 \pm \Gamma^7\right) \,. \tag{6.2}$$

The minimal spinor representation of the Lorentz group are 4-component chiral fermions $\Psi_\pm = P_\pm \Psi$. Each of the 6D-chiral fields contains two four dimensional Weyl fermions of opposite 4D-chirality. Such considerations are quite general and apply to different models (see for example Refs. [14,17] for a more detailed discussion of the formalism).

For example, in the case of two flat extra dimensions, the Lagrangian for fermions reads

$$\begin{aligned} \mathcal{L}_{Fermions} &= \int dx_5 \int dx_6 \, \left\{ i\bar{\psi}_\pm \Gamma^M \partial_M \psi_\pm \right\} \\ &= \int dx_5 \int dx_6 \, i \left\{ \bar{\psi}_{\pm L}\Gamma^\mu \partial_\mu \psi_{\pm L} + \bar{\psi}_{\pm R}\Gamma^\mu \partial_\mu \psi_{\pm R} \right. \\ &\quad \left. + \bar{\psi}_{\pm L}\Gamma^\pm \partial_\mp \psi_{\pm R} + \bar{\psi}_{\pm R}\Gamma^\mp \partial_\pm \psi_{\pm L} \right\} \,, \end{aligned} \tag{6.3}$$

where $\Gamma^\pm = \frac{1}{2}(\Gamma^5 \pm i\Gamma^6)$ and $\partial_\pm = \partial_5 \pm i\partial_6$. The way in which 4D chiral zero modes describing the SM fermions are obtained differs in different models. Most often a quotient of the original symmetry group by a discrete Z_2 symmetry is necessary, to eliminate one 4D degree of freedom and to allow a 4D chiral fermion [13], but it can also be obtained directly from the properties of the orbifold as in Ref. [17]. Higher massive modes are vector-like fermions.

6.1.2 Scalars

The Lagrangian for a scalar field Φ is

$$\mathcal{L}_{Scalars} = \int dx_5 \int dx_6 \left\{ \partial_\alpha \Phi^\dagger \partial^\alpha \Phi - M^2 \Phi^\dagger \Phi \right\} , \tag{6.4}$$

where $\alpha = 1, \dots 6$ and the corresponding equations of motion are

$$\left(\partial_5^2 + \partial_6^2 + p^2 - M^2\right) \Phi = 0 \,, \tag{6.5}$$

where $p^2 = -\partial_\mu \partial^\mu$. After Fourier decomposition along the extra coordinates, the fields can be written as a sum of KK modes. The wave functions satisfy the above equation with p^2 replaced by the mass squared of the mode. The

solutions of this equation are usually combinations of sines and cosines (with frequencies determined by the periodicity) in flat extra dimensions, while in the case of the 2-sphere inspired orbifolds the solutions are the spherical harmonics. The masses are given by the formula

$$m_{k,l}^2 = M^2 + k^2 + l^2 \,, \tag{6.6}$$

and the mass eigenstates can be labeled by their parity assignment with respect to the generators of the symmetry group of the orbifold and by the KK numbers (k, l).

6.1.3 Gauge bosons

The Lagrangian for an Abelian gauge field (also for non-Abelian gauge symmetries at quadratic level) is

$$\begin{aligned} \mathcal{L}_{Gauge+GF} &= \int dx_5 \int dx_6 \, \left[-\frac{1}{4} F^{\alpha\beta} F_{\alpha\beta} \right. \\ &\quad \left. - \frac{1}{2\xi} [\partial_\mu A^\mu - \xi(\partial_5 A_5 + \partial_6 A_6)]^2 \right] \,, \end{aligned} \tag{6.7}$$

where ξ is the gauge fixing parameter, and $F_{\alpha\beta} = \partial_\alpha A_\beta - \partial_\beta A_\alpha$. The gauge fixing term eliminates the mixing between A_μ and the extra polarization A_5 and A_6. Once the parities are assigned, the spectrum and wave functions will be the same as for the scalar field (without a mass term):

$$m_{k,l}^2 = k^2 + l^2 \,. \tag{6.8}$$

In the Feynman-'t Hooft gauge $\xi = 1$, the equations of motion for A_5 and A_6 decouple from the rest:

$$(\partial_5^2 + \partial_6^2 - \partial_\mu^2) A_{5,6} = 0 \,, \tag{6.9}$$

where the two extra-components of the gauge field can be treated as two independent scalar fields. Spectra and wave functions are again similar to the scalar case, with some additional constraints. Therefore each of the gauge fields has six components [14] and decomposes into towers of 4D spin-1 fields and two towers of real scalars belonging to the adjoint representation. The phenomenology of these spinless adjoints has been investigated in detail in Ref. [49].

6.1.4 Yukawa interactions

Yukawa interactions are built in the usual way in terms of 6D fields:

$$\mathcal{L}_{Yukawa} = \int dx_5 \int dx_6 \, Y^{ab} \left\{ i \bar{\psi}^a_{\pm R} \phi \psi^b_{\mp L} \right\} \,. \tag{6.10}$$

Any 6D field (fermion/gauge or scalar) $\Phi(x^\mu, x^5, x^6)$ can be decomposed as:

$$\Phi(x^\mu, x^5, x^6) = \frac{1}{L}\sum_{j,k} f^{(j,k)}(x^5, x^6)\phi^{(j,k)}(x^\mu) \,, \tag{6.11}$$

where in the flat case $f^{(j,k)}(x^5, x^6)$ is given by Eq. (3.64).

Note that the 4D fields $\phi^{(j,k)}(x^\mu)$ are the $(j,k)^{th}$ KK modes of the 6D fields $\Phi(x^M)$. These Yukawa interactions will give rise to the usual SM Yukawa interactions plus those related to the towers of KK states.

6.1.5 Model dependence of the spectra

In general a fixed value of the KK numbers (k, l) will correspond to a tier of states (including scalars, but also fermions and gauge bosons) and for each type of particle there will be more than one state (corresponding to the different possible parities of the orbifold). However, not all the possible states will be present, as some states may not be possible due to symmetry constraints and boundary conditions. Indeed, looking to the typical spectra of the 2UED models we listed in the introduction, one can check that this is the case only if at least one of the two KK numbers (k, l) is equal to zero, while the higher tiers with require the $k, l \neq 0$ states be fully populated. This is an important observation for the calculation of the RGE, as the fact that only a few of the first KK modes are absent (and which ones depends on the model) has little effect on the numerical results, thus reducing considerably the model dependence of the evolution equations, as we shall see in more detail in the following (see Appendix C also).

6.2 Gauge couplings evolution

Armed now with our 2UED model we derive the gauge coupling RGEs, where our results agree with Refs. [82, 83] for all matter fields propagating in the bulk. Apart from the SM field contributions, there will be new contributions from the spinless adjoints $A_H^{(j,k)}$, where the calculation is similar to that of the 5D UED model but with an additional factor of 2 due to the 6D gauge field having two extra dimensional components. Note that for the case of all matter fields being restricted to the brane there will be no contributions from the KK excited states of the fermions. The generic structure of the one-loop RGEs for the gauge couplings is then given by:

$$16\pi^2 \frac{dg_i}{dt} = b_i^{SM} g_i^3 + \pi \left(S(t)^2 - 1\right) b_i^{6D} g_i^3 \,, \tag{6.12}$$

where $t = \ln(\frac{\mu}{M_Z})$, $S(t) = e^t M_Z R$, or $S(\mu) = \mu R = \frac{\mu}{M_{KK}}$ for $M_Z < \mu < \Lambda$ (Λ is the cut-off scale as shall be discussed in more detail in section 6.4). More

details about the calculation of the $S^2(t)$ factor can be found in Appendix C. The numerical coefficients appearing in equation (6.12) are given by:

$$b_i^{SM} = \left[\frac{41}{10}, -\frac{19}{6}, -7\right] \ , \tag{6.13}$$

and

$$b_i^{6D} = \left[\frac{1}{10}, -\frac{13}{2}, -10\right] + \left[\frac{8}{3}, \frac{8}{3}, \frac{8}{3}\right] \eta \ , \tag{6.14}$$

η being the number of generations of fermions propagating in the bulk. In the two cases we shall consider, that of all fields propagating in the bulk ($\eta = 3$) we have [53]:

$$b_i^{6D} = \left[\frac{81}{10}, \frac{3}{2}, -2\right] \ . \tag{6.15}$$

Similarly, for all matter fields localized to the brane ($\eta = 0$) we have:

$$b_i^{6D} = \left[\frac{1}{10}, -\frac{13}{2}, -10\right] \ . \tag{6.16}$$

In appendix A a sample calculation of the numerical coefficient of the gauge couplings for various models is presented from the SM all the way to 2UED models.

We present in Fig.6.1 the evolution of the bulk field and brane localized cases for several choices of compactification scale for the extra-dimensions in the 2UED model. We find that there is a difference in the g_2 evolution, where it increases in the bulk propagating case and decreases in the brane localized case. We also see that the three gauge coupling constants, as expected in extra-dimensional theories, can unify at some value of t depending on the radius of compactification. As an example, for 1 TeV we see an approximation unification at $t = 4$.

In Fig.6.2 we show for comparison the gauge couplings between the 1UED and 2UED cases for a compactification scale of 2 TeV. From the plots and the discussion in Ref. [72], we see that in both cases the gauge couplings have a similar behaviour, however, in the 2UED case we have asymptotes at lower t values, that is, a lower energy scale. As such the range of validity for the 2UED is less than the 1UED case, this being due to the $S^2(t)$ factor present in Eq.(6.12), there only being a linear dependence on $S(t)$ for the 1UED case. The solid line (which corresponds to the 2UED case) drops off faster than the dashed line (1UED case) when the gauge couplings decrease with energy scale. For the g_1 coupling, it increases faster than in the 2UED case (at $t \sim 6$) with a roughly constant evolution in the 1UED case. As such one can see in the brane case a large difference in the evolution of this coupling, a feature which can distinguish these two models.

In Fig.6.3 we present the evolution of $\sin^2\theta_W$ in the 2UED for the bulk and brane cases. Once the KK states begin to contribute the new contributions from the extra-dimensions change the behaviour, that is, it increases until we

reach the cut-off scale. One can see that for $R^{-1} = 1$ TeV $\sin^2\theta_W$ can rise to ~ 0.4. This result may be useful, at least from a model building perspective, as many extra-dimensional models (such as gauge-Higgs unification models in two extra dimensions, see for example Ref. [84]) predict, for many choices of the gauge group, large values of $\sin^2\theta_W$ from a group theory point of view. However, this value is the one expected in the energy range of coupling unification, which once evolved back to the electroweak scale may indeed be close or compatible to the measured value.

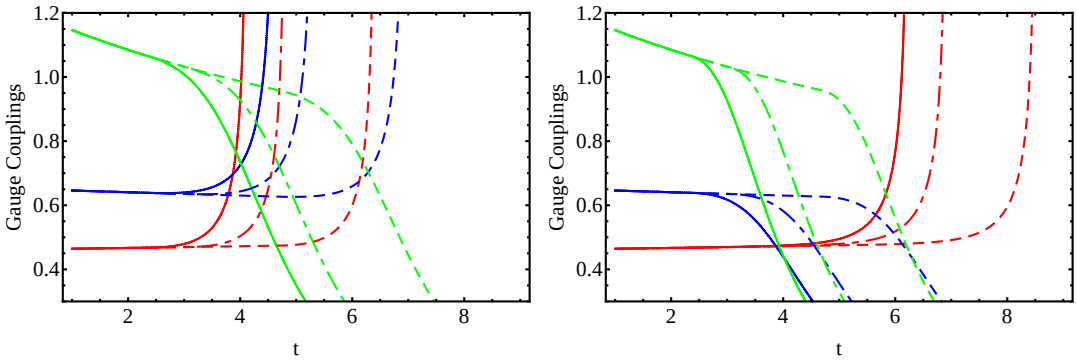


Figure 6.1: *The evolution of gauge couplings g_1 (red), g_2 (blue) and g_3 (green), with: in the left panel, all matter fields in the bulk; and the right panel for all matter fields on the brane; for three different values of the compactification scales 1 TeV (solid line), 2 TeV (dot-dashed line) and 10 TeV (dashed line), as a function of the scale parameter t.*

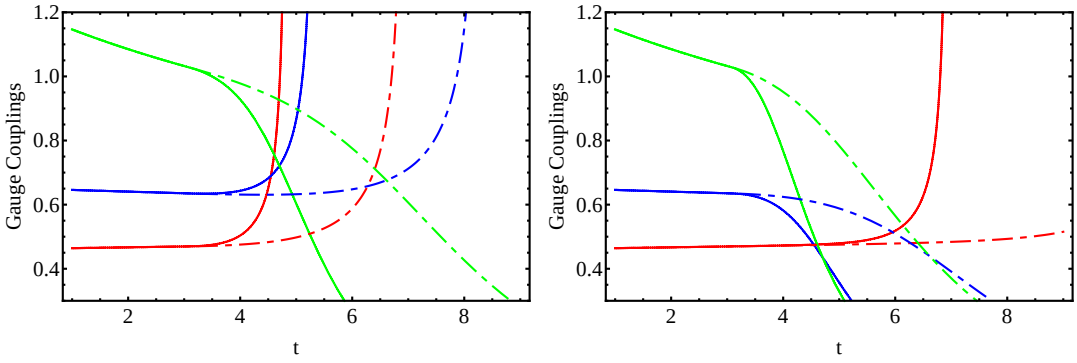


Figure 6.2: *Comparison of the gauge coupling evolutions g_1 (red), g_2 (blue), g_3 (green) between the 1UED case (dashed line) and the 2UED case (solid line) with: in the left panel, all matter fields in the bulk; and the right panel for all matter fields on the brane; for a compactification scale of 2 TeV as a function of the scale parameter t.*

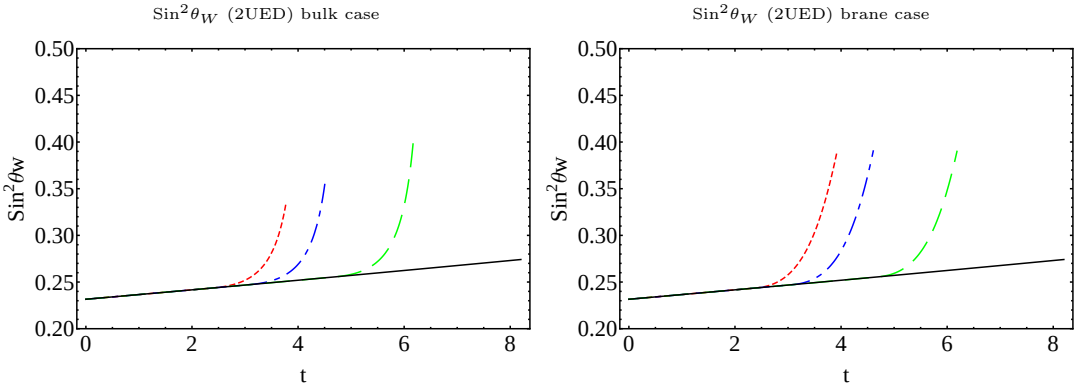


Figure 6.3: *The evolution of the Weinberg angle ($sin^2\theta_W$) where the solid line represents the SM case with: in the left panel, all matter fields in the bulk; and the right panel for all matter fields on the brane; for three different values of the compactification scales 1 TeV (solid line) with the first KK threshold at $t = 2.394$, 2 TeV (dot-dashed line) with the first KK threshold at $t = 3.0879$ and 10 TeV (dashed line) with the first KK threshold at $t = 4.697$, as a function of the scale parameter t.*

6.3 Beta functions of the Yukawa couplings and CKM matrix elements in 1UED and 2UED models

In the 1UED and 2UED models the β-function for the Yukawa couplings can be written as:

$$16\pi^2 \frac{dY_i}{dt} = \beta_i^{SM} + \beta_i^{5,6D} , \quad \text{for } i = u, d, e, \tag{6.17}$$

where β_i^{SM} is the SM contribution, and can be found in Refs. [56, 72]. The $\beta_i^{5,6D}$ are the contributions from the excited KK modes and $S(t)$ is the number of KK levels that fulfills the inequality $1 \leq j^2 + k^2 \leq (\frac{\mu}{M_{KK}})^2$ in this general 2UED model. Recall that μ is the energy scale and $M_{KK} = R^{-1}$ is the energy for which the first KK mode is generated. Detailed calculations of β_i^{6D} can be found in Appendix B.

6.3.1 Bulk 1UED case

For all matter fields propagating in the bulk, the Yukawa coupling RGEs take the following forms:

$$\beta_u^{5D} = (S(t)-1)Y_u\left[-\frac{28}{3}g_3^2-\frac{15}{8}g_2^2-\frac{101}{120}g_1^2+\frac{3}{2}(Y_u^\dagger Y_u-Y_d^\dagger Y_d)\right.$$
$$\left.+2Tr(3Y_u^\dagger Y_u+3Y_d^\dagger Y_d+Y_e^\dagger Y_e)\right], \qquad (6.18)$$

$$\beta_d^{5D} = (S(t)-1)Y_d\left[-\frac{28}{3}g_3^2-\frac{15}{8}g_2^2-\frac{17}{120}g_1^2+\frac{3}{2}(Y_d^\dagger Y_d-Y_u^\dagger Y_u)\right.$$
$$\left.+2Tr(3Y_u^\dagger Y_u+3Y_d^\dagger Y_d+Y_e^\dagger Y_e)\right], \qquad (6.19)$$

$$\beta_e^{5D} = (S(t)-1)Y_e\left[-\frac{15}{8}g_2^2-\frac{99}{40}g_1^2+\frac{3}{2}Y_e^\dagger Y_e\right.$$
$$\left.+2Tr(3Y_u^\dagger Y_u+3Y_d^\dagger Y_d+Y_e^\dagger Y_e)\right]. \qquad (6.20)$$

6.3.2 Bulk 2UED case

For all matter fields propagating in the bulk, we get:

$$\beta_u^{6D} = \pi(S(t)^2-1)Y_u\left[-\frac{32}{3}g_3^2-\frac{3}{2}g_2^2-\frac{5}{6}g_1^2+3(Y_u^\dagger Y_u-Y_d^\dagger Y_d)\right.$$
$$\left.+2Tr(3Y_u^\dagger Y_u+3Y_d^\dagger Y_d+Y_e^\dagger Y_e)\right], \qquad (6.21)$$

$$\beta_d^{6D} = \pi(S(t)^2-1)Y_d\left[-\frac{32}{3}g_3^2-\frac{3}{2}g_2^2-\frac{1}{30}g_1^2+3(Y_d^\dagger Y_d-Y_u^\dagger Y_u)\right.$$
$$\left.+2Tr(3Y_u^\dagger Y_u+3Y_d^\dagger Y_d+Y_e^\dagger Y_e)\right], \qquad (6.22)$$

$$\beta_e^{6D} = \pi(S(t)^2-1)Y_e\left[-\frac{3}{2}g_2^2-\frac{27}{10}g_1^2+3Y_e^\dagger Y_e\right.$$
$$\left.+2Tr(3Y_u^\dagger Y_u+3Y_d^\dagger Y_d+Y_e^\dagger Y_e)\right]. \qquad (6.23)$$

Note that the coupling constant g_1 is chosen to follow the conventional $SU(5)$ normalisation.

According to the discussion of section 4.2, these Yukawa coupling matrices can be diagonalized by using two unitary matrices U and V, where

$$UY_u^\dagger Y_u U^\dagger = \mathrm{diag}(f_u^2, f_c^2, f_t^2)\,, \qquad VY_d^\dagger Y_d V^\dagger = \mathrm{diag}(h_d^2, h_s^2, h_b^2)\,, \qquad (6.24)$$

in which f_u^2, f_c^2, f_t^2 and h_d^2, h_s^2, h_b^2 are the eigenvalues of $Y_u^\dagger Y_u$ and $Y_d^\dagger Y_d$ respec-

tively. As such we obtain the following two relations:

$$\begin{aligned}
16\pi^2\frac{df_i^2}{dt} &= f_i^2\Bigg[2\left(2\pi(S(t)^2-1)+1\right)T-2G_u+6\left(\pi(S(t)^2-1)+1\right)f_i^2 \\
&\qquad -6\left(\pi(S(t)^2-1)+1\right)\sum_j h_j^2|V_{ij}|^2\Bigg]\,, \\
16\pi^2\frac{dh_j^2}{dt} &= h_j^2\Bigg[2\left(2\pi(S(t)^2-1)+1\right)T-2G_d+6\left(\pi(S(t)^2-1)+1\right)h_i^2 \\
&\qquad -6\left(\pi(S(t)^2-1)+1\right)\sum_i f_i^2|V_{ij}|^2\Bigg]\,, \qquad (6.25)
\end{aligned}$$

where $i=(u,c,t)$ and $j=(d,s,b)$. Similarly the variation of the lepton Yukawa couplings y_a^2 $(a=e,\mu,\tau)$ is

$$16\pi^2\frac{dy_a^2}{dt}=y_a^2\left[2\left(2\pi(S(t)^2-1)+1\right)T-2G_e+6\left(\pi(S(t)^2-1)+1\right)y_a^2\right] \qquad (6.26)$$

In Eqs.(6.25, 6.26) we have used the following expressions:

$$\begin{aligned}
G_u &= 8g_3^2+\frac{9}{4}g_2^2+\frac{17}{20}g_1^2+\pi\left(S(t)^2-1\right)\left(\frac{32}{3}g_3^2+\frac{3}{2}g_2^2+\frac{5}{6}g_1^2\right)\,, \\
G_d &= 8g_3^2+\frac{9}{4}g_2^2+\frac{1}{4}g_1^2+\pi\left(S(t)^2-1\right)\left(\frac{32}{3}g_3^2+\frac{3}{2}g_2^2+\frac{1}{30}g_1^2\right)\,, \\
G_e &= \frac{9}{4}g_2^2+\frac{9}{4}g_1^2+\pi\left(S(t)^2-1\right)\left(\frac{3}{2}g_2^2+\frac{27}{10}g_1^2\right)\,, \\
T &= Tr(3Y_u^\dagger Y_u+3Y_d^\dagger Y_d+Y_e^\dagger Y_e)\,.
\end{aligned}$$

The CKM matrix is then obtained upon diagonalisation of the quark mass matrices, $V_{CKM}=UV^\dagger$. The variation of the CKM matrix and its evolution equation for all matter fields in the bulk is:

$$\begin{aligned}
16\pi^2\frac{dV_{ik}}{dt} &= -6\left(\pi(S(t)^2-1)+1\right)\Bigg[\sum_{m,j\neq i}\frac{f_i^2+f_j^2}{f_i^2-f_j^2}h_m^2V_{im}V_{jm}^*V_{jk} \\
&\qquad +\sum_{j,m\neq k}\frac{h_k^2+h_m^2}{h_k^2-h_m^2}f_j^2V_{jm}^*V_{jk}V_{im}\Bigg] \qquad (6.27)
\end{aligned}$$

The RGEs for the squares of the absolute values of the CKM matrix ele-

ments, i.e. the rephasing invariant variables, can now be calculated as:

$$16\pi^2\frac{d|V_{ij}|^2}{dt} = 2\left(\pi(S(t)^2-1)+1\right)\left[3|V_{ij}|^2\left(f_i^2+h_j^2-\sum_k f_k^2|V_{kj}|^2-\sum_k h_k^2|V_{ik}|^2\right)\right.$$
$$-3f_i^2\sum_{k\neq i}\frac{1}{f_i^2-f_k^2}\left(2h_j^2|V_{kj}|^2|V_{ij}|^2+\sum_{l\neq j}h_l^2V_{iklj}\right)$$
$$\left.-3h_j^2\sum_{l\neq j}\frac{1}{h_j^2-h_l^2}\left(2f_i^2|V_{il}|^2|V_{ij}|^2+\sum_{k\neq i}f_k^2V_{iklj}\right)\right] , \quad (6.28)$$

where

$$V_{iklj} = 1-|V_{il}|^2-|V_{kl}|^2-|V_{kj}|^2-|V_{ij}|^2-|V_{il}|^2|V_{kj}|^2-|V_{kl}|^2|V_{ij}|^2 . \quad (6.29)$$

6.3.3 Brane 1UED case

In this case the Yukawa coupling RGEs are given by:

$$\beta_u^{5D} = 2(S(t)-1)Y_u\left[-8g_3^2-\frac{9}{4}g_2^2-\frac{17}{20}g_1^2+\frac{3}{2}(Y_u^\dagger Y_u-Y_d^\dagger Y_d)\right], \quad (6.30)$$

$$\beta_d^{5D} = 2(S(t)-1)Y_d\left[-8g_3^2-\frac{9}{4}g_2^2-\frac{1}{4}g_1^2+\frac{3}{2}(Y_d^\dagger Y_d-Y_u^\dagger Y_u)\right], \quad (6.31)$$

$$\beta_e^{5D} = 2(S(t)-1)Y_e\left[-\frac{9}{4}g_2^2-\frac{9}{4}g_1^2+\frac{3}{2}Y_e^\dagger Y_e\right] . \quad (6.32)$$

6.3.4 Brane 2UED case

We shall now consider the case of brane localized matter fields for Yukawa couplings in a 6D model. In this case there are no contributions from the KK excited states of the fermions to the Yukawa couplings, in which case we obtain:

$$\beta_u^{6D} = 4\pi(S(t)^2-1)Y_u\left[-8g_3^2-\frac{9}{4}g_2^2-\frac{17}{20}g_1^2+\frac{3}{2}(Y_u^\dagger Y_u-Y_d^\dagger Y_d)\right], \quad (6.33)$$

$$\beta_d^{6D} = 4\pi(S(t)^2-1)Y_d\left[-8g_3^2-\frac{9}{4}g_2^2-\frac{1}{4}g_1^2+\frac{3}{2}(Y_d^\dagger Y_d-Y_u^\dagger Y_u)\right], \quad (6.34)$$

$$\beta_e^{6D} = 4\pi(S(t)^2-1)Y_e\left[-\frac{9}{4}g_2^2-\frac{9}{4}g_1^2+\frac{3}{2}Y_e^\dagger Y_e\right] . \quad (6.35)$$

By imposing the unitary transformation on both sides of the evolution equations of $Y_u^\dagger Y_u$ and $Y_d^\dagger Y_d$, we derive the RGEs for the eigenvalues of the

square of these Yukawa coupling matrices as follows:

$$16\pi^2\frac{df_i^2}{dt} = f_i^2\Bigg[2T-2G_u+3\left(4\pi(S(t)^2-1)+1\right)f_i^2 -3\left(4\pi(S(t)^2-1)+1\right)\sum_j h_j^2|V_{ij}|^2\Bigg]\,, \quad (6.36)$$

$$16\pi^2\frac{dh_j^2}{dt} = h_j^2\Bigg[2T-2G_d+3\left(4\pi(S(t)^2-1)+1\right)h_j^2 -3\left(4\pi(S(t)^2-1)+1\right)\sum_i f_i^2|V_{ij}|^2\Bigg]\,, \quad (6.37)$$

$$16\pi^2\frac{dy_a^2}{dt} = y_a^2\Bigg[2T-2G_e+3\left(4\pi(S(t)^2-1)+1\right)y_a^2\Bigg]\,, \quad (6.38)$$

where

$$\begin{aligned}
G_u &= 8g_3^2+\frac{9}{4}g_2^2+\frac{17}{20}g_1^2+4\pi\left(S(t)^2-1\right)\left(8g_3^2+\frac{9}{4}g_2^2+\frac{17}{20}g_1^2\right)\,,\\
G_d &= 8g_3^2+\frac{9}{4}g_2^2+\frac{1}{4}g_1^2+4\pi\left(S(t)^2-1\right)\left(8g_3^2+\frac{9}{4}g_2^2+\frac{1}{4}g_1^2\right)\,,\\
G_e &= \frac{9}{4}g_2^2+\frac{9}{4}g_1^2+4\pi\left(S(t)^2-1\right)\left(\frac{9}{4}g_2^2+\frac{9}{4}g_1^2\right)\,,\\
T &= Tr(3Y_u^\dagger Y_u+3Y_d^\dagger Y_d+Y_e^\dagger Y_e)\,.
\end{aligned}$$

Consequently the CKM running of the quark flavor mixing matrix ($16\pi^2\frac{dV_{ik}}{dt}$ and $16\pi^2\frac{d|V_{ij}|^2}{dt}$) for all matter fields on the brane is the same as in the bulk case, except that the prefactor $2\left(\pi(S(t)^2-1)+1\right)$ is replaced by $(4\pi(S(t)^2-1)+1)$ in Eqs.(6.27, 6.28) for more details see section 4.2.

6.4 Numerical results and discussions

For our numerical calculations we assume that the fundamental scale is not far from the range of the LHC and set the compatification radii to be $R^{-1}=1$ TeV, 2 TeV and 10 TeV. Only some selected plots will be shown and we will comment on the other similar cases not explicitly presented. We quantitatively analyse these quantities in the 2UED model with the initial values adopted at the M_Z scale presented in Table E.1.

Once the first KK threshold is reached, the contributions from the KK states become more and more significant due to the power law running, where the second term on the right hand side of Eq.(6.17) depends explicitly on the

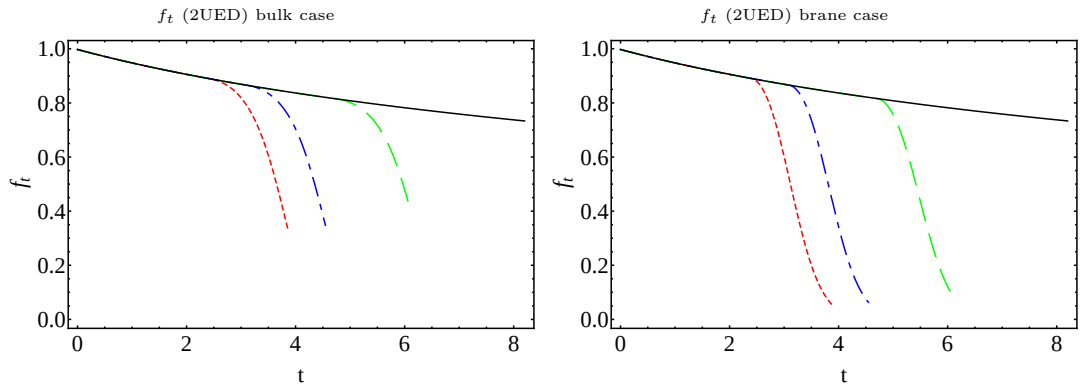


Figure 6.4: *The evolution of top Yukawa coupling f_t where the solid line represents the SM case with: in the left panel all matter fields in the bulk; and the right panel for all matter fields on the brane; for three different values of the compactification scales 1 TeV (solid line) with the first KK threshold at $t = 2.394$, 2 TeV (dot-dashed line) with the first KK threshold at $t = 3.0879$ and 10 TeV (dashed line) with the first KK threshold at $t = 4.697$, as a function of the scale parameter t.*

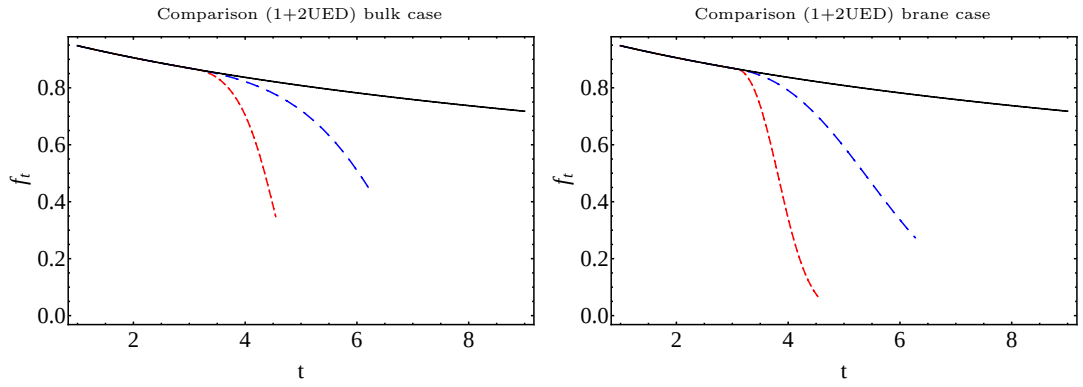


Figure 6.5: *Comparison of the top Yukawa coupling evolution between the 1UED case (blue) and the 2UED case (red), where the solid line represent the SM case with: in the left panel all matter fields in the bulk; and the right panel for all matter fields on the brane; for a compactification scale of 2 TeV as a function of the scale parameter t.*

cut-off, which has quantum corrections to the beta functions at each massive KK excitation level. Therefore, the running of the Yukawa couplings deviates from their normal orbits and starts to evolve faster. Similarly, for the Yukawa couplings, where we show in Fig.6.4 the evolution of the top Yukawa coupling in the 2UED case, the cases of bulk fields and brane localized fields for different radii of compactification, the Yukawa couplings decrease when the first two towers of KK states are reached (that is, when $t > \ln\left(\frac{1}{M_Z R}\right)$). However, as

the cut-off is reached quickly in the bulk case, the resulting decrease is of 50% from the initial value, while in the brane case, the top Yukawa coupling can reach a smaller value by running in a larger energy range (a decrease of about 90% from the initial value). This is due to the theory being valid to a higher cut-off scale in the brane case.

A comparison between the 1UED and 2UED cases for the evolution of the top Yukawa coupling is shown in Fig.6.5, where a rapid decrease appears in the 2UED case, due to the presence of two towers of KK states, which manifest in Eqs.(6.23, 6.35) as the $S^2(t)$ factor. In the 1UED case we have one tower of KK states and a linear dependence of $S(t)$, so we observe that f_t decreases less rapidly than the 2UED case. Note that the evolution of other Yukawa couplings have similar behaviours of decreasing when the quantum corrections from the extra-dimensions set in.

We should explicitly state, at this point, that the cut-offs used for the bulk and brane cases in both five and six dimensions (1UED and 2UED) are summarized in Tab.6.1. From this we see that the theory in 6D is valid only up to a smaller value of t than the 5D case, where beyond these cut-offs the model would be superseded by new physics. Note that these values are found by finding the scale at which $g_1 = g_2$, which is lowered compared to the 4D SM case, by the effects of the compactification.

Table 6.1: *The cut-offs in 5D and 6D for both bulk and brane cases for the three compactification radii R^{-1} =1, 2 and 10 TeV, where $t = \ln\left(\frac{\mu}{M_Z}\right)$.*

Scenarios	$t(R_1)$	$t(R_2)$	$t(R_3)$
Brane and Bulk 5D (1UED)	5.61	6.27	7.81
Brane and Bulk 6D (2UED)	3.87	4.55	6.12

We next turn our attention to the quark flavour mixings, where due to the arbitrary choice of phases for the quark fields, the phases of individual matrix elements of V_{CKM} are not themselves directly observable. We therefore use the absolute values of the matrix element $|V_{ij}|$ as the independent set of rephasing invariant variables. Of the nine elements of the CKM matrix, only four of them are independent, which is consistent with the four independent variables of the standard parameterization of the CKM matrix.

We plot in Fig.6.6 the evolution of the CKM parameter $|V_{ub}|$ in the bulk and brane cases and note that the other CKM parameters have similar behaviours. We see that once the KK threshold is reached, we have new contributions from the new KK states, resulting in a rapidly increasing evolution of the parameter in both cases. Recall that the range of validity for the brane case is bigger than the bulk one, where both cases have a smaller range of validity in the

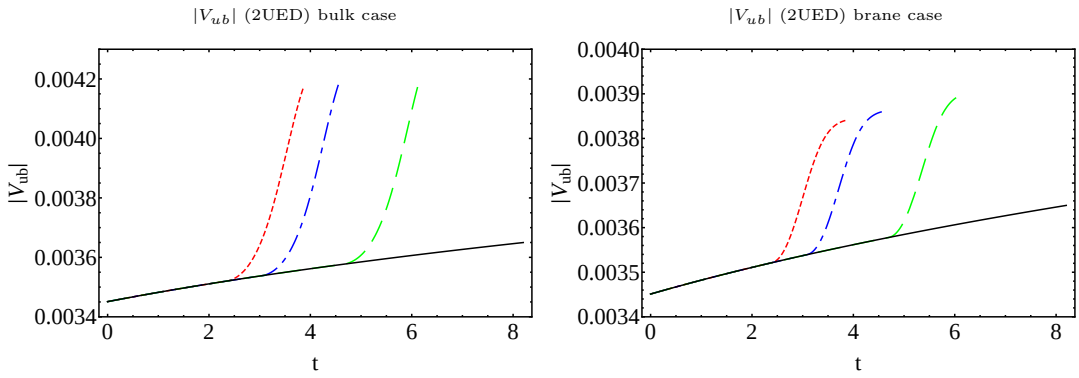


Figure 6.6: *The evolution of CKM element $|V_{ub}|$ where the solid line represents the SM case with: in the left panel all matter fields in the bulk; and the right panel for all matter fields on the brane; for three different values of the compactification scales 1 TeV (solid line), 2 TeV (dot-dashed line) and 10 TeV (dashed line), as a function of the scale parameter t.*

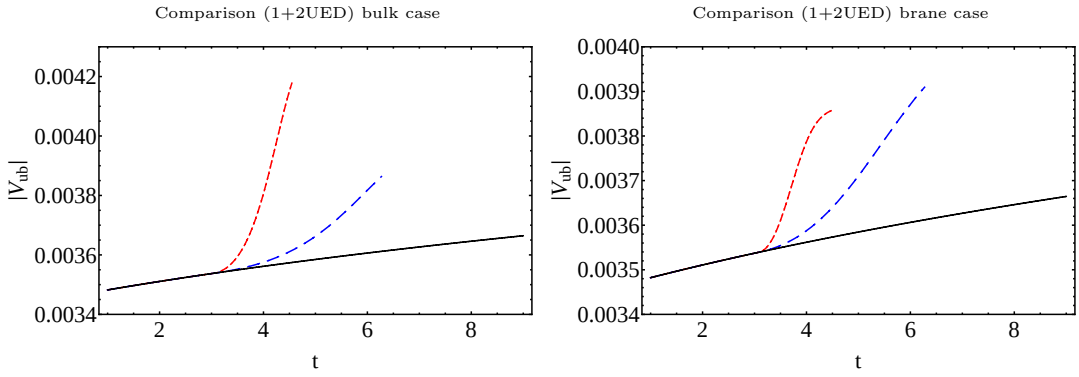


Figure 6.7: *Comparison of the $|V_{ub}|$ evolution between the 1UED case (blue) and the 2UED case (red), where the solid line represents the SM case with: in the left panel all matter fields in the bulk; and the right panel for all matter fields on the brane; for a compactification scale of 2 TeV as a function of the scale parameter t.*

2UED model when compared to the 1UED model, due to the cut-off in two extra dimensions being smaller. For comparison see Fig.6.7.

We plot the Jarlskog parameter in Fig.6.8 in the 2UED model for both cases considered here for different radius of compactification. The Jarlskog rephasing invariant parameter $J = \mathrm{Im} V_{ud} V_{cs} V_{us}^* V_{cd}^*$, gives us an indication of the amount of CP violation in the quark sector. As can be seen from the Fig. 6.8, once the first KK threshold is crossed, we have a sharp increase in the value of J up to the cut-off scale for both cases. For the bulk case as approximately 45%, and the brane localized of 20%. In Fig.6.9 we compare the 2UED to the 1UED model, and observe similar phenomenologies as for the

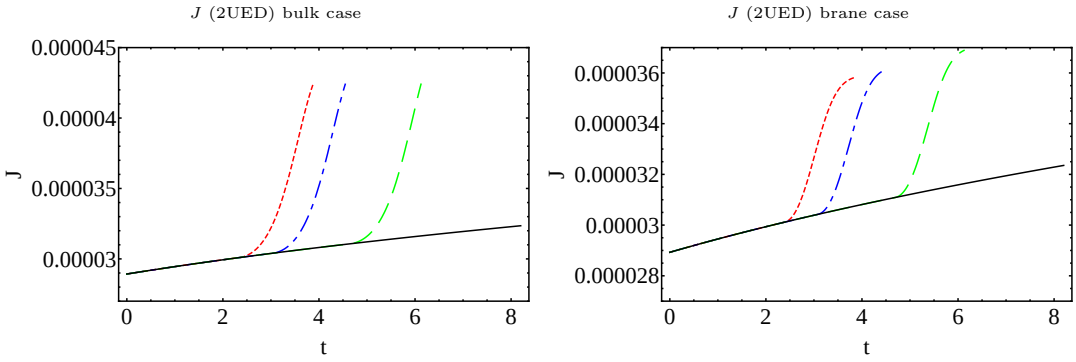


Figure 6.8: *The evolution of the Jarlskog parameter J where the solid line represents the SM case with: in the left panel all matter fields in the bulk; and the right panel for all matter fields on the brane; for three different values of the compactification scales 1 TeV (solid line) with the first KK threshold at $t = 2.394$, 2 TeV (dot-dashed line) with the first KK threshold at $t = 3.0879$ and 10 TeV (dashed line) with the first KK threshold at $t = 4.697$, as a function of the scale parameter t.*

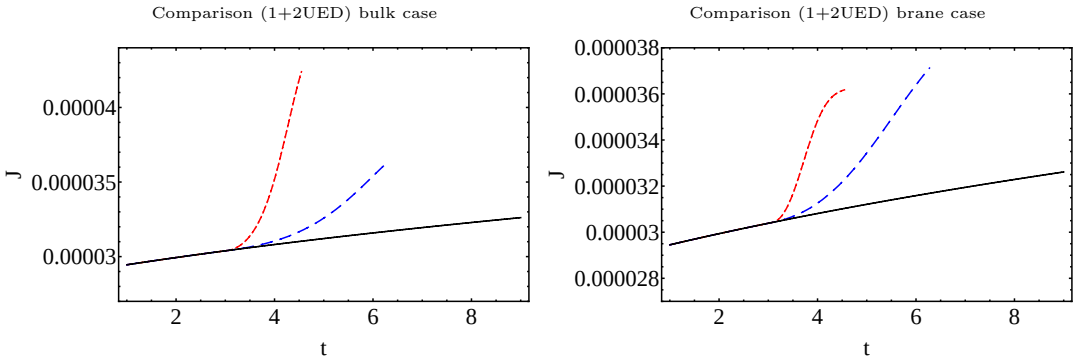


Figure 6.9: *Comparison of the Jarlskog parameter J evolution between the 1UED case (blue) and the 2UED case (red), where the solid line represent the SM case with: in the left panel all matter fields in the bulk; and the right panel for all matter fields on the brane; for a compactification scale of 2 TeV as a function of the scale parameter t.*

$|V_{ub}|$ evolution. Note that the main difference between the two models (1UED and 2UED) is the cut-off scale, which for $R^{-1} = 1$ TeV is $\Lambda \sim 25$ TeV in the 5D model, which is larger than in the 6D model where $\Lambda \sim 4.5$ TeV. Therefore, the typical 2UED model can be tested, detected or ruled out more easily.

Chapter 7

Evolution of Quark Masses and Flavour Mixings in the 2UED

This chapter shall study the evolution of quark masses and flavour mixings in 2UED models (note that this work is an extension to chapter 6), we use a complete set of all observables related to up and down quarks and quark flavour mixings at one-loop level. Specifically we study the evolution of mass ratios, the renormalisation invariance R_{13} and R_{23}, and $\sin\beta$ in this model. These invariants exhibit explicitly the correlation between quark flavour mixings and mass ratios in the context of the SM, MSSM and extra-dimensions of electroweak interactions.

7.1 Mass Ratios, Mixings and Renormalisation invariance

The evolution of the Yukawa couplings were derived in Refs. [133, 134], where the one-loop RGEs in the 2UED we study are given in Eq. (6.23, 6.35). That is, when the energy scale $\mu > \frac{1}{R}$, or when the energy scale parameter $t > \ln(\frac{1}{M_Z R})$, we shall use Eq.(6.23, 6.35). However, when the energy scale $M_Z < \mu < \frac{1}{R}$, the Yukawa evolution equations are dictated by the usual SM ones, see Refs. [72, 133, 134].

The mixing matrix V_{CKM} in Eqs.(6.27, 6.28) satisfies the unitarity condition, providing the following constraint

$$V_{ud}\, V_{ub}^{*} + V_{cd}\, V_{cb}^{*} + V_{td}\, V_{tb}^{*} = 0. \tag{7.1}$$

That is, we have a triangle in the complex plane and the three inner angles α, β and γ are given by

$$\sin\beta = \frac{J}{|V_{td}|\,|V_{tb}^{*}|\,|V_{cd}|\,|V_{cb}^{*}|}\,, \tag{7.2}$$

$$\sin\gamma = \frac{J}{|V_{ud}|\,|V_{ub}^*|\,|V_{cd}|\,|V_{cb}^*|}\ , \tag{7.3}$$

with $\alpha = \pi - \beta - \gamma$. The shape of the unitarity triangle can be used as a tool to explore new symmetries or other interesting properties that give a deeper insight into the physical content of new physics models.

On the other hand, in the quark sector both the mass ratios are related to mixing angles as

$$\theta_{13} \sim \frac{m_d}{m_b}, \qquad \theta_{23} \sim \frac{m_s}{m_b}. \tag{7.4}$$

In Refs. [62, 63] a set of renormalisation invariants is constructed

$$R_{13} = \sin(2\theta_{13})\sinh\left[\ln\frac{m_b}{m_d}\right] \sim \text{constant}\ , \tag{7.5}$$

$$R_{23} = \sin(2\theta_{23})\sinh\left[\ln\frac{m_b}{m_s}\right] \sim \text{constant}\ . \tag{7.6}$$

7.2 Numerical Results and Discussions

For our numerical calculations we set the compatification radii to be $R^{-1} = 1$ TeV, 2 TeV and 10 TeV. Only some selected plots will be shown and we will comment on the other similar cases not explicitly presented. We quantitatively anlayse these quantities in 2UED models, though we observed similar behaviours for all values of R^{-1}. The initial values we shall adopt at the M_Z scale can be found in the appendix E.

As illustrated in Figs. 7.1, 7.2, mass ratios evolve in the usual logarithmic fashion when the energies are below 1 TeV, 2 TeV and 10 TeV respectively. However, once the first KK threshold is reached the contributions from the KK states become increasingly significant and the effective 4D SM couplings begin to deviate from their normal trajectories. One finds that the running behaviours of the mass ratios are governed by the combination of the third family Yukawa couplings and the CKM matrix elements. This implies that the mass ratios of the first two light generations have a slowed evolution well before the unification scale. Beyond that point, their evolution diverges due to the faster running of the gauge couplings, where any new physics would then come into play, and we find the scaling dependence of m_d/m_s and m_e/m_μ is very slow.

On the other hand, Grand Unification Theories (such as $SU(5)$ and $SO(10)$) imply the well-known quark-lepton symmetric relation for fermion masses $m_d = m_e$. Due to power law running of the Yukawa couplings, the renormalisation effects on these relations can be large for m_b/m_τ, for both scenarios, see Fig.7.2. We have shown by numerical analysis of the one-loop calculation that the mass ratio m_b/m_τ, as one crosses the KK threshold at $\mu = R^{-1}$ for

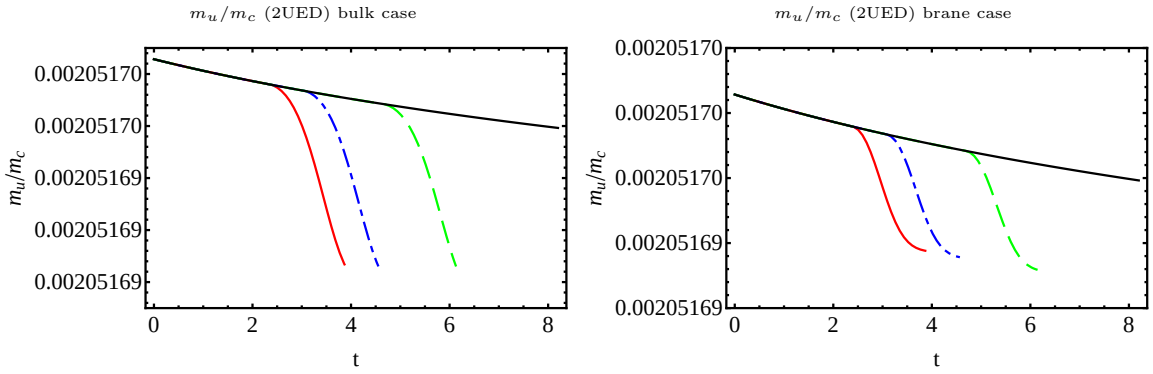


Figure 7.1: *Evolution of the mass ratio* $\frac{m_u}{m_c}$ *with: in the left panel all matter fields in the bulk; and the right panel for all matter fields on the brane. Three different values of the compactification radius have been used* $R^{-1} = 1$ *TeV (solid line) with the first KK threshold at* $t = 2.394$*, 2 TeV (dot-dashed line) with the first KK threshold at* $t = 3.0879$*, and 10 TeV (dashed line) with the first KK threshold at* $t = 4.697$*, all as a function of the scale parameter* t*.*

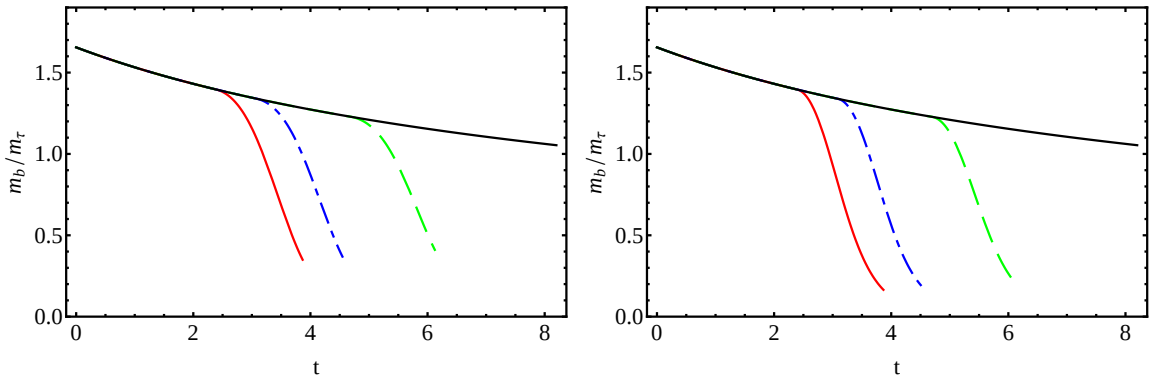


Figure 7.2: *Evolution of the mass ratio* $\frac{m_b}{m_\tau}$*, with the same notations as Fig.7.1*

both scenarios, results in a rapid approach to a singularity before the unification scale is reached, which agrees with what is observed in the SM. However, the mass ratios decrease at a much faster rate. Note that we observed similar behaviour for m_d/m_e and m_s/m_μ.

Let us now focus on the evolution of the set of renormalisation invariants R_{13} and R_{23} that describe the correlation between the mixing angles and mass ratios to a good approximation. With a variation of the order of λ^4 and λ^5 under energy scaling respectively, as shown in Fig.7.3, the energy scale dependence is weak, because the increase of the mixing angles are compensated by the deviation of the mass ratios. Therefore the effect is not large.

In Fig.7.4 we present the evolution of the inner angle from the electroweak scale to the unification scale by using the one-loop RGE for the 2UED model,

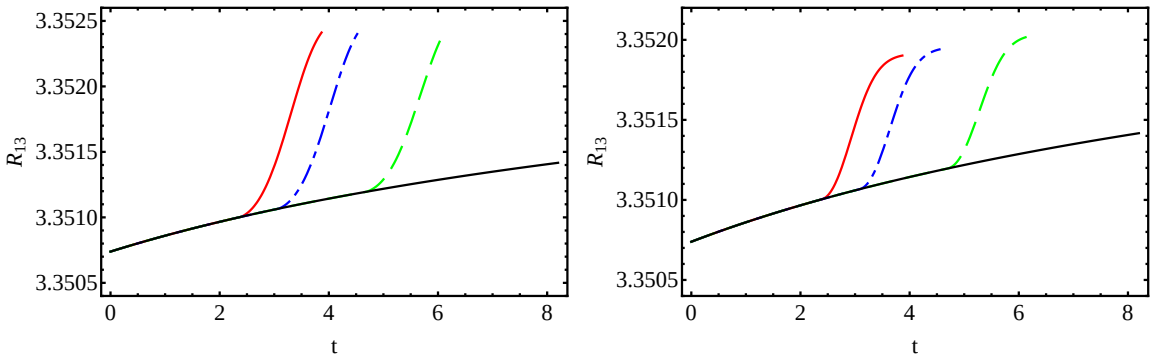


Figure 7.3: *Evolution of the R_{13}, with the same notations as Fig.7.1*

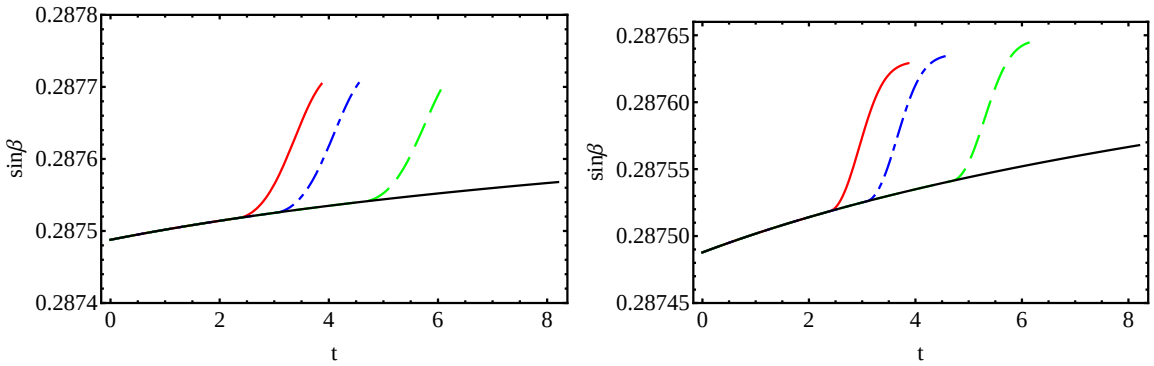


Figure 7.4: *Evolution of* $\sin\beta$*, with the same notations as Fig.7.1*

and demonstrate that the angle has a small variation against radiative corrections. To be more precise, the relative deviation for $\sin\beta$ is only up to 0.05% in the whole range studied. Similar analysis can also be found for the angles α and γ. This result makes sense, since both the triangle's sides and area become larger and larger as the energy scale increases, and the unitarity triangle (UT) is only rescaled, its shape does not change much during the renormalisation group evolution. The fact that inner angles are rather stable against radiative corrections indicates that it is not possible to construct an asymptotic model with some simple, special form of the CKM matrix from this simple scenario. The stability against radiative corrections suggests that the shape of the UT is almost unchanged from RGE effects. In this regard, the UT is not a sensitive test of this model in current and upcoming experiments.

Chapter 8

Higgs Quartic Coupling, Neutrino Masses and Mixing Angles in 2UED Models

In this chapter we shall derive and discuss the Higgs quartic coupling RGEs in 2UED models. Comparisons of the limits on the effective theory obtained by requiring the stability of the Higgs potential with other effective rules for the cutoff theory are made. These other rules are obtained from requirements such as perturbativity of the interactions, gauge coupling unification, etc. This shall be followed by the study of the neutrino mixing and masses evolution.

8.1 Introduction

The Higgs mechanism has intrigued both theorists and experimentalists for a long time, being one of the central pieces in the construction of the SM and its extensions. The LHC was indeed built to discover the missing pieces of the SM and to search for new particles BSM. The ATLAS and CMS experiments announced in 2012 the discovery of a Higgs particle compatible with the SM expectations with a mass of about 126 GeV [3, 4], and updated results with more data have been recently released (see for example Refs. [85, 86]). As we increase the energy scale above the electroweak scale, the quartic couplings may become smaller and eventually become negative, where as a consequence, the potential becomes unbounded from below and the electroweak vacuum becomes unstable. In the context of the SM this problem was investigated a long time ago (see for example Ref. [87]) and continuously reinvestigated till recently (see for example Ref. [88]) as Higgs data and more precise calculations became available.

This is also relevant for BSM and in particular those we shall consider, as this can give bounds on the limit of validity of the effective theory. In this case the problem of vacuum stability and the triviality of the Higgs potential can be quite relevant, as running effects are more pronounced in these models (with

respect to the SM). For some recent work concerning 5 and 6-dimensional UED models see Ref. [82].

Another important point connected to BSM physics is that in the SM the neutrino does not have a mass, but neutrino oscillations suggest that neutrinos have finite mass and lepton flavours mix. The most recent evidence is the measurement of a large θ_{13} mixing parameter [89–91]. In the context of UED models [92], one can use the dimension-five Weinberg operator [93] to give Majorana masses to neutrinos and study RGEs for the physical observables in this sector. In general two extra dimensional models have different (and faster) evolution properties with respect to one extra dimensional models. It is therefore interesting to check if signs of the evolution of neutrino parameters are within experimental reach or not. Note that the discussion of the neutrino sector appear in this chapter as its evolution equations are related to the Higgs quartic evolution equations.

8.2 The Quartic coupling RGEs

This section shall study a generic model with two universal extra dimensions, where in the following we summarise the evolution equations. We shall use a notation similar to the ones of Refs. [56, 133], noting that the beta functions contain terms quadratic in the cut-off, where this part dominates the evolution of the Yukawa couplings and of k (the coefficient of the Weinberg operator). The top Yukawa coupling becomes non-perturbative only after the gauge coupling unification. As such, the limit on the range of validity for the effective theory will be determined by which condition is reached first: unification of the gauge couplings or instability of the Higgs potential. We shall first write down the results of the SM for completeness and then generalise it to include the effects arising from the extra dimensional degrees of freedom. The initial values we shall adopt at the M_Z scale can be found in appendix E.

8.2.1 SM evolution equations

The evolution equations for the SM are a limiting case when the KK scale becomes heavy and the KK modes decouple. We introduce them to fix the notation and as they are relevant below the KK threshold. When $0 < t < \ln(\frac{1}{M_Z R})$, where $t = \ln\left(\frac{\mu}{M_Z}\right)$, μ being the energy, that is, for the evolution between $M_Z < \mu < 1/R$; the Yukawa evolution equations can be found in chapter 6, the Higgs quartic couplings and neutrino parameter evolution equations are

dictated by the usual SM ones:

$$\begin{aligned}\beta_\lambda^{SM} &= \left[12\lambda^2 - \left(\frac{9}{5}g_1^2 + 9g_2^2\right)\lambda + \frac{9}{4}\left(\frac{3}{25}g_1^4 + g_2^4 + \frac{2}{5}g_1^2 g_2^2\right)\right. \\ &\quad + 4\lambda Tr\left(3Y_u^\dagger Y_u + 3Y_d^\dagger Y_d + Y_e^\dagger Y_e\right) \\ &\quad \left. - 4Tr\left(3(Y_u^\dagger Y_u)^2 + 3(Y_d^\dagger Y_d)^2 + (Y_e^\dagger Y_e)^2\right)\right] , \qquad (8.1) \\ \beta_k^{SM} &= \left[\left(-3g_2^2 + \lambda + 2Tr(3Y_u^\dagger Y_u + 3Y_d^\dagger Y_d + Y_e^\dagger Y_e)\right)k\right. \\ &\quad \left. - \frac{3}{2}\left(kY_e^\dagger Y_e + (Y_e^\dagger Y_e)^T k\right)\right] . \qquad (8.2)\end{aligned}$$

Where k comes from the $d = 5$ Weinberg operator structure as

$$-\frac{k_{ij}}{M}(l_a^i \epsilon^{ab}\phi_b)(l_c^j \epsilon^{cd}\phi_d) + h.c.$$

M is an energy scale distinctive for the low energy effective theory description. The notation is as follows: g_1, g_2, g_3 are respectively the $U(1)$, $SU(2)$, $SU(3)$ gauge couplings; Y_i are the Yukawa coupling matrices where the index refers to the corresponding sector (u for up-type, d for down-type and e for leptons); λ is the Higgs quartic coupling and k the coefficient of the Weinberg operator. These equations are modified when we enter the energy regime where the effects of the extra dimensions set in. The modifications depend on the particles non-decoupled at that energy scale and on the structure of the model. We shall consider two cases, one in which all particles can propagate in the extra dimensions (bulk case) and the other in which SM particles are constrained to the brane (brane case).

8.2.2 The 1UED and 2UED scenarios

The RGEs for the Yukawa couplings were derived in chapter 6, Higgs quartic couplings and neutrino running parameter in the 1UED [58] and 2UED models, for all three generations propagating in the bulk, can be expressed as:

$$\begin{aligned}\beta_\lambda^{5D} &= (S(t)-1)\left[12\lambda^2 - \left(\frac{9}{5}g_1^2 + 9g_2^2\right)\lambda + \left(\frac{9}{25}g_1^4 + 3g_2^4 + \frac{6}{5}g_1^2 g_2^2\right)\right. \\ &\quad + 8\lambda Tr\left(3Y_u^\dagger Y_u + 3Y_d^\dagger Y_d + Y_e^\dagger Y_e\right) \\ &\quad \left. - 8Tr\left(3(Y_u^\dagger Y_u)^2 + 3(Y_d^\dagger Y_d)^2 + (Y_e^\dagger Y_e)^2\right)\right] , \qquad (8.3) \\ \beta_k^{5D} &= (S(t)-1)\left[\left(-\frac{3}{20}g_1^2 - \frac{11}{4}g_2^2 + \lambda + 4Tr(3Y_u^\dagger Y_u + 3Y_d^\dagger Y_d + Y_e^\dagger Y_e)\right)k\right. \\ &\quad \left. - \frac{3}{2}(kY_e^\dagger Y_e + (Y_e^\dagger Y_e)^T k)\right] . \qquad (8.4)\end{aligned}$$

$$\beta_\lambda^{6D} = \pi(S(t)^2-1)\left[12\lambda^2 - \left(\frac{9}{5}g_1^2+9g_2^2\right)\lambda + \left(\frac{9}{20}g_1^4+\frac{15}{4}g_2^4+\frac{3}{2}g_1^2g_2^2\right) + 8\lambda Tr\left(3Y_u^\dagger Y_u + 3Y_d^\dagger Y_d + Y_e^\dagger Y_e\right) - 8Tr\left(3(Y_u^\dagger Y_u)^2 + 3(Y_d^\dagger Y_d)^2 + (Y_e^\dagger Y_e)^2\right)\right], \quad (8.5)$$

$$\beta_k^{6D} = \pi(S(t)^2-1)\left[\left(-\frac{3}{20}g_1^2 - \frac{5}{2}g_2^2 + \lambda + 4Tr(3Y_u^\dagger Y_u + 3Y_d^\dagger Y_d + Y_e^\dagger Y_e)\right)k - 3(kY_e^\dagger Y_e + (Y_e^\dagger Y_e)^T k)\right]. \quad (8.6)$$

The corresponding evolution equations, for all three generations restricted to the brane are given by:

$$\beta_\lambda^{5D} = (S(t)-1)\left[12\lambda^2 - \left(\frac{9}{5}g_1^2+9g_2^2\right)\lambda + \left(\frac{9}{25}g_1^4+3g_2^4+\frac{6}{5}g_1^2g_2^2\right)\right], \quad (8.7)$$

$$\beta_k^{5D} = (S(t)-1)\left[(-3g_2^2+\lambda)\,k - \frac{3}{2}\left(kY_e^\dagger Y_e + (Y_e^\dagger Y_e)^T k\right)\right], \quad (8.8)$$

$$\beta_\lambda^{6D} = \pi(S(t)^2-1)\left[12\lambda^2 - \left(\frac{9}{5}g_1^2+9g_2^2\right)\lambda + \left(\frac{9}{20}g_1^4+\frac{15}{4}g_2^4+\frac{3}{2}g_1^2g_2^2\right)\right], \quad (8.9)$$

$$\beta_k^{6D} = 2\pi(S(t)^2-1)\left[(-3g_2^2+\lambda)\,k - 3\left(kY_e^\dagger Y_e + (Y_e^\dagger Y_e)^T k\right)\right], \quad (8.10)$$

where $S(t) = M_Z Re^t$, assuming that all modes contribute. Note that these coefficients are model dependent, as discussed further in Appendix C. The bulk and brane sets of evolution equations share the same structure, but bring about quite different evolutions for the physical parameters. For example, if you compare Eq. (8.5) for the bulk case against the corresponding one for the brane case, Eq. (8.9), you can see that the presence of the Yukawa terms adds a negative contribution which will affect the evolution. Numerically we will show in the following that this term is dominant and drives the quartic coupling to zero in the bulk case as the energy scale increases, whilst in the brane model, which does not contain such a contribution, has the opposite behaviour and the quartic coupling grows with the energy scale. Our calculation agrees with Ref. [75] in the general structure, but the coefficient of g_1^2 in the running of the k parameter is different and the number of the KK particles taken into

account in the factor $S^2(t)$ is also different (see Appendix C). In particular we have explicitly calculated the KK modes contributing up to the cut-off in different 6D models, while Ref. [75] only has a factor of two with respect to the 5D case. Using a factor of two amounts to considering only the modes $(j, 0)$ and $(0, k)$, while disregarding all the "mixed" modes (j, k) with $j, k \neq 0$. Even if the numerical differences are not very large, excluding the mixed modes is inconsistent.

8.2.3 The 2UED bulk and brane quartic results

The numerical calculation of the RGEs confirms the results expected from inspection of the analytical formulae above for the brane and for the bulk UED models. We show in Fig. 8.1 the evolution of the Higgs quartic coupling in these two scenarios (for all matter fields propagating in the bulk (downward evolution with increasing energy scale) or brane localised matter fields (upward evolution with increasing energy scale)). As can be seen, for the brane case the quartic Higgs coupling $\lambda(t)$ is positive and remains finite as we run from the electroweak scale all the way up to the unification scale. In contrast to the bulk case (and also in the SM) the evolution of $\lambda(t)$ goes to zero at some energy scale before reaching the unification scale, which implies the vacuum instability of the model and requires the introduction of a cut-off which is typically lower than the one usually determined by other means. A discussion of this point was already performed in the literature for the bulk case [75] for a particular scenario (assuming that the number of modes in the 6D case is twice the one of the corresponding 5D model). Our numerical results agree qualitatively with them, as the running has a similar behaviour, but we consider realistic models taking into account explicitly all the KK modes up to the cut-off. Recall, as defined earlier in section 8.2, our effective theories cut-off is determined by either reaching the gauge coupling unification (see Fig. 6.1 in section 6.2) or the instability of the Higgs potential.

More general results were also obtained in Ref. [82] for 2UED results. We use the updated experimental values for the Higgs sector from the ATLAS and CMS collaborations and updated values for the top quark mass, and also consider more general bulk and brane scenarios. We have checked that the dependence on the Higgs boson and top quark masses in their experimentally allowed ranges does not affect significantly the result of the evolution. The evolution is also only weakly sensitive to the particular choice of 2UED model (we have considered the two broad classes of models issued from the compactifications of the crystallographic groups of the plane and of the sphere S^2). A more detailed discussion of the model dependence of the results is given in Appendix C.

In Fig.8.2 we present a comparison of the evolution of Higgs quartic couplings in the bulk case between the 1UED and 2UED models for different values of compactification scale (1, 4 and 10 TeV). We find that the evolution has the same behaviour, but in the 2UED model the cut-off is lower than the

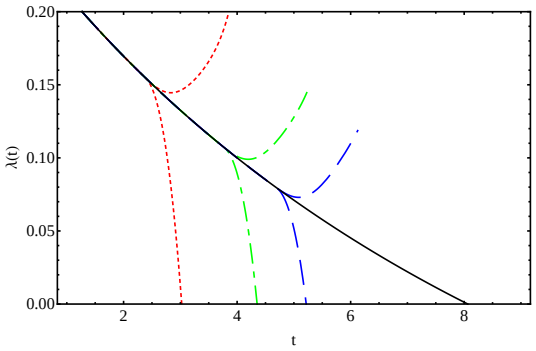


Figure 8.1: *The evolution of the Higgs quartic coupling λ, where the solid line represents the SM case with: downward trajectories for all matter fields in the bulk; and upward for all matter fields on the brane; for three different values of the compactification scales 1 TeV (dotted line), 4 TeV (dot-dashed line) and 10 TeV (dashed line), as a function of the scale parameter t.*

1UED model, this being due to the presence of $S^2(t)$ in Eq. (6.23) instead of the linear dependence on $S(t)$ as in the 1UED model.

8.3 Neutrino mixing and masses

This section is concerned with the neutrino sector, where we first state our conventions for the mixing angles and phases and briefly discuss different scenarios for neutrino masses. The mixing matrix which relates gauge and mass eigenstates is defined to diagonalise the neutrino mass matrix in the basis where the charged lepton mass matrix is diagonal [94]:

$$U = \begin{pmatrix} c_{12}c_{13} & s_{12}c_{13} & s_{13}e^{-i\delta} \\ -s_{12}c_{23} - c_{12}s_{23}s_{13}e^{-i\delta} & c_{12}c_{23} - s_{12}s_{23}s_{13}e^{i\delta} & s_{23}c_{13} \\ s_{12}s_{23} - c_{12}c_{23}s_{13}e^{i\delta} & -c_{12}s_{23} - s_{12}c_{23}s_{13}e^{i\delta} & c_{23}c_{13} \end{pmatrix} \begin{pmatrix} e^{i\phi_1} & & \\ & e^{i\phi_2} & \\ & & 1 \end{pmatrix},$$

with $c_{ij} = \cos\theta_{ij}$ and $s_{ij} = \sin\theta_{ij}$ $(ij = 12, 13, 23)$. We follow the conventions of Ref. [95] to extract mixing parameters from the PMNS matrix.

Experimental information on neutrino mixing parameters and masses is obtained mainly from oscillation experiments [96, 97]. In general Δm^2_{atm} is assigned to a mass difference between ν_3 and ν_2, whereas Δm^2_{sol} to a mass difference between ν_2 and ν_1. The current observational values are summarised in Table E.2. Data indicates that $\Delta m^2_{sol} \ll \Delta m^2_{atm}$, but the masses themselves are not determined. In this work we have adopted the masses of the neutrinos at the M_Z scale as $m_1 = 0.1$ eV, $m_2 = 0.100379$ eV, and $m_3 = 0.11183$ eV, as the *normal* hierarchy (whilst any reference to an *inverted* hierarchy would refer to $m_3 = 0.1$ eV, with $m_3 < m_1 < m_2$ and satisfying the above bounds).

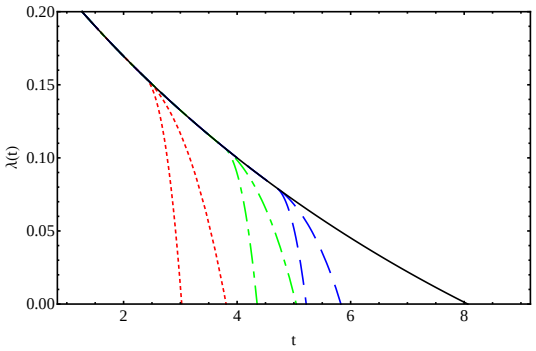


Figure 8.2: *Comparison of the Higgs quartic coupling evolution between the 1UED case and the 2UED case, where the solid line represent the SM case; all matter fields are in the bulk; for a compactification scale of 1 TeV (dotted line), 4 TeV (dot-dashed line) and 10 TeV (dashed line), as a function of the scale parameter t. The 2UED line is always steeper than the corresponding 1UED one.*

For the purpose of illustration, we choose values for the angles and phases at the M_Z scale as: $\theta_{12} = 34^o$, $\theta_{13} = 8.83^o$, $\theta_{23} = 46^o$, $\delta = 30^0$, $\phi_1 = 80^o$ and $\phi_2 = 70^o$.

Using the 2UED model [57], the transition to the 2UED bulk case will be done by making the replacement of $C = \pi(S(t)^2 - 1)$ and $\alpha = \pi(S(t)^2 - 1)\left[-\frac{9}{10}g_1^2 - \frac{5}{2}g_2^2 + \lambda + 4Tr(3Y_u^\dagger Y_u + 3Y_d^\dagger Y_d + Y_e^\dagger Y_e)\right]$ in Eqs. (B1–D3) in Ref. [57], and Eq. (A.3) in Ref. [72]. Similarly, we will also have the same equations in the 2UED brane case, with $C = 2\pi(S(t)^2-1)$ and $\alpha = 2\pi(S(t)^2-1)(-3g_2^2+\lambda)S(t)$.

In Fig. 8.3 we plot the cut-off of the Higgs quartic coupling and gauge couplings for all matter fields propagating in the bulk. As we observed before in Fig. 8.1 for the bulk case, the Higgs self-couplings evolve towards zero at high energies, requiring the introduction of an ultraviolet cut-off for the theory. As can be seen from the plot, the cut-off required by the λ evolution reaching zero is lower than the gauge couplings unification scale.

The evolution of the mass squared differences Δm^2_{atm} , both for the matter fields on the brane and for all fields in the bulk is presented in Fig. 8.4. Only some selected plots will be shown and we will comment on the other similar cases not explicitly presented. As depicted in Fig. 8.4, the mass squared difference increases rapidly once the KK threshold is crossed at $\mu = R^{-1}$ for the bulk case, resulting in a rapid approach to a singularity before the unification scale is reached. Note however that the cut-off imposed by the requirement of the stability of the Higgs potential is reached much faster. For the brane localised case the contribution from the gauge couplings is important, and the evolution decreases instead of increasing. Note that Δm^2_{sol} has the same shape as Δm^2_{atm} for both cases. To see the running behaviours of neutrino mixing

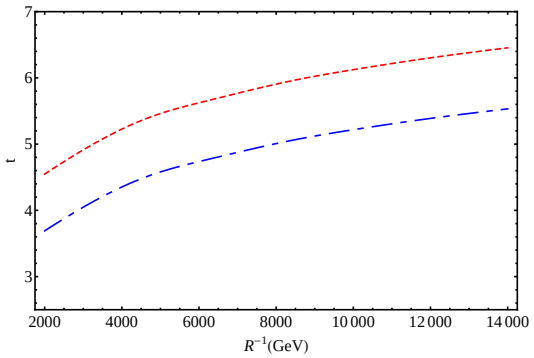


Figure 8.3: *The cut-off of the Higgs quartic coupling λ (dot-dashed line) and gauge couplings (dashed line) for all matter fields in the bulk; for different values of the compactification scales from 2 TeV to 14 TeV, as a function of the energy scale parameter t.*

parameters in the 2UED model, we carry out similar numerical analyses by using the beta function derived in section 8.2 for both the bulk case and the brane case. From this we observe that the correction to θ_{13} and θ_{23} are quite small and milder than θ_{12}. For θ_{12} the largest variations are of the order of 0.3% on the full energy range of validity for the effective theory. For θ_{13} and θ_{23} the variations are negligible. There is therefore no substantial difference in all cases with respect to the SM.

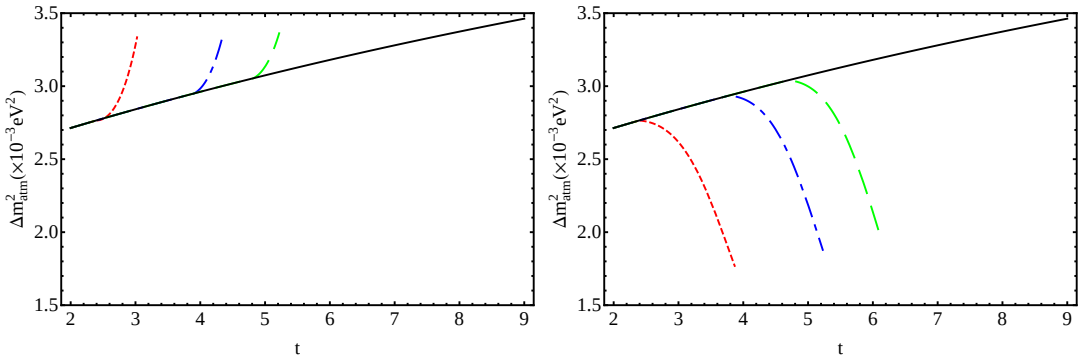


Figure 8.4: *The evolution of Δm^2_{atm} where the solid line represents the SM case with: in the left panel all matter fields in the bulk; and the right panel for all matter fields on the brane; for three different values of the compactification scales 1 TeV (dotted line), 4 TeV (dot-dashed line) and 10 TeV (dashed line), as a function of the scale parameter t.*

As such the appropriate cut-off for the three radii considered in this work, for the brane localized matter fields case, will be determined by the instability of the Higgs quartic condition. This will correspond to $t(R^{-1} = 1 \text{ TeV}) \sim 3.0$, $t(R^{-1} = 4 \text{ TeV}) \sim 4.3$ and $t(R^{-1} = 10 \text{ TeV}) \sim 5.7$ (see Fig.8.2). For the bulk case, the cut-off has been presented in Table 6.1. Note that this corresponds to approximately 5 KK modes in the 2UED $R^{-1} = 1$ TeV case being accommodated before the cut-off is reached; these being the (j, k) modes (1,0), (1,1), (2,0), (1,2) and (2,1) (note that (0,1) and (0,2) are excluded by the selection rules given in section 6.1 of Ref. [133]).

Chapter 9

Large A_t Without the Desert

This chapter will explore the RGEs of a number of parameters from the unification scale to the electroweak scale, in particular focusing on achieving a large Trilinear soft parameter A_t, then using the achieved values of A_t in our models to estimate the necessary size of the lightest stop mass that fits with the currently observed Higgs mass.

9.1 Introduction

The discovery of a scalar particle of mass $m_h \sim 125.5$ GeV [3, 4], consistent with the SM Higgs boson, in the context of the MSSM, motivates us to consider models of SUSY breaking in which stop masses are heavy (of the order of 10 TeV or greater), or models in which a sufficiently large A_t can be generated at low scales. In most models of SUSY breaking, choosing heavy stops results in the entire coloured sparticle spectrum becoming rather heavy, beyond the reach of the LHC, and is consequently phenomenologically less interesting.[1] The second possibility, of large A_t, allows for light stops perhaps below 1 TeV, which is allowed by current collider bounds [101, 102], and is aesthetically preferred as it greatly reduces the required fine tuning of the Higgs mass from $\delta m^2_{H_u}$.

Models of SUSY breaking with a large A_t at the electroweak scale are usually considered rather difficult to obtain however. For example, in a generic supergravity mediated scenario, one should expect all trilinear soft breaking terms, $A_{u/d/e}(i, j)$, to be of the same order, such that a model in which $A_u(3, 3) = A_t$ is sufficiently large is already excluded by flavour constraints on the other off-diagonal elements. Additional *ad hoc* symmetries are then required without motivation, to reduce the soft breaking terms to the diagonal elements only. Equally, in minimal gauge mediated SUSY breaking (mGMSB) trilinear terms, such as A_t , are vanishing at the SUSY breaking scale M, and a large A_t can only be generated via a rather long period of renormalisation

[1] Some recent interesting alternatives may be found in Refs. [98–100].

group evolution. This requires the SUSY breaking scale to be very high, which is also detrimental to the naturalness of the theory.

A purely radiatively generated A_t does, however, have some positive features: the relative hierarchy of Yukawas and the large size of the top Yukawa, Y_t, allows for a hierarchy amongst the trilinear soft breaking terms in which A_t is driven through RGEs almost entirely from the gluino mass M_3, where such a hierarchy between trilinear breaking terms can naturally satisfy flavour changing neutral current (FCNC) constraints. It is therefore worthwhile to consider extensions of the MSSM that may accelerate the RGE evolution of Y_t or A_t or both.

In this chapter we will show that a 5D MSSM with compactification scale of $O(10-10^3)$ TeV, [2] and correspondingly a low unification scale of 10^9 TeV or lower, can naturally (through power law running [105]) achieve a large A_t at low scales. The largeness of A_t is driven by the size of the gluino mass M_3, which is necessary to be above collider bounds, but is largely independent of how SUSY is broken. We simply assume that $A_t(M_{GUT}) \sim 0$ and is entirely generated through renormalisation. In addition we have explored the case when all three generations are on the boundary and the "split families" case when the 3^{rd} generation of matter multiplets is on the boundary and the first two are in the bulk. Our results hold similarly for both cases, but the second may be more favourable to generate a hierarchy of soft masses $m^2_{(Q,U,D)_3} \ll m^2_{(Q,U,D)_{1,2}}$, which should be more natural and phenomenologically more interesting as stops can then be much lighter, and within reach of the LHC.

9.2 Generating large A_t in the 5D MSSM

In this section we describe the details and the setup of our model, we describe our parameterisation of the UV boundary conditions (such as the SUSY breaking and the electroweak boundary conditions). We then discuss our results for the evolution of various parameters of our model.

9.2.1 The setup

We define the 5D MSSM to be a field theory on a four dimensional spacetime, times an interval of length R in which the SM $SU(3)_c \times SU(2)_L \times U(1)_Y$ gauge fields and the Higgses (H_u, H_d) propagate into the fifth dimension. As a result, these fields will have KK modes which contribute to the RGEs at $Q > 1/R$, and additional matter associated with the five dimensional $\mathcal{N} = 1$ super Yang-Mills. Different possibilities of localisation for the matter fields can be studied, however, we shall consider first the limiting case with SM matter fields restricted to the $y = 0$ brane, and we supply the RGEs for this scenario in section 9.5. Therefore there will be no additional KK contributions from

[2] As in our model the KK mode of the bulk $U(1)$ supplies a Z', collider exclusions set a lower bound on the compactification scale to be a O(5 TeV).

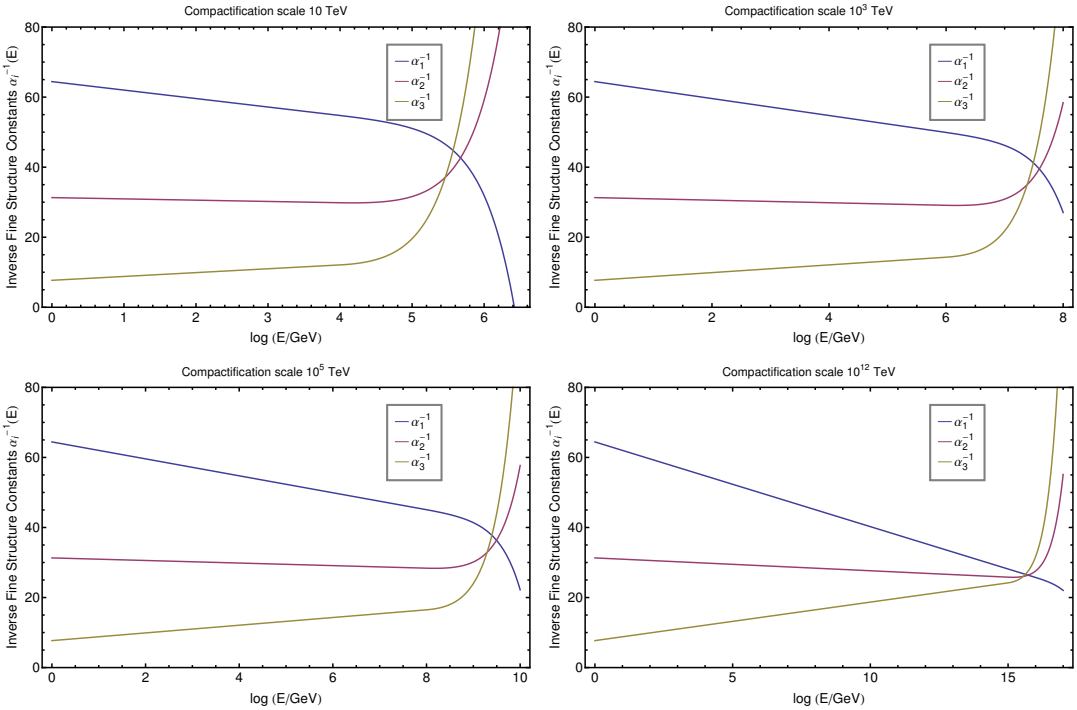


Figure 9.1: *Running of the inverse fine structure constants $\alpha^{-1}(E)$, for three different values of the compactification scales 10 TeV (top left panel), 10^3 TeV (top right), 10^5 TeV (bottom left) and 10^{12} TeV (bottom right), with M_3 of 1.7 TeV, as a function of log(E/GeV).*

these matter fields to the RGEs. In a specific setup, only the third family is restricted to the brane, while the light generations are allowed to propagate in the bulk. Note, however, that from the point of view of numerical results this case is not greatly different from restricting all the three generations to the brane, as the only large effects in the renormalisation group evolution are due to the third family coefficients, while the first two generations play only a minor role. Even if in the following we will explicitly discuss the case of all three fermion families restricted to the brane, we have checked numerically that restricting to the brane only the third family does not qualitatively change our conclusions. Note also that five dimensional super Yang-Mills has additional matter fields, such as colour adjoint chiral superfields [106, 107], compared to its four dimensional counterparts and these can influence the RGEs.

Regarding the breaking of SUSY, whilst gauge mediation is favoured (and some recent work on gauge mediated SUSY breaking in a five dimensional context may be found in Refs. [108–114]), ultimately the universality of squark massses in GMSB means that even though the gaugino mediated limit [115–118] might allow for light squarks (and 5D RGE evolution allows for a large A_t and the observed Higgs mass), the collider bounds on first and second generation squarks [119, 123], in the supra-TeV range, would apply also to

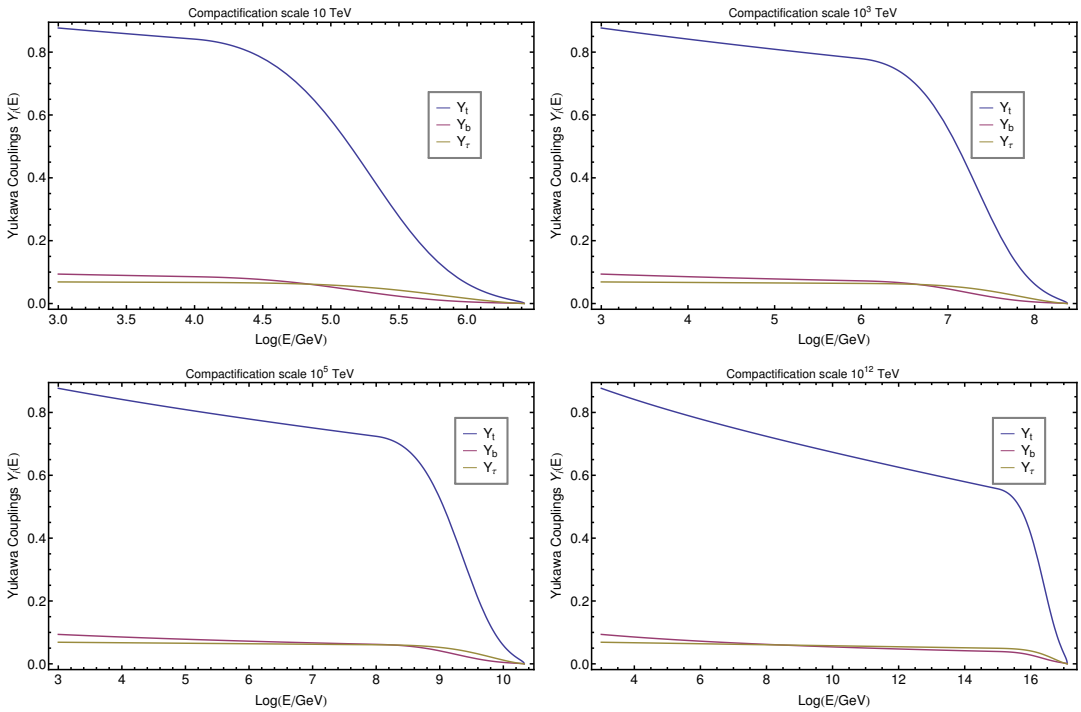


Figure 9.2: *Running of Yukawa couplings Y_i, for three different values of the compactification scales: 10 TeV (top left panel),* 10^3 *TeV (top right),* 10^5 *TeV (bottom left) and* 10^{12} *TeV (bottom right), with* $M_3[10^3]$ *of 1.7 TeV, as a function of log(E/GeV).*

the 3^{rd} generation squarks, i.e. the stops, which as discussed before is both phenomenologically less interesting and unnatural. Therefore we wish for some other description of SUSY breaking that may allow for stops to be lighter than their first and second generation counterparts, such as in Refs. [99, 100]. In this work we will therefore be rather agnostic about the precise details of how SUSY is broken, and as a result our conclusions will apply quite generally. We do, however, make some minimal specifications:

- We take as inputs the Yukawa and gauge couplings at the SUSY scale, 1 TeV.
- We will assume SUSY breaking occurs at the unification scale, which is found by finding the scale at which $g_1 = g_2$, which is lowered compared to the 4D MSSM, by the effects of the compactification.
- We specify the value of the gluino mass, M_3 at 1 TeV.
- We take the trilinear soft breaking terms, $A_{u/d/e}$, to vanish at the unification scale.

Our procedure is to solve the combined set of differential equations numerically using the above conditions, taking the "third family" approximation

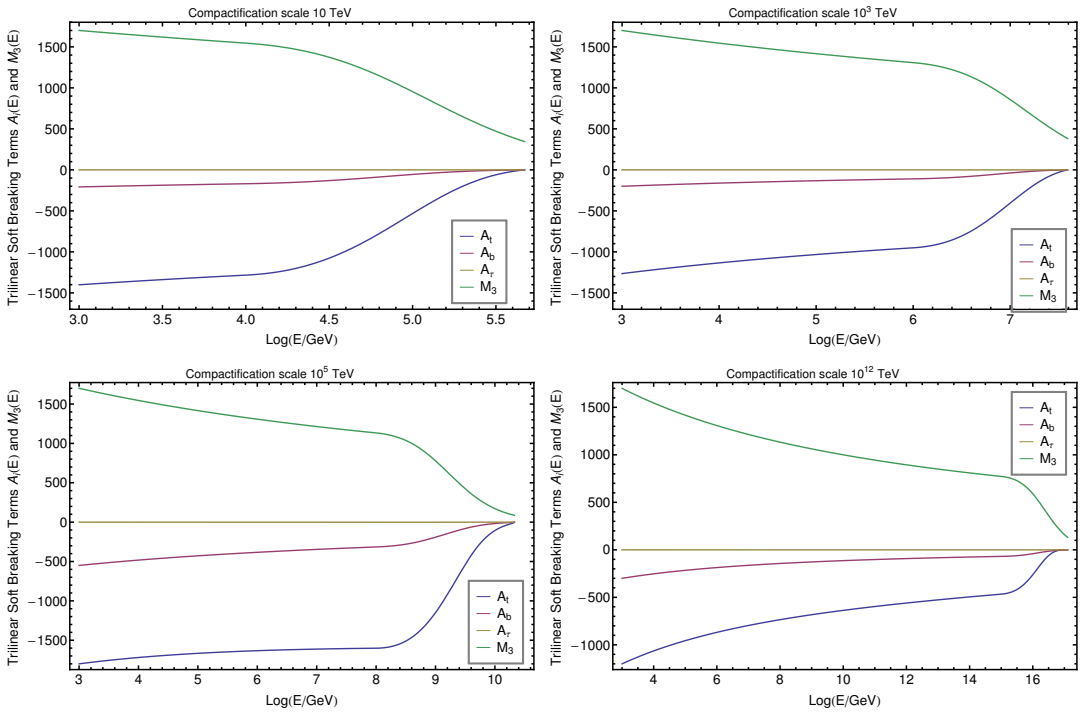


Figure 9.3: *Running of trilinear soft terms* $A_i(3,3)(E)$*, for three different values of the compactification scales 10 TeV (top left panel),* 10^3 *TeV (top right),* 10^5 *TeV (bottom left) and* 10^{12} *TeV (bottom right), with* $M_3[10^3]$ *of 1.7 TeV, as a function of log(E/GeV).*

in which we only evolve the third generation RGEs; although the full RGEs are supplied in section 9.5. This approximation is quite standard and is due to the relative smallness of the other Yukawa couplings (at least one order of magnitude) compared to those of the third generation, and as a result the other A-term values are also very small. We further specified some parameters such as μ, B_μ and the value of the sfermion masses ($\sim$ 1 TeV) so as to allow for the RGEs to be solved, but these do not affect the overall result. We solved the differential equations between $Q_{min} = 10^3$ GeV and Q_{max}, which was typically only one order larger than the unification scale, for each scenario explored. The details of the RGEs and how the KK summation is accounted for is discussed in section 9.5.

An interesting feature of the 5D MSSM is the approximate unification of gauge couplings [127–131], which is here calculated to one-loop and presented in Fig. 9.1 for various compactification scales. The key feature of Fig. 9.1 is that with a larger compactification radius the unification scale can be significantly lowered, lowering the desert of scales between the electroweak scale and unification. In this work we will take the unification scale to be the scale of SUSY breaking such that a lower SUSY breaking scale will also assist in improving the naturalness of each model, as we shall see later.

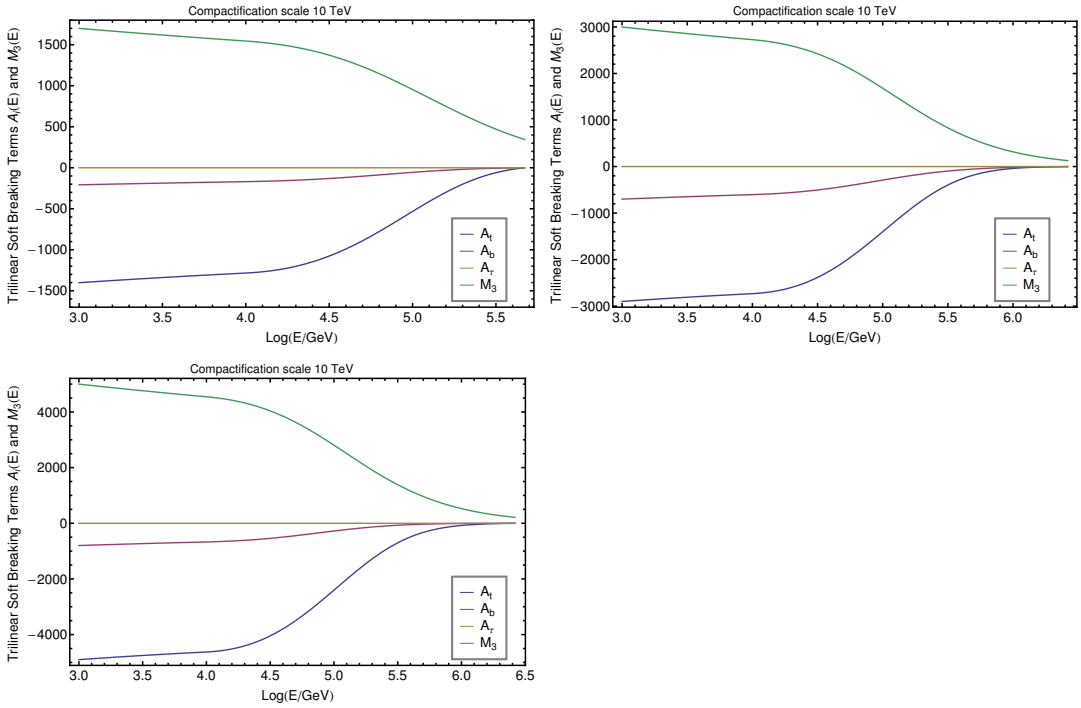


Figure 9.4: *Running of trilinear soft terms $A_i(3,3)(E)$, for three different values of gluino masses, M_3: 1.7 TeV (top left panel), 3 TeV (top right panel) and 5 TeV (bottom panel), with R^{-1} of 10 TeV, as a function of log(E/GeV).*

We also specify the Yukawa coupling RGE [53, 57, 72, 133, 134] boundary conditions at 1 TeV, which interestingly appears to vanish when evolved to the unification scale as shown in Fig. 9.2.

Let us now focus on the evolution of the A_t terms. As mentioned before, we fix a low scale value of the gluino mass M_3 and set a high scale boundary condition that the A_i's vanish, and then solve the set of equations. The results are presented in Fig. 9.3 for various compactification radii, and then for a fixed radius of 10 TeV but for varying gluino mass M_3 in Fig. 9.4. We see in Fig. 9.3 that by increasing the compactificaton radius one can increase the size of the trilinear soft breaking term. Fig. 9.4 shows that after a reasonable period of renormalisation group evolution, the A_t mimics the magnitude of the final value of the gluino mass at $1/R \sim 10$ TeV, such that at low scales $|A_t| \sim M_3$. Therefore, for this compacitification radius an $\mathcal{O}(2$ TeV) gluino can generate a reasonably large size A_t at low scales, but with an initially low unification scale. If we associate the unification scale with the messenger scale, which is where we assume the A-terms vanish, in the context of GMSB for example, this suggests that we can still have a low messenger scale of $10^6 - 10^9$ GeV, for a sufficiently large compactification radius. Equally we could have a small compactification radius, in which case we would need a very high initial scale of running to obtain similar sized A-terms, which is detrimental to the naturalness of the theory, as pictured Fig. 9.3 bottom right panel. To summarise, we may

achieve a large A_t term by exchanging a high initial SUSY breaking scale such as in the four dimensional MSSM, for a larger compactification radius and a lower initial SUSY breaking scale. Such a scenario has improved naturalness properties and is favourable from this perspective.

9.3 Light Stops Without the Desert

An important result of obtaining a large A_t at low scales is that one may then achieve the correct Higgs mass with a lower stop mass scale. Using the (MSSM) one-loop Higgs mass in the limit $m_{A^0} \gg m_Z$ [137–141] one has

$$m_{h,1}^2 \simeq m_z^2 \cos^2 2\beta + \frac{3}{4\pi^2}\frac{m_t^4}{v_{ew}^2}\left[\ln\frac{M_S^2}{m_t^2} + \frac{X_t^2}{M_S^2}\left(1 - \frac{X_t^2}{12M_S^2}\right)\right], \tag{9.1}$$

where v_{ew} is the electroweak Higgs VEV, $X_t = A_t - \mu\cot\beta$ and $M_S^2 = m_{\tilde{t}_1} m_{\tilde{t}_2}$. Fixing $m_{h,1} = 125.5$ GeV, $m_Z = 91$ GeV, $\mu = 200$ for $\tan\beta = 10$ we can see in Fig. 9.5 that for representative values of A_t achievable in the 5D MSSM, one may easily accommodate the lightest stop mass in the sub-TeV range.

Note that the Higgs mass at low scale is below the KK scale, which justify the use of a pure MSSM one-loop Higgs mass formula.

Let us also discuss the model's dependence on the value of $\tan\beta$ as pictured in Fig. 9.6. The precise value of $\tan\beta$ will depend greatly on how μ and B_μ are addressed in the context of SUSY breaking, and hence the solution of the vacuum tadpole equations. Regardless of this, for values of $\tan\beta > 10$ the functions are approximately flat and we expect the value to fall within this interval. We expect that the μ term is naturally of the order of the electroweak scale, where in Fig. 9.5 we took a slightly large μ value of 400 GeV and in Fig. 9.6 we took 200 GeV, leading typically to light Higgsinos and Winos.

These models have an interesting additional naturalness feature: the lowered unification and SUSY breaking scale necessary, compared to the 4D MSSM, results in a lowered cutoff to radiative corrections, for example, on stops from the gluino:

$$\delta m_{\tilde{t}}^2 = \frac{2g_3^2}{3\pi^2} M_3^2 \log\left(\frac{M_{\not{\text{SUSY}}}}{M_3}\right). \tag{9.2}$$

If the SUSY breaking scale can then be kept low enough, this can allow for stops remaining light as well as reduced radiative corrections on the Higgs mass,

$$\delta m_{H_u}^2 = -\frac{3y_t^2}{8\pi^2}(m_{Q_3}^2 + m_{U_3}^2 + A_t^2)\log\left(\frac{M_{\not{\text{SUSY}}}}{m_{\tilde{t}}}\right). \tag{9.3}$$

The details will depend on how SUSY is parameterised at the SUSY breaking scale and as such will be part of a future study, however it should be clear that an $M_{\not{\text{SUSY}}} \sim M_{GUT}$ of 10^6 GeV would fair much better than 10^{16} GeV, with regard to radiative corrections to fine tuning.

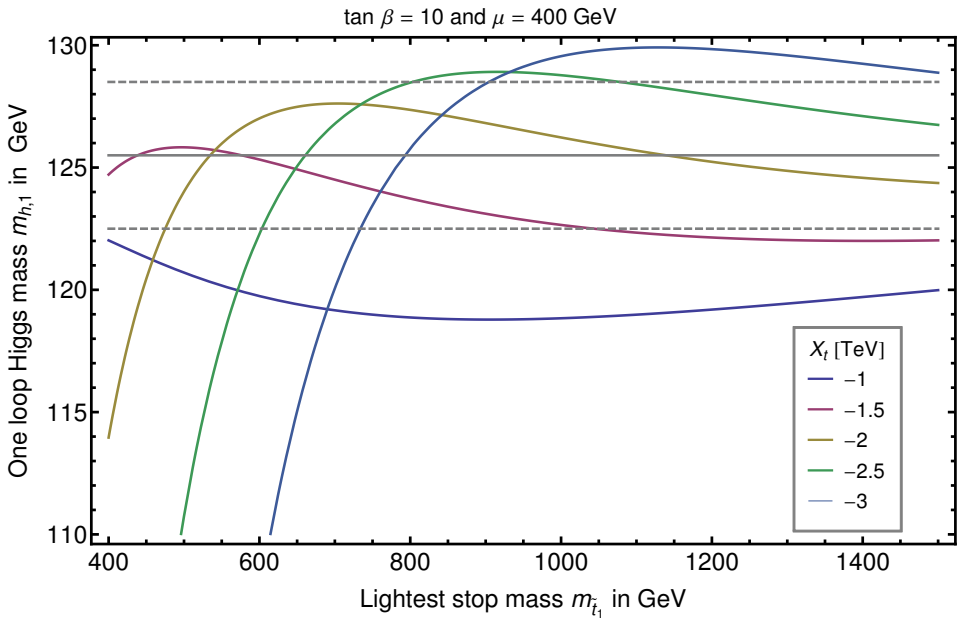


Figure 9.5: *A plot of the one loop Higgs mass versus the lightest stop mass for representative values of* $X_t = A_t - \mu \cot \beta$*, corresponding to those of the 5D MSSM.*

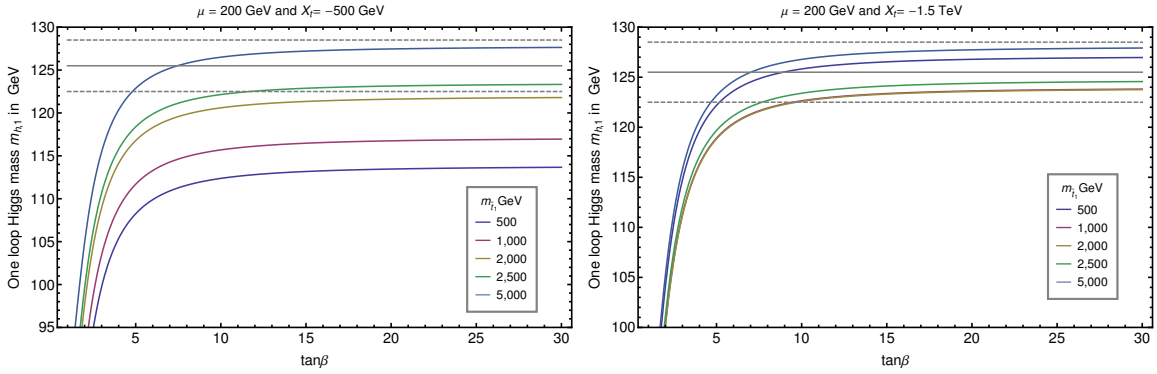


Figure 9.6: *A plot of the one loop Higgs mass versus* $\tan \beta$ *for different values of the stop mass, for* $X_t = A_t - \mu \cot \beta$ *of* -500 *GeV (left panel) and* -1.5 *TeV (right panel).*

9.4 Compatible models of SUSY breaking

As the feature of a large A_t term from renormalisation group evolution with a small compactification scale is rather generic, we have so far been agnostic about the specific details of how SUSY is broken. There are a number of models of SUSY breaking that may be compatible with our setup, so here we describe them and some additional features of the sparticle spectrum that we can infer.

9.4.1 Sequestered super-gravity mediation

Four dimensional super-gravity mediation has a number of issues that need to be overcome. Firstly the theory is non-renormalisable and as such one-loop calcutions of the soft masses should not be trusted. Even if the resulting soft masses are all set from dimensional analysis arguments, this leads to large FCNCs as all entries in the $A_{u/d/e}(3,3)$ would be of the same order, as discussed in the section 9.1. Furthermore one should generically expect large mixings between the Kähler potentials of the visible sector and SUSY breaking matter fields, such that soft scalar masses are not flavour universal.

Sequestered or brane to brane super-gravity mediation [142–146] overcomes many of these drawbacks: SUSY breaking effects are calculable and finite at one-loop. Mixing of Kähler potentials at tree level does not arise due to spatial separation of the visible and hidden sectors. In this scenario, A-terms would be vanishing at the high scale and our results might then be compatible with this scenario by having purely radiatively induced A-terms. Sequestered supergravity mediation is therefore a favourable model compatible with our results.

Even though we do not specify many details of the setup, we may already make some comments on the sort of spectrum of this scenario:

- The lightest superparticle may be the sneutrino (stau) or neutralino (neutral Wino, Bino or Higgsino), generically.
- The gravitino mass is given by $M_{3/2} \sim F/\sqrt{3}M_{Pl}$ and may arguably be related to that of the gluino mass, $M_3 = -3g_3^2 m_{3/2}/16\pi^2$, which we took to be just above the current exclusion, 1.7 TeV [150].

Any physical effect due to "anomaly mediation" is an effect of integrating out the non-propagating degrees of freedom of the super-gravity multiplet, it should also, by default, be accounted for in the parameterisation of the soft terms.

Of course a more complete picture will have some drawbacks that should be overcome. A natural model should have third generation squarks lighter than the first and second (perhaps from spatially localising the fields away from the source of SUSY breaking). Yet, it should also explain the generation of the Higgs sector soft masses that allow for a solution of μ/B_μ and generate electroweak symmetry breaking, and such problems are easier to address in the context of gravity mediation. We have checked that having the first and second generations in the bulk and the third generation on the boundary does not effect our results, essentially as the modification of the RGEs between each case only effects the Yukawa terms and not the terms proportional to gauge couplings, and in particular the dominant effect is from the gluino soft mass.

9.4.2 Gauge mediation

We may also expect a gauge mediated scenario compatible with this setup. In this case:

- The gravitino is the LSP with sneutrino or neutralino the NLSP.
- We expect approximately flavour diagonal (if not flavour universal) soft terms.
- The gaugino mass is $M_3 = g_3^2 \Lambda_{\tilde{f}}/16\pi^2$ and is not directly related to $m_{3/2} \sim F/\sqrt{3}M_{Pl}$, although we could take $\Lambda_{\tilde{f}} = F/M_{mess}$ and $M_{mess} \sim M_{unification}$, where $M_{unification} \sim \mathcal{O}(10-100) \times 1/R$ i.e. ten times the compacitifaction radius, as can be seen in Fig. 9.1.

Again the μ/B_μ problem should be addressed and indeed the issue of a natural spectrum in the squark sector (light stops). A μ-term of a few hundred GeV should also lead to light Higgsinos, observable at the ILC.

In either scenario we intend for naturally light stops, as can be accommodated by the large A_t term, but for which we do not yet specify a fully complete picture. This setup may also be compatible with other models of SUSY breaking, although a "natural spectrum" is possible in some scenarios, light stops may not always be achievable in all models. In the cases discussed above, the soft terms are finite and do not depend on the cutoff, all three being non-local, the first two being due to one loop diagrams that propagate in the bulk from boundary to boundary, where the radius acts as a regulator on the loop diagrams.

9.5 RGEs for 5D MSSM

In this section we supply the beta functions used in this main chapter's. We define $t = \log(Q^2/Q_0^2)$ where we take the reference scale $Q_0^2 = m_Z^2$ and $\beta_A = 16\pi^2 dA/dt$. For reference, the gauge theory and the Higgs are in the bulk and matter fields are all localised to a brane.

9.5.1 Gauge couplings

The one loop beta function for the gauge couplings if $t > \log(1/R)/\log(10)$ are given by

$$16\pi^2 \frac{dg_i(t)}{dt} = b^i_{MSSM} g_i^3(t) + b^i_{5D} g_i^3(t)(S(t)-1) \,, \tag{9.4}$$

where $i = 1,2,3$ and $S(p) = (m_Z R)e^p$, where $p = t\log(10) - \log(m_Z)$. For the 4D MSSM $b^i = (33/5, 1, -3)$ and for five dimensions $b^i_{5D} = (6/5, -2, -6)$. The

fine structure constants may be defined from $\alpha_i = g_i^2/4\pi$. Instead one could consider including one KK mode at a time, in which case one finds

$$\beta_{g_i} = \frac{g_i^3}{16\pi^2}\left(b^i_{MSSM} + n\tilde{b}^i_{5D}\right) \quad , \quad \beta_{M_i} = \frac{2g_i^2 M_i}{16\pi^2}\left(b^i_{MSSM} + n\tilde{b}^i_{5D}\right). \tag{9.5}$$

We instead use the KK summed expression above.

9.5.2 Yukawa couplings

The beta functions for the Yukawa couplings may be related to the matrices of anomalous dimensions

$$\beta_Y^{ijk} = \gamma_n^i Y^{njk} + \gamma_n^i Y^{ink} + \gamma_n^k Y^{ijn}. \tag{9.6}$$

The one-loop RGEs for Yukawa couplings in the 4D MSSM are given by (see Fig. 9.7)

$$\beta^{(1)}_{Y_u} = 3Y_u Y_u^\dagger Y_u + Y_u Y_d^\dagger Y_d - \frac{1}{15}Y_u\Big(13g_1^2 + 45g_2^2 + 80g_3^2 - 45\mathrm{Tr}\Big(Y_u Y_u^\dagger\Big)\Big) \tag{9.7}$$

$$\beta^{(1)}_{Y_d} = 3Y_d Y_d^\dagger Y_d + Y_d Y_u^\dagger Y_u + Y_d\Big(-3g_2^2 - \frac{16}{3}g_3^2 - \frac{7}{15}g_1^2 + \mathrm{Tr}\Big(Y_e Y_e^\dagger + 3Y_d Y_d^\dagger\Big)\Big) \tag{9.8}$$

$$\beta^{(1)}_{Y_e} = 3Y_e Y_e^\dagger Y_e + Y_e\Big(-3g_2^2 - \frac{9}{5}g_1^2 + \mathrm{Tr}\Big(Y_e Y_e^\dagger\Big) + 3\mathrm{Tr}\Big(Y_d Y_d^\dagger\Big)\Big). \tag{9.9}$$

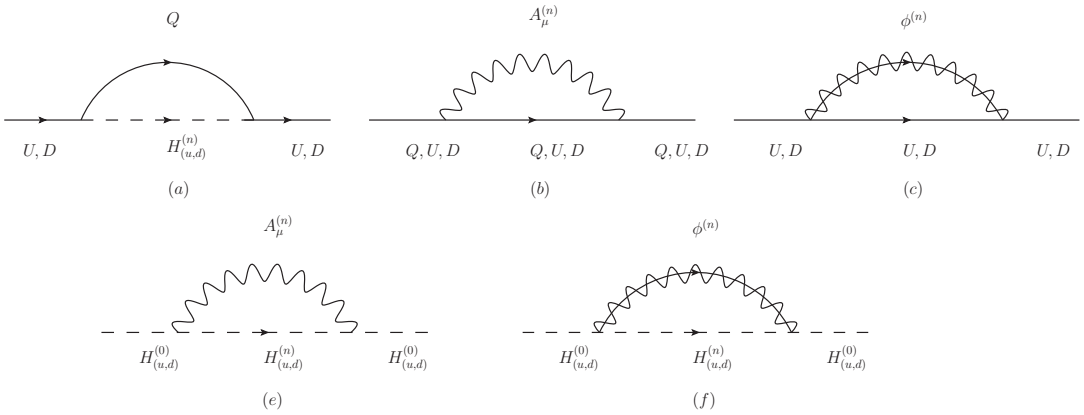


Figure 9.7: *The wavefunction renormalisation contribution for the five dimensional Yukawas.*

The five dimensional contribution is given by

$$\beta^{(1)}_{(5D)Y_u}[t] = Y_u\left[\left(6Y_u^\dagger Y_u + 2Y_d^\dagger Y_d\right) - \left(\frac{34}{30}g_1^2 + \frac{9}{2}g_2^2 + \frac{32}{3}g_3^2\right)\right] \quad (9.10)$$

$$\beta^{(1)}_{(5D)Y_d}[t] = Y_d\left[(6Y_d^\dagger Y_d + 2Y_u^\dagger Y_u) - \left(\frac{19}{30}g_1^2 + \frac{9}{2}g_2^2 + \frac{32}{3}g_3^2\right)\right] \quad (9.11)$$

$$\beta^{(1)}_{(5D)Y_e}[t] = Y_e\left[6Y_e^\dagger Y_e - \left(\frac{33}{10}g_1^2 + \frac{9}{2}g_2^2\right)\right]. \quad (9.12)$$

9.5.3 Trilinear soft breaking parameters

The 4D MSSM soft breaking parameters at one loop, as pictured in Fig. 9.8 are given by

$$\begin{aligned}\beta^{(1)}_{A_u} &= +2Y_uY_d^\dagger A_d + 4Y_uY_u^\dagger A_u + A_uY_d^\dagger Y_d + 5A_uY_u^\dagger Y_u - \frac{13}{15}g_1^2A_u - 3g_2^2A_u - \frac{16}{3}g_3^2A_u \\ &\quad +3A_u\mathrm{Tr}\Big(Y_uY_u^\dagger\Big) + Y_u\Big(6g_2^2M_2 + 6\mathrm{Tr}\Big(Y_u^\dagger A_u\Big) + \frac{26}{15}g_1^2M_1 + \frac{32}{3}g_3^2M_3\Big) \quad (9.13)\\ \beta^{(1)}_{A_d} &= +4Y_dY_d^\dagger A_d + 2Y_dY_u^\dagger A_u + 5A_dY_d^\dagger Y_d + A_dY_u^\dagger Y_u - \frac{7}{15}g_1^2A_d - 3g_2^2A_d - \frac{16}{3}g_3^2A_d \\ &\quad +3A_d\mathrm{Tr}\Big(Y_dY_d^\dagger\Big) + A_d\mathrm{Tr}\Big(Y_eY_e^\dagger\Big) + Y_d\Big(2\mathrm{Tr}\Big(Y_e^\dagger A_e\Big) \\ &\quad +6g_2^2M_2 + 6\mathrm{Tr}\Big(Y_d^\dagger A_d\Big) + \frac{14}{15}g_1^2M_1 + \frac{32}{3}g_3^2M_3\Big) \quad (9.14)\\ \beta^{(1)}_{A_e} &= +4Y_eY_e^\dagger A_e + 5A_eY_e^\dagger Y_e - \frac{9}{5}g_1^2A_e - 3g_2^2A_e + 3A_e\mathrm{Tr}\Big(Y_dY_d^\dagger\Big) + A_e\mathrm{Tr}\Big(Y_eY_e^\dagger\Big) \\ &\quad +Y_e\Big(2\mathrm{Tr}\Big(Y_e^\dagger A_e\Big) + 6g_2^2M_2 + 6\mathrm{Tr}\Big(Y_d^\dagger A_d\Big) + \frac{18}{5}g_1^2M_1\Big). \quad (9.15)\end{aligned}$$

In the 5D MSSM these are given by:

$$\begin{aligned}\beta^{(1)}_{(5D)A_u}[t] &= A_u\left(\left(18Y_u^\dagger Y_u + 2Y_d^\dagger Y_d\right) - \left(\frac{34}{30}g_1^2 + \frac{9}{2}g_2^2 + \frac{32}{3}g_3^2\right)\right) + 4A_dY_d^\dagger Y_u \\ &\quad +Y_u\left(\frac{34}{15}g_1^2M_1 + 9g_2^2M_2 + \frac{64}{3}g_3^2M_3\right) \quad (9.16)\\ \beta^{(1)}_{(5D)A_d}[t] &= A_d\left(\left(18Y_d^\dagger Y_d + 2Y_u^\dagger Y_u\right) - \left(\frac{19}{30}g_1^2 + \frac{9}{2}g_2^2 + \frac{32}{3}g_3^2\right)\right) \\ &\quad +4A_uY_u^\dagger Y_d + 2A_eY_e^\dagger Y_d + Y_d\left[\frac{19}{15}g_1^2M_1 + 9g_2^2M_2 + \frac{64}{3}g_3^2M_3\right] \quad (9.17)\\ \beta^{(1)}_{(5D)A_e}[t] &= A_e\left(18Y_e^\dagger Y_e - \left(\frac{33}{10}g_1^2 + \frac{9}{2}g_2^2\right)\right) + 6A_dY_d^\dagger Y_e + Y_e\left(\frac{33}{5}g_1^2M_1 + 9g_2^2M_2\right). \quad (9.18)\end{aligned}$$

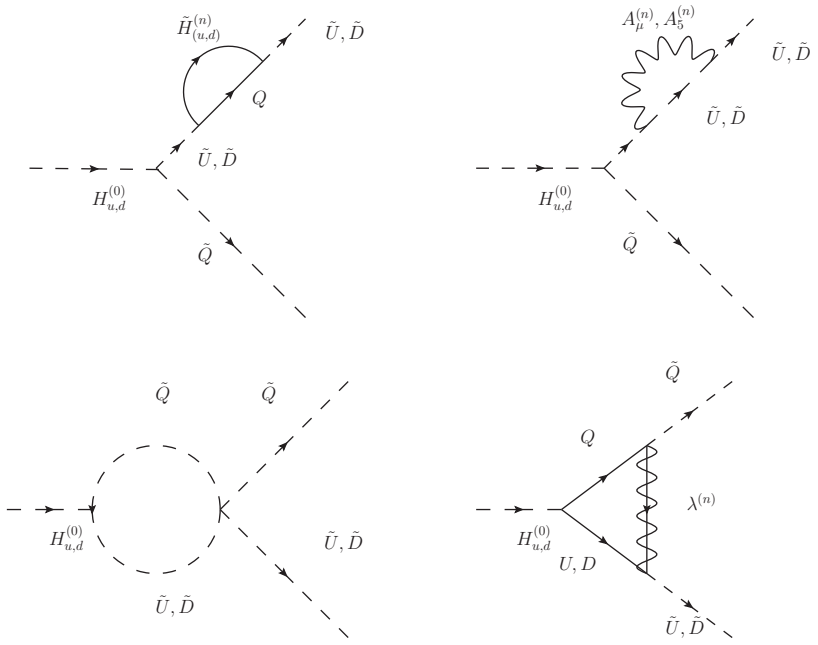


Figure 9.8: *The diagrams contributing to the five dimensional RGEs of the trilinear soft breaking parameters.*

9.5.4 Soft masses

We expect the gaugino soft masses to run as following

$$\beta^{(1)}_{M_i}(t) = 2b^i_{MSSM} M_i(t) g_i^2(t) + 2b^i_{(5D)} M_i(t) g_i^2(t)(S(t)-1). \tag{9.19}$$

The scalar soft masses have five dimensional RGE contributions as pictured in Fig. 9.9. The four dimensional MSSM contribution is

$$\begin{aligned}
\beta^{(1)}_{m_q^2} &= -\frac{2}{15}g_1^2\mathbf{1}|M_1|^2 - \frac{32}{3}g_3^2\mathbf{1}|M_3|^2 - 6g_2^2\mathbf{1}|M_2|^2 + 2m_{H_d}^2 Y_d^\dagger Y_d + 2m_{H_u}^2 Y_u^\dagger Y_u + 2A_d^\dagger A_d \\
&\quad + 2A_u^\dagger A_u + m_q^2 Y_d^\dagger Y_d + m_q^2 Y_u^\dagger Y_u + 2Y_d^\dagger m_d^2 Y_d + Y_d^\dagger Y_d m_q^2 + 2Y_u^\dagger m_u^2 Y_u \\
&\quad + Y_u^\dagger Y_u m_q^2 + \frac{1}{\sqrt{15}}g_1\mathbf{1}\sigma_{1,1} \qquad (9.20) \\
\beta^{(1)}_{m_u^2} &= -\frac{32}{15}g_1^2\mathbf{1}|M_1|^2 - \frac{32}{3}g_3^2\mathbf{1}|M_3|^2 + 4m_{H_u}^2 Y_u Y_u^\dagger + 4A_u A_u^\dagger + 2m_u^2 Y_u Y_u^\dagger + 4Y_u m_q^2 Y_u^\dagger \\
&\quad + 2Y_u Y_u^\dagger m_u^2 - 4\frac{1}{\sqrt{15}}g_1\mathbf{1}\sigma_{1,1} \qquad (9.21) \\
\beta^{(1)}_{m_d^2} &= -\frac{8}{15}g_1^2\mathbf{1}|M_1|^2 - \frac{32}{3}g_3^2\mathbf{1}|M_3|^2 + 4m_{H_d}^2 Y_d Y_d^\dagger + 4A_d A_d^\dagger + 2m_d^2 Y_d Y_d^\dagger + 4Y_d m_q^2 Y_d^\dagger \\
&\quad + 2Y_d Y_d^\dagger m_d^2 + 2\frac{1}{\sqrt{15}}g_1\mathbf{1}\sigma_{1,1} \qquad (9.22) \\
\beta^{(1)}_{m_l^2} &= -\frac{6}{5}g_1^2\mathbf{1}|M_1|^2 - 6g_2^2\mathbf{1}|M_2|^2 + 2m_{H_d}^2 Y_e^\dagger Y_e + 2A_e^\dagger A_e + m_l^2 Y_e^\dagger Y_e + 2Y_e^\dagger m_e^2 Y_e \\
&\quad + Y_e^\dagger Y_e m_l^2 - \sqrt{\frac{3}{5}}g_1\mathbf{1}\sigma_{1,1} \qquad (9.23) \\
\beta^{(1)}_{m_e^2} &= -\frac{24}{5}g_1^2\mathbf{1}|M_1|^2 + 2\Big(2m_{H_d}^2 Y_e Y_e^\dagger + 2A_e A_e^\dagger + 2Y_e m_l^2 Y_e^\dagger + m_e^2 Y_e Y_e^\dagger + Y_e Y_e^\dagger m_e^2\Big) \\
&\quad + 2\sqrt{\frac{3}{5}}g_1\mathbf{1}\sigma_{1,1} \qquad (9.24)
\end{aligned}$$

where

$$\sigma_{1,1} = \sqrt{\frac{3}{5}}g_1\Big(-2\mathrm{Tr}\Big(m_u^2\Big) - \mathrm{Tr}\Big(m_l^2\Big) - m_{H_d}^2 + m_{H_u}^2 + \mathrm{Tr}\Big(m_d^2\Big) + \mathrm{Tr}\Big(m_e^2\Big) + \mathrm{Tr}\Big(m_q^2\Big)\Big). \qquad (9.25)$$

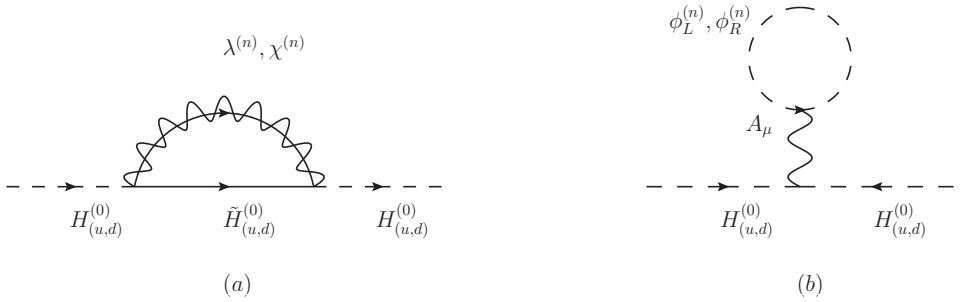


Figure 9.9: *The diagrams for the five dimensional RGEs of the soft scalar masses at one loop.*

In the 5D MSSM these are given by:

$$\beta^{(1)}_{(5D)m_q^2} = \left[-\frac{4}{15}g_1^2\mathbf{1}|M_1|^2 - \frac{64}{3}g_3^2\mathbf{1}|M_3|^2 - 9g_2^2\mathbf{1}|M_2|^2 + \frac{\sqrt{2}}{\sqrt{15}}g_1\mathbf{1}\sigma_{1,1}\right] \quad (9.26)$$

$$\beta^{(1)}_{(5D)m_l^2} = \left[-\frac{12}{5}g_1^2\mathbf{1}|M_1|^2 - 9g_2^2\mathbf{1}|M_2|^2 - \sqrt{\frac{6}{5}}g_1\mathbf{1}\sigma_{1,1}\right] \quad (9.27)$$

$$\beta^{(1)}_{(5D)m_u^2} = \left[-\frac{64}{15}g_1^2\mathbf{1}|M_1|^2 - \frac{64}{3}g_3^2\mathbf{1}|M_3|^2 - 4\frac{\sqrt{2}}{\sqrt{15}}g_1\mathbf{1}\sigma_{1,1}\right] \quad (9.28)$$

$$\beta^{(1)}_{(5D)m_d^2} = \left[-\frac{16}{15}g_1^2\mathbf{1}|M_1|^2 - \frac{64}{3}g_3^2\mathbf{1}|M_3|^2 + 2\frac{\sqrt{2}}{\sqrt{15}}g_1\mathbf{1}\sigma_{1,1}\right] \quad (9.29)$$

$$\beta^{(1)}_{(5D)m_e^2} = \left[-\frac{48}{5}g_1^2\mathbf{1}|M_1|^2 + 2\sqrt{\frac{6}{5}}g_1\mathbf{1}\sigma_{1,1}\right]. \quad (9.30)$$

The one-loop RGEs for the two Higgs doublet soft masses in the 4D MSSM are given by

$$\begin{aligned}\beta^{(1)}_{m_{H_d}^2} = & -\frac{6}{5}g_1^2|M_1|^2 - 6g_2^2|M_2|^2 - \sqrt{\frac{3}{5}}g_1\sigma_{1,1} + 6m_{H_d}^2\mathrm{Tr}\Big(Y_dY_d^\dagger\Big) + 2m_{H_d}^2\mathrm{Tr}\Big(Y_eY_e^\dagger\Big) \\ & +6\mathrm{Tr}\Big(A_d^*A_d^T\Big) + 2\mathrm{Tr}\Big(A_e^*A_e^T\Big) + 6\mathrm{Tr}\Big(m_d^2Y_dY_d^\dagger\Big) + 2\mathrm{Tr}\Big(m_e^2Y_eY_e^\dagger\Big) \\ & +2\mathrm{Tr}\Big(m_l^2Y_e^\dagger Y_e\Big) + 6\mathrm{Tr}\Big(m_q^2Y_d^\dagger Y_d\Big) \quad (9.31)\end{aligned}$$

$$\begin{aligned}\beta^{(1)}_{m_{H_u}^2} = & -\frac{6}{5}g_1^2|M_1|^2 - 6g_2^2|M_2|^2 + \sqrt{\frac{3}{5}}g_1\sigma_{1,1} + 6m_{H_u}^2\mathrm{Tr}\Big(Y_uY_u^\dagger\Big) \\ & +6\mathrm{Tr}\Big(A_u^*A_u^T\Big) + 6\mathrm{Tr}\Big(m_q^2Y_u^\dagger Y_u\Big) + 6\mathrm{Tr}\Big(m_u^2Y_uY_u^\dagger\Big). \quad (9.32)\end{aligned}$$

In 5D MSSM the two Higgs doublet soft masses obey the RGEs

$$\beta^{(1)}_{(5D)m_{H_d}^2} = \left[-\frac{12}{5}g_1^2|M_1|^2 - 9g_2^2|M_2|^2 - 2\sqrt{\frac{3}{5}}g_1\sigma_{1,1}\right] \quad (9.33)$$

$$\beta^{(1)}_{(5D)m_{H_u}^2} = \left[-\frac{12}{5}g_1^2|M_1|^2 - 9g_2^2|M_2|^2 + 2\sqrt{\frac{3}{5}}g_1\sigma_{1,1}\right]. \quad (9.34)$$

9.5.5 Bilinear parameters μ and B_μ

The one-loop beta function of μ and B_μ in the 4D MSSM are given by:

$$\beta_\mu^{(1)} = 3\mu \mathrm{Tr}\Big(Y_d Y_d^\dagger\Big) - \frac{3}{5}\mu\Big(5g_2^2 - 5\mathrm{Tr}\Big(Y_u Y_u^\dagger\Big) + g_1^2\Big) + \mu \mathrm{Tr}\Big(Y_e Y_e^\dagger\Big) \tag{9.35}$$

$$\begin{aligned}\beta_{B_\mu}^{(1)} &= 3B_\mu \mathrm{Tr}\Big(Y_d Y_d^\dagger\Big) - \frac{3}{5}B_\mu\Big(5g_2^2 - 5\mathrm{Tr}\Big(Y_u Y_u^\dagger\Big) + g_1^2\Big) + B_\mu \mathrm{Tr}\Big(Y_e Y_e^\dagger\Big) \\ &\quad +6\mu \mathrm{Tr}\Big(A_d Y_d^\dagger\Big) + \frac{6}{5}\mu\Big(5g_2^2 M_2 + 5\mathrm{Tr}\Big(A_u Y_u^\dagger\Big) + g_1^2 M_1\Big) + 2\mu \mathrm{Tr}\Big(A_e Y_e^\dagger\Big)\end{aligned} \tag{9.36}$$

.

In the 5D MSSM these are given by:

$$\beta_{(5D)\mu}^{(1)} = \mu\left[-\frac{6}{5}g_1^2 - \frac{9}{2}g_2^2\right] \tag{9.37}$$

$$\beta_{B_\mu}^{(1)} = -B_\mu\Big(\frac{9}{2}g_2^2 + \frac{6}{5}g_1^2\Big) + \mu\Big(9g_2^2 M_2 + \frac{12}{5}g_1^2 M_1\Big). \tag{9.38}$$

Chapter 10

Conclusions

In this thesis we derived the RGEs for Yukawa and gauge couplings in the general 2UED model for different scenarios, that of all matter fields propagating in the bulk or constrained to the brane. We observed that the physical observables in this model undergo rapid evolutions once the first KK threshold is crossed. However, in comparison with 1UED models, we find that this model is valid up to energy scales less than that of the 1UED model cases. This should lead to a means of distinguishing these two models. Note that the case of two extra spatial dimensions opens up a range of different compactification scenarios, as discussed in Appendix C, where we have found that in the general (all KK modes included) 2UED model the leading behaviour, as encompassed in the $S^2(t)$, dominates. Indeed, the fact that only a few of the first KK modes are absent has little effect on the numerical results, thus allowing us to make robust predictions, reducing considerably the impact of model dependence on the evolution equations and the results described in chapter 6.

The mass ratios in a 5D MSSM on a S^1/Z_2 orbifold, for different possibilities of matter field localisation, were discussed. That is, where they are either bulk propagating or localised to the brane. We found that the 5D MSSM has substantial effects on the scaling of fermion masses for both cases, including both quark and lepton sectors. We quantitatively analysed these quantities in the 5D MSSM with small, intermediate, and large $\tan\beta$ values, though we observed similar behaviours for all values of $\tan\beta$. We have shown that the scale dependence is no longer logarithmic, having a power law behaviour. We also found that for both scenarios the theory is valid up to the unification scale, receiving significant renormalization group corrections. Therefore the 5D MSSM promises exciting phenomenology for upcoming collider physics results.

In this thesis we also derived the RGEs for the Higgs quartic coupling and neutrino mass running for two distinct classes of 2UED models, again of all matter fields propagating in the bulk or localised to the brane. We obtain stronger constraints on the cut-off scale from the requirement of the stability of the Higgs potential in the bulk case. Whilst in the brane case the evolution of the quartic Higgs coupling has improved vacuum stability and λ is positive and finite from the electroweak scale all the way up to the unification scale.

We also compare our results with the 1UED model, where we find a more rapid evolution of the physical observables in the 2UED models.

On the other hand, in the neutrino sector, the evolution equations for the mixing angles, phases, and Δm^2_{atm} and Δm^2_{sol} are also considered. Once the first KK threshold is reached, these quantities increase as energy increase for the bulk case and decrease with energy in the brane case. However the effect is almost negligible for the mixing angles, while it can be sizeable for the evolution of the squared mass differences.

Finally we explored how a five dimensional extension of the MSSM may generate a sufficiently large A_t parameter to achieve the observed Higgs mass and have sub-TeV stops, perhaps observable at the LHC. We computed the full one-loop RGEs for all SUSY and soft breaking parameters, and then solved these equations for a given set of boundary conditions. The results were rather interesting: We found that Yukawa couplings may be made to unify and approximately vanish at the unification scale of the gauge couplings, for a low compactification scale, in this setup. Furthermore we found that the magnitude of A_t follows closely that of the magnitude of the gluino mass M_3 and increases as the compactification scale decreases, such that a large negative A_t may be achieved at low energies from a $10 - 10^4$ TeV compactification radius and RGE evolution from the unification scale, for a gluino mass above but not far from the current collider bounds of around 1600 GeV [150]. Such a result is sufficiently general and independent of how SUSY is broken. A key and generic point of this work is that one may achieve larger A_t terms at lower scales than are usually associated with the MSSM, by changing the UV physics and the RGEs. As such we should perhaps take the relative heavy size of the Higgs, at 125.5 GeV, as a prediction of new non-miminal physics that can effect RGEs, and not necessarily pessimistically conclude that stops are supra-TeV in scale. The compactification scale could be as low as a few TeV, with collider bounds on Z''s being the main lower bound on this value, though electroweak precision tests may also be an interesting indirect constraint to explore further, due to the additional matter in this type of scenario.

The size of $|A_t|$ is also bounded, and cannot be too large, as it results in an instability of the electroweak vacua to tunnel charge and colour breaking vacua. It is interesting to consider then the relationship between gluino mass M_3, the radius of compactification R, and the magnitude of A_t. For a fixed 10 TeV radius one cannot make M_3 arbitrarily large, or it induces too large an $|A_t|$ and the electroweak vacuum becomes unstable. Similarly for a fixed M_3, the radius cannot be made arbitrarily large, giving an indirect bound on the size of the extra dimension.

To extend this work it would be interesting to explore if warped or holographic scenarios [109, 112, 148] may also achieve a large A_t, as one expects logarithmic [130] rather than power law running in these models. In five dimensions one may also take advantage of non-decoupled D-terms [149,151,152] such as in Ref. [98] to achieve a larger tree level Higgs mass. More ambitiously, whilst in this work these RGEs have been solved numerically at one-loop, a full

and dedicated spectrum generator which implemented these 5D RGEs and various features may then give a far richer phenomenological study. Furthermore, this work may be extended up to two-loop level, where we would expect to find minor corrections compared to the one-loop level. It is therefore important to confirm that results and conclusions made at one loop are insensitive and still consistent (that is under control at two (and higher) loops. For instance one might be concerned that one loop linear sensitivity to the cutoff behaves as ΛR does not result in terms of the form $(\Lambda R)^2$ at two-loop, which would then indicate a break down of perturbation theory at renormalisation scales of the order of the compactification radius.

Appendix A

One-loop correction for gauge coupling coefficients in the SM, MSSM, 5D MSSM, 1UED and 2UED

In this appendix I will derive the numerical coefficients b_i of gauge couplings in various models.

One-loop correction for gauge coupling constants in the SM

The one-loop correction to gauge coupling constant RGEs in the SM can be found in Ref. [32]. It can be written as

$$16\pi^2 \frac{dg_i}{dt} = b_i^{SM} g_i^3 \ , \tag{A.1}$$

where

$$b_G^{SM} = \Big(\frac{11}{3} C_2(G) - \frac{4}{3} n_g C(R) - \frac{1}{3} n_h C_2(R) \Big) \ , \tag{A.2}$$

with n_g being the number of generations, n_h is the number of Higgs scalars and $C(R)\delta_{ij} = Tr(T_i T_j)$ for the representation R; $C_2(G)$, $C(R)$ and $C_2(R)$ refer to the guage bosons, fermions and Higgs scalar contribution respectively. Note that the gauge bosons belong to the adjoint representation of the group $SU(N)$; $C_2(G) = N$. The coefficient b_i can be determined as follows:

Firstly for the strong interaction: $SU(3)$

The gauge bosons (gluons) belong to the adjoint representation which imply $C_2(SU(3)) = 3$, and the fermion is belonging to the fundamental representatio.

For one generation of fermion only u_α and d_α contribute, therefore

$$T(1\text{generation}) = T_F(3) + T_F(3) = \frac{1}{2} + \frac{1}{2} = 1 \ .$$

If we work with Weyl fermions u_L, d_L, u_R and d_R , then we must include the factor $\frac{1}{2}$ for each helicity, which follows from $TrL(R) = \frac{1}{2}$, $L(R) = \frac{1}{2}(1 \pm \gamma_5)$. Hence

$$C(R) = 4 \times \frac{1}{2} \times \frac{1}{2} = 1 \ .$$

Since the Higgs is not coloured under $SU(3)$, then $C_2(R) = 0$.

We have finally

$$b_3^{SM} = \Big(\frac{11}{3} \times 3 - \frac{4}{3} \times 1 \times 3\Big) = 7 \ . \tag{A.3}$$

Secondly for the weak interaction: $SU(2)_L$

We have $C_2(SU(2)) = 2$, $C(R) = 1$ and $C_2(R) = \frac{1}{2}$. Thus we get

$$b_2^{SM} = \Big(\frac{11}{3} \times 2 - \frac{4}{3} \times 1 \times 3 - \frac{1}{3} \times 1 \times \frac{1}{2}\Big) = \frac{19}{6} \ . \tag{A.4}$$

Finally for $U(1)_Y$

There are no gauge boson contributions in b_Y since they do not carry hypercharge. For the fermions and Higgs scalar we take their hypercharges from Table 3.1, therefore

$$b_1^{SM} = \Big(- 3 \times \frac{4}{3}\Big(\frac{2}{36} \times 3 + \frac{4}{9} \times 3 + \frac{1}{9} \times 3 + \frac{2}{4} + 1\Big) \times \frac{1}{2} - \frac{1}{6}\Big) = -\frac{41}{6} \ . \tag{A.5}$$

But we always use the $SU(5)$ normalisation, that is $g' = \sqrt{\frac{3}{5}} g_1$. Therefore

$$b_1^{SM} = -\frac{41}{6} \times \frac{3}{5} = -\frac{41}{10} \ . \tag{A.6}$$

As such $b_i^{SM} = (-\frac{41}{10}, \frac{19}{6}, 7)$.

One-loop correction for gauge coupling constants in the MSSM

The one-loop correction to gauge coupling constant RGEs in the MSSM have been calculated in Refs. [34, 41] and can be written as

$$16\pi^2 \frac{dg_i}{dt} = b_i^{MSSM} g_i^3 \ , \tag{A.7}$$

where

$$b_G^{MSSM} = \Big(-\frac{11}{3}C_2(G)+\frac{2}{3}C_2(G)+\frac{4}{3}n_g C(R)+\frac{2}{3}n_g C(R)+\frac{1}{3}n_h C_2(R)+\frac{2}{3}n_h C_2(R)\Big) \,. \tag{A.8}$$

Here the first two terms correspond to the SM gauge bosons and gauginos contributions respectively, the 3^{rd} and 4^{th} terms correspond to SM fermions and sfermions respectively, and the last two terms correspond to the Higgs and Higgsinos contributions respectively.

Firstly the strong interaction: $SU(3)$

The gluinos belong to the adjoint representation and sfermions belong to the fundamental representation, therefore

$$b_3^{MSSM} = \left(-\frac{11}{3}\times 3+\frac{2}{3}\times 3+\frac{4}{3}\times 3+\frac{2}{3}\times 3\right) = -3 \,. \tag{A.9}$$

Secondly for the weak interaction: $SU(2)$

The gaugino $\tilde{W}$ and $\tilde{B}$ belong to the adjoint representation, the Higgsinos belong to the fundamental representation and $n_h = 2$. We get

$$b_2^{MSSM} = \left(-\frac{11}{3}\times 2+\frac{2}{3}\times 2+\frac{4}{3}\times 3+\frac{2}{3}\times 3+\frac{1}{3}+\frac{2}{3}\right) = 1 \,. \tag{A.10}$$

Finally for $U(1)_Y$

There are no contributions from the gauge bosons and gauginos, we obtain

$$\begin{aligned} b_1^{MSSM} \;=\; & 3\times\frac{4}{3}\Big(\frac{2}{36}\times 3+\frac{4}{9}\times 3+\frac{1}{9}\times 3+\frac{2}{4}+1\Big)\times\frac{1}{2} \\ & +3\times\frac{2}{3}\Big(\frac{2}{36}\times 3+\frac{4}{9}\times 3+\frac{1}{9}\times 3+\frac{2}{4}+1\Big)\times\frac{1}{2} \\ & +\frac{2}{6}+\frac{4}{6}\Big) = \frac{66}{6}\times\frac{3}{5} = \frac{33}{5} \,. \end{aligned} \tag{A.11}$$

Therefore $b_i^{MSSM} = (\frac{33}{5}, 1, -3)$.

One-loop correction for gauge coupling constants in the 5D MSSM

At each excited KK level the one-loop corrections to the gauge couplings are given by:

$$16\pi^2\frac{dg_i}{dt} = b_i^{MSSM} g_i^3 + (S(t)-1) b_i^{5DMSSM} g_i^3 \,, \tag{A.12}$$

where

$$b_G^{5DMSSM} = \Big(-\frac{11}{3}C_2(G) + \frac{2}{3}C_2(G) + C_2(G) + 4\eta C(R) + 2n_h C_2(R) \Big) \ . \quad \text{(A.13)}$$

The first two terms correspond to the gauge bosons and gauginos contributions respectively, the 3^{rd} is the contribution from the supefield χ scalar and fermion, the 4^{th} terms correspond to η generations of matter contribution and the last term corresponds to the Higgs superfield (mirror to 4D MSSM) and Higgs superfield Φ^c contribution.

Therefore, for g_3 at each excited KK level

$$b_3^{5DMSSM} = \Big(-\frac{11}{3} \times 3 + \frac{2}{3} \times 3 + 3 + 4\eta \Big) = -6 + 4\eta \ , \quad \text{(A.14)}$$

for g_2 at each excited KK level

$$b_2^{5DMSSM} = \Big(-\frac{11}{3} \times 2 + \frac{2}{3} \times 2 + 2 + 4\eta + 2 \Big) = -2 + 4\eta \ , \quad \text{(A.15)}$$

and for g_1 at each excited KK level

$$b_1^{5DMSSM} = \Big(4\eta(\frac{10}{6}) + 2 \Big) \times \frac{3}{5} = \Big(\frac{6}{5} + 4\eta \Big) \ . \quad \text{(A.16)}$$

So $(b_1^{5DMSSM}, b_2^{5DMSSM}, b_3^{5DMSSM}) = (\frac{6}{5}, -2, -6) + 4\eta$.

One-loop correction for gauge coupling constants in the UED model

At each excited KK level, the one-loop corrections to the gauge couplings arise from the diagrams exactly mirroring those of the SM ground states. Note that for the closed fermion loop diagrams one needs to count the contributions from both the left-handed and right-handed KK modes of each chiral fermion to the self-energy of the gauge filed. Additional contributions to the self-energy of the gauge boson from the fifth component of the 5D gauge field A_M $(M = 0, 1, 2, 3, 5)$ at each KK excited level are as shown in Fig. A.1.

Note that we use dimensional regularisation to calculate the contribution from the Fig. A.1 as follows:

$$\begin{aligned} \Pi_{\mu\nu} &= \frac{1}{2} \int \frac{d^d p}{(2\pi)^d} \, \frac{i}{p^2} \times \frac{i}{(p+q)^2} \times g^2 (2p+q)^\mu (-(2p+q)^\nu) f^{ace} f^{bde} \delta^{ac} \\ &= \frac{1}{2} g^2 C_2(G) \delta^{ab} \int \frac{d^d p}{(2\pi)^d} \, \frac{(4p^\mu p^\nu + 2p^\mu q^\nu + 2q^\mu p^\nu + q^\mu q^\nu)}{p^2 (p+q)^2} \ . \end{aligned} \quad \text{(A.17)}$$

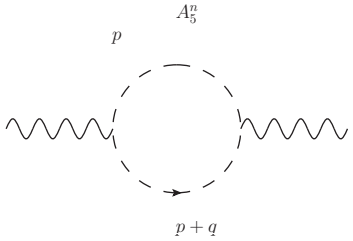


Figure A.1: *The one-loop gauge field self correction involving the scalar A_5^n loop.*

Using Feynman parametrisation

$$\frac{1}{ab} = \int_0^1 dz \frac{1}{(b+(a-b)z)^2} \ , \tag{A.18}$$

we get

$$\Pi_{\mu\nu} = \frac{1}{2} g^2 C_2(G) \delta^{ab} \int \frac{d^d p}{(2\pi)^d} \int_0^1 dz \ \frac{4p^\mu p^\nu + 2p^\mu q^\nu + 2q^\mu p^\nu + q^\mu q^\nu}{(p^2 + (q^2 + 2qp)z)^2} \ . \tag{A.19}$$

By introducing a new variable $p = l - qz$, the denominator becomes $(l^2 + q^2 z(1-z))^2$ and the numerator $4l^\mu l^\nu + q^\mu q^\nu (2z-1)^2$. Note that odd powers of l are dropped in the numerator. Thus

$$\Pi_{\mu\nu} = \frac{1}{2} g^2 C_2(G) \delta^{ab} \int \frac{d^d l}{(2\pi)^d} \int_0^1 dz \ \frac{4l^\mu l^\nu + q^\mu q^\nu (2z-1)^2}{(l^2 + q^2 z(1-z))^2} \ . \tag{A.20}$$

Using the standard integrals

$$\int d^d q \frac{q^\mu q^\nu}{(q^2+\Delta)^n} = i\pi^{\frac{d}{2}} \frac{\Gamma(n - \frac{d}{2} - 1) g^{\mu\nu}}{2\Gamma(n)\Delta^{n-\frac{d}{2}-1}} \ , \tag{A.21}$$

$$\int d^d q \frac{q^2}{(q^2+\Delta)^n} = i\pi^{\frac{d}{2}} \frac{\Gamma(n - \frac{d}{2} - 1) d}{2\Gamma(n)\Delta^{n-\frac{d}{2}-1}} \ , \tag{A.22}$$

and

$$\int d^d q \frac{1}{(q^2+\Delta)^n} = i\pi^{\frac{d}{2}} \frac{\Gamma(n - \frac{d}{2})}{\Gamma(n)\Delta^{n-\frac{d}{2}}} \ , \tag{A.23}$$

Eq. (A.20) becomes

$$\begin{aligned} \Pi_{\mu\nu} \ &= \ \frac{g^2 C_2(G) \delta^{ab}}{(4\pi)^{\frac{d}{2}}} \int_0^1 dz \ \frac{1}{\Delta^{2-\frac{d}{2}}} \left(g^{\mu\nu} q^2 z(1-z) \Gamma\left(1 - \frac{d}{2}\right) \right. \\ &\left. + \frac{(2z-1)^2}{2} q^\mu q^\nu \Gamma\left(2 - \frac{d}{2}\right) \right) \ , \end{aligned} \tag{A.24}$$

where $\Delta = q^2 z(1-z)$. Integrating over z and substituting $d = 4 - \epsilon$, we obtain

$$i\Pi_{\mu\nu} = \frac{ig^2 C_2(G)\delta^{ab}}{(4\pi)^2}\Big(-\frac{1}{6}(g^{\mu\nu}q^2 - q^\mu q^\nu)\Big).\frac{2}{\epsilon}\ . \tag{A.25}$$

Thus Eq. (A.1) is modified in the UED model as

$$16\pi^2\frac{dg_i}{dt} = b_i^{SM}g_i^3 + (S(t)-1)b_i^{UED}g_i^3\ , \tag{A.26}$$

where

$$b_G^{UED} = \Big(\frac{11}{3}C_2(G) - \frac{1}{6}C_2(G) - 2\frac{4}{3}n_g C(R) - \frac{1}{3}n_h C_2(R)\Big)\ . \tag{A.27}$$

As we did previously, the coefficients b_i^{UED} can be calculated:

$$b_i^{UED} = (b_1^{UED}, b_2^{UED}, b_3^{UED}) = \left(-\frac{81}{10}, -\frac{7}{6}, \frac{5}{2}\right)$$

.

One-loop correction for gauge coupling constants in the 2UED model

The calculation is similar to the UED model, but now there will be factor 2 due to the 6D gauge filed, which has two extra dimensional components. Eq. (A.25) then becomes

$$i\Pi_{\mu\nu} = \frac{ig^2 C_2(G)\delta^{ab}}{(4\pi)^2}\Big(-\frac{1}{3}(g^{\mu\nu}q^2 - q^\mu q^\nu)\Big).\frac{2}{\epsilon}\ . \tag{A.28}$$

As such Eq. (A.26) is modified in the 2UED model as

$$16\pi^2\frac{dg_i}{dt} = b_i^{SM}g_i^3 + \pi(S^2(t)-1)b_i^{2UED}g_i^3\ , \tag{A.29}$$

where

$$b_G^{2UED} = \Big(\frac{11}{3}C_2(G) - \frac{1}{3}C_2(G) - 2\frac{4}{3}n_g C(R) - \frac{1}{3}n_h C_2(R)\Big)\ , \tag{A.30}$$

and the coefficients b_i^{2UED} are given by

$$b_i^{2UED} = (b_1^{2UED}, b_2^{2UED}, b_3^{2UED}) = \left(-\frac{81}{10}, -\frac{3}{2}, 2\right)$$

.

Appendix B

Calculation of the one-loop beta functions in the 2UED model

This appendix is concerned with our RGEs calculation for various parameters, such as the Yukawa and Higgs quartic couplings. Note that we shall ignore the sum of KK modes for simplicity, and we will calculate the KK number in Appendix C.

Note that our fields in 2UED models will have KK modes which contribute to the RGEs at the scale $E = 1/R$. Up to this energy scale the evolution is logarithmic and controlled by the SM evolution, beyond it the contributions of KK states should be considered. However, we do make some considerations in this setup:

- The KK number (k, l) is conserved at each vertex.
- The KK states of fermions (quarks and leptons) are vector-like, whilst the zero mode fermions are chiral due to the orbifolding mechanism.
- The extra components of the gauge bosons (A_5 and A_6) are scalars belonging to the adjoint representation.

One-loop Yukawa couplings

Figs. B.1($a - c$ and $g - i$) are the new contributions to the RGEs of the Yukawa couplings. To calculate the wave function renormalisation constants we usually ignore the mass term in the propagators, since they have nothing to do with the divergent part of the one-loop diagrams.

Calculation the factor of the g_3^2 for up-type

$$Fig.B.1(a) = \int \frac{d^d p}{(2\pi)^d} \left(\frac{g_3^5}{\sqrt{\pi R}}\gamma^5 \frac{\lambda^A}{2}\right) \frac{i}{(\not{q} - \not{p})} \left(-\frac{i}{2}\frac{Y_u^5}{\sqrt{\pi R}}\right) \frac{i}{(\not{q} - \not{p})} \left(\frac{g_3^5}{\sqrt{\pi R}}\gamma^5 \frac{\lambda^A}{2}\right) \frac{i}{p^2} ,$$

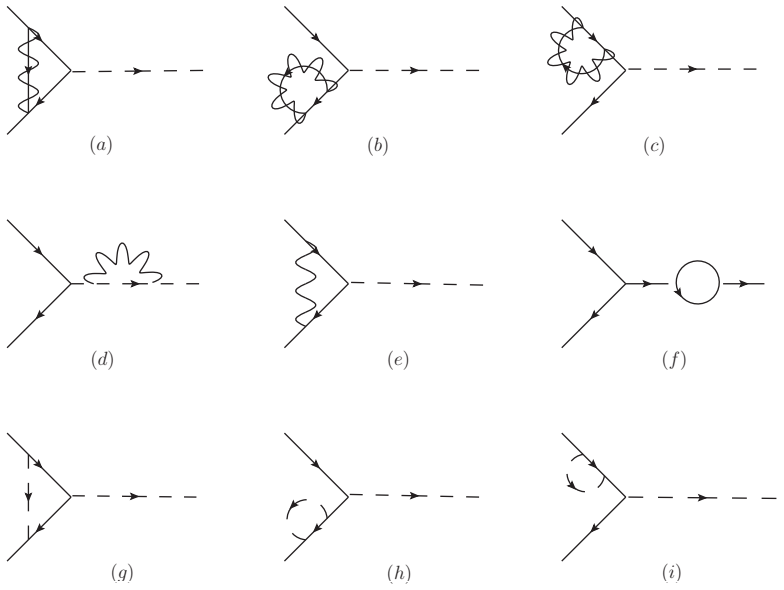


Figure B.1: *Diagrams contributing to Yukawa coupling RGEs in 2UED models in the Landau gauge. Solid (broken) lines correspond to fermions (SM scalars), while wavy lines (wavy+solid lines) represent ordinary gauge bosons (fifth components of gauge bosons).*

We use the relations $(\gamma_5)^2 = 1$, $\{\gamma^5, \gamma^\mu\} = 0$, $\frac{g_3^5}{\sqrt{\pi R}} = g_3$ and $\frac{Y_u^5}{\sqrt{\pi R}} = Y_u$, and dimensional regularisation, the above integral yields

$$Fig.B.1(a) = -2\frac{1}{\sqrt{2}}\frac{N^2-1}{2N}Y_u g_3^2 \frac{1}{16\pi^2}\frac{1}{\epsilon}(\mu^2)^{-\epsilon} i \ . \tag{B.1}$$

For $SU(3)$; $N = 3$ therefore

$$Z_{coupling} = 1 - 2\frac{8}{6}Y_u g_3^2 \frac{1}{16\pi^2}\frac{1}{\epsilon}(\mu^2)^{-\epsilon} \ . \tag{B.2}$$

Then

$$-\mu\frac{\partial}{\partial\mu}Z_{coupling} = -2\frac{8}{3}Y_u g_3^2 \frac{1}{16\pi^2} \ . \tag{B.3}$$

Calculation of Fig. B.1 (b) give us

$$\begin{aligned} Fig.B.1(b) &= 2\int \frac{d^dp}{(2\pi)^d}\left(\frac{g_3^5}{\sqrt{\pi R}}\gamma^5\frac{\lambda^A}{2}\right)\frac{i}{(\not{q}-\not{p})}\left(-\frac{i}{2}\frac{Y_u^5}{\sqrt{\pi R}}\right)\left(\frac{g_3^5}{\sqrt{\pi R}}\gamma^5\frac{\lambda^A}{2}\right)\frac{i}{p^2} \\ &= 2\frac{8}{12}Y_u g_3^2\frac{1}{16\pi^2}\frac{1}{\epsilon}(\mu^2)^{-\epsilon} i \ , \end{aligned} \tag{B.4}$$

where we now get

$$Z_{U_R} = 1 - 2\frac{8}{12} Y_u g_3^2 \frac{1}{16\pi^2} \frac{1}{\epsilon} (\mu^2)^{-\epsilon} \ . \tag{B.5}$$

Then

$$\frac{1}{2}\mu \frac{\partial}{\partial \mu} Z_{U_R} = 2\frac{8}{12} Y_u g_3^2 \frac{1}{16\pi^2} \ . \tag{B.6}$$

Likewise, Fig. B.1 (c) gives us

$$\frac{1}{2}\mu \frac{\partial}{\partial \mu} Z_{q_L} = 2\frac{8}{12} Y_u g_3^2 \frac{1}{16\pi^2} \ . \tag{B.7}$$

Fig. B.1 (e), like the SM gives us

$$-\mu \frac{\partial}{\partial \mu} Z_{coupling} = -8 Y_u g_3^2 \frac{1}{16\pi^2} \ . \tag{B.8}$$

Adding Eq. (B.3), Eq. (B.6), Eq. (B.7) and Eq. (B.8) yields

$$\left(-2\frac{8}{3} + 2\frac{8}{12} + 2\frac{8}{12} + \frac{8}{12} - 8 \right) Y_u g_3^2 \frac{1}{16\pi^2} = -\frac{32}{3} Y_u g_3^2 \frac{1}{16\pi^2} \ , \tag{B.9}$$

which exactly matches the g_3^2 factor appearing in Eq. (6.23).

Calculation the factor of the g_2^2 for up-type

$$\begin{aligned} Fig.B.1(c) &= 2\int \frac{d^d p}{(2\pi)^d} \left(\frac{g_2^5}{\sqrt{\pi R}} \gamma^5 \frac{\lambda^A}{2} \right) \frac{i}{(\not{q} - \not{p})} \left(-\frac{i}{2} \frac{Y_u^5}{\sqrt{\pi R}} \right) \left(\frac{g_2^5}{\sqrt{\pi R}} \gamma^5 \frac{\lambda^A}{2} \right) \frac{i}{p^2} \\ &= 2\frac{3}{8} Y_u g_2^2 \frac{1}{16\pi^2} \frac{1}{\epsilon} (\mu^2)^{-\epsilon} i \ , \end{aligned} \tag{B.10}$$

therefore

$$Z_{q_L} = 1 - 2\frac{3}{8} Y_u g_2^2 \frac{1}{16\pi^2} \frac{1}{\epsilon} (\mu^2)^{-\epsilon} \ . \tag{B.11}$$

Then

$$\frac{1}{2}\mu \frac{\partial}{\partial \mu} Z_{q_L} = \frac{3}{8} Y_u g_2^2 \frac{1}{16\pi^2} \ . \tag{B.12}$$

Note that Fig. B.1 (b) has no contribution to g_2^2, because the right handed fermion does not couple to W bosons.
Fig. B.1 (d) contribution is the same as the SM, giving us

$$\frac{1}{2}\mu \frac{\partial}{\partial \mu} Z_{\phi} = -\frac{9}{4} Y_u g_2^2 \frac{1}{16\pi^2} \ . \tag{B.13}$$

Adding Eq. (B.12) and Eq. (B.13) we get

$$\left(\frac{3}{4} - \frac{9}{4} \right) Y_u g_2^2 \frac{1}{16\pi^2} = -\frac{3}{2} Y_u g_2^2 \frac{1}{16\pi^2} \ . \tag{B.14}$$

Which is the same factor of g_2^2 in Eq. (6.23).

Calculation the factor of the g_1^2 for up-type

The calculation of Fig. B.1 (c) is the same as Eq. (B.10), but the vertex factor $\frac{3}{4}$ is replaced with $(\frac{Y_Q}{2})^2 = (\frac{1}{6})^2$, so

$$\frac{1}{2}\mu\frac{\partial}{\partial\mu}Z_{q_L} = \left(\frac{1}{6}\right)^2 Y_u g_1^2 \frac{1}{16\pi^2} \ . \tag{B.15}$$

Similarly Fig. B.1 (b) gives us

$$\frac{1}{2}\mu\frac{\partial}{\partial\mu}Z_{U_R} = \left(\frac{2}{3}\right)^2 Y_u g_1^2 \frac{1}{16\pi^2} \ . \tag{B.16}$$

The calculation of Fig. B.1 (a) is the same as Eq. (B.4), where we take off the vertex factor $\frac{8}{6}$ and replace it with

$$\frac{Y_Q}{2}\frac{Y_u}{2} = \frac{1}{6}\frac{2}{3} \ .$$

Thus

$$-\mu\frac{\partial}{\partial\mu}Z_{coupling} = -4\frac{1}{6}\frac{2}{3}Y_u g_1^2 \frac{1}{16\pi^2} \ . \tag{B.17}$$

Fig. B.1 (d) and Fig. B.1 (e), like the SM give us

$$-\frac{17}{12}Y_u g_1^2 \frac{1}{16\pi^2} \ .$$

Adding the above results with Eq. (B.15), Eq. (B.16) and Eq. (B.17) yields

$$\left(-\frac{17}{12} - \frac{9}{4} + \frac{9}{4} + \frac{1}{36}\right) Y_u g_1^2 \frac{1}{16\pi^2} = -\frac{50}{36}\frac{Y_u g_1^2}{16\pi^2} \times \frac{3}{5} = -\frac{5}{6}\frac{Y_u g_1^2}{16\pi^2} \ . \tag{B.18}$$

The above result matches the factor of g_1^2 in Eq. (6.23).

The down-type calculations are similar to the up-type except for the g_1^2 calculations, where we get

$$-\frac{1}{30}\frac{Y_d g_1^2}{16\pi^2} \ . \tag{B.19}$$

Calculation the factor of the g_1^2 for leptons

Again the calculation is similar to the calculation of g_1^2 factor for the quarks, except for the vertex factors. We obtain

$$-\frac{27}{10}\frac{Y_e g_1^2}{16\pi^2} \ . \tag{B.20}$$

The calculation of the g_2^2 factor is the same as quarks calculation.

Calculating the factor of Y_u

$$Fig.B.1(f) \;=\; -2\int \frac{d^dp}{(2\pi)^d}\, Tr\left(\frac{i(\not{q}+\not{p})\gamma_5 i\not{p}\gamma_5}{(q+p)^2p^2}\right)\times Tr(3Y_u^\dagger Y_u + 3Y_d^\dagger Y_d + Y_e^\dagger Y_e)\;. \tag{B.21}$$

The factor 2 is due to the fact that both sines and cosines will contribute, after some algebra, and using the following trace technology

$$\begin{aligned}\mathrm{Tr}\left[\text{odd }\gamma^{'}s\right] &= 0\;,\\ \mathrm{Tr}\left[\gamma^\mu\right] &= 0\;,\\ \mathrm{Tr}\left[\gamma^\mu\gamma^\nu\right] &= 4g^{\mu\nu}\;,\end{aligned}$$

we get

$$\frac{1}{2}\mu\frac{\partial}{\partial\mu}Z_\phi = 2Y_u\frac{1}{16\pi^2}Tr(3Y_u^\dagger Y_u + 3Y_d^\dagger Y_d + Y_e^\dagger Y_e)\;. \tag{B.22}$$

Figs. B.1 (g-h-i) are the same as the SM, giving us

$$Y_u\left(\frac{3}{2}Y_u^\dagger Y_u - \frac{3}{2}Y_d^\dagger Y_d\right)\frac{1}{16\pi^2}\;. \tag{B.23}$$

Similarly for the down-types, we get

$$Y_d\left(\frac{3}{2}Y_d^\dagger Y_d - \frac{3}{2}Y_u^\dagger Y_u\right)\frac{1}{16\pi^2}\;. \tag{B.24}$$

Finally for leptons we get

$$Y_e\frac{3}{2}Y_e^\dagger Y_e\frac{1}{16\pi^2}\;. \tag{B.25}$$

Plugging all the ingredients in Eq. (4.1), the beta function for the Yukawa couplings are

$$\begin{aligned}\beta_{Y_u}^{2UED} &= Y_u\left[2\mathrm{Tr}\left(3Y_u^\dagger Y_u + 3Y_d^\dagger Y_d + Y_e^\dagger Y_e\right) + \frac{3}{2}\left(Y_u^\dagger Y_u - Y_d^\dagger Y_d\right)\right.\\ &\quad\left. - \left(\frac{32}{3}g_3^2 + \frac{3}{2}g_2^2 + \frac{5}{6}g_1^2\right)\right]\;,\end{aligned} \tag{B.26}$$

$$\begin{aligned}\beta_{Y_d}^{2UED} &= Y_d\left[2\mathrm{Tr}\left(3Y_u^\dagger Y_u + 3Y_d^\dagger Y_d + Y_e^\dagger Y_e\right) + \frac{3}{2}\left(Y_d^\dagger Y_d - Y_u^\dagger Y_u\right)\right.\\ &\quad\left. - \left(\frac{32}{3}g_3^2 + \frac{3}{2}g_2^2 + \frac{1}{30}g_1^2\right)\right]\;,\end{aligned} \tag{B.27}$$

$$\beta_{Y_e}^{2UED} = Y_e \left[2\mathrm{Tr}\left(3Y_u^\dagger Y_u + 3Y_d^\dagger Y_d + Y_e^\dagger Y_e\right) + \frac{3}{2} Y_e^\dagger Y_e - \left(\frac{3}{2} g_2^2 + \frac{27}{10} g_1^2\right)\right] . \tag{B.28}$$

Which exactly confirms Eq. (6.23).

One-loop Higgs quartic couplings

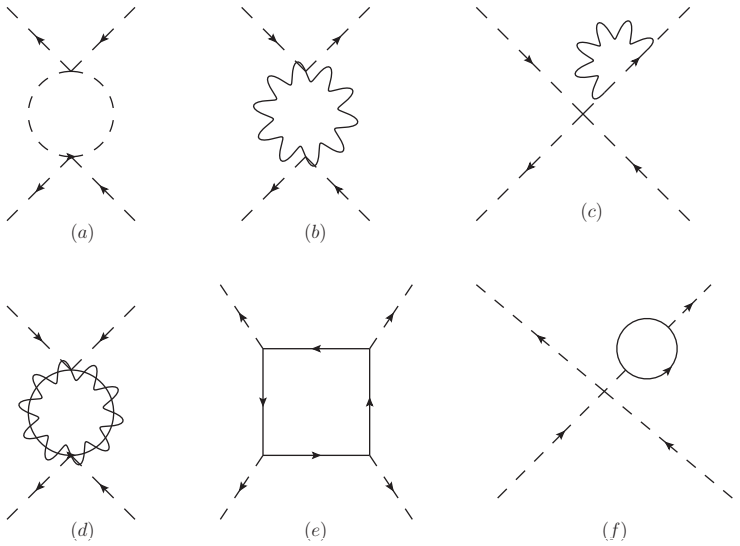


Figure B.2: *Diagrams contributing to Higgs quartic coupling RGEs in the 2UED models in the Landau gauge. The notation is the same as in Fig. B.1.*

Calculation of the λ^2 factor

$$Fig.B.2(a) + 2\mathrm{permutations} = \frac{3\lambda^2}{2} \int \frac{d^d p}{(2\pi)^d} \frac{1}{(p-q)^2} \frac{1}{p^2} . \tag{B.29}$$

By making use of Eq. (A.18) and Eq. (A.23), we obtain

$$Fig.B.2(a) + 2\mathrm{permutations} = \frac{12 i \lambda^2}{16\pi^2} \left(\frac{1}{\epsilon} + \mathrm{finite} - \mathrm{terms}\right) . \tag{B.30}$$

Calculation of the λ factor

Fig. B.2 (f) is identical to the SM one, giving us

$$Fig.B.2(f) = \frac{4\lambda}{16\pi^2} \times 2\mathrm{Tr}\left(3Y_u^\dagger Y_u + 3Y_d^\dagger Y_d + Y_e^\dagger Y_e\right) . \tag{B.31}$$

Fig. B.2 (e) is also identical to the SM one, giving us

$$Fig.B.2(e) = -4\frac{1}{16\pi^2} \times 2\mathrm{Tr}\left(3(Y_u^\dagger Y_u)^2 + 3(Y_d^\dagger Y_d)^2 + (Y_e^\dagger Y_e)^2\right) . \tag{B.32}$$

Calculation of the g_2^4 factor

$$Fig.B.2(b) = \frac{1}{2}\int \frac{d^dp}{(2\pi)^d} \frac{-i(g_{\mu\nu} - p_\mu p_\nu/p^2)}{(p)^2} \left(\frac{ig^2}{2}\right)^2 \frac{-i(g_{\mu\nu} - p_\mu p_\nu/p^2)}{p^2} \tag{B.33}$$

$$Fig.B.2(b) + 2\mathrm{permutations} = 3\frac{3g_2^4}{8}\int \frac{d^dp}{(2\pi)^d} \frac{1}{(p)^2} = \frac{9}{4}g_2^4\frac{1}{16\pi^2}\frac{1}{\epsilon} . \tag{B.34}$$

Fig. B.2 (d) has been calculated without the external line in the previous appendix (see Eq. (A.25)), we need only replace the vertex by g_2^2, to get

$$2\frac{3}{4}g_2^4\frac{1}{16\pi^2} = \frac{3}{2}g_2^4\frac{1}{16\pi^2} . \tag{B.35}$$

Adding the above equations to Eq. (B.34) gives us the coefficient of g_2^4 as

$$\left(\frac{9}{4} + \frac{3}{2}\right) g_2^4\frac{1}{16\pi^2} = \frac{15}{4}g_2^4\frac{1}{16\pi^2} . \tag{B.36}$$

Calculation of the g_1^4 factor

The calculation is similar to the calculation for the g_2^4 factor, except the vertex factor ($\frac{3}{4}$) in Eq. (B.36) is replaced by

$$\left(\frac{Y_\phi}{2}\right)^2 = \frac{1}{4} .$$

Thus the coefficient of g_1^4 is

$$\frac{15}{4} \times \frac{4}{3} \times \frac{1}{4} \times \frac{3}{5} \times \frac{3}{5} \times g_1^4\frac{1}{16\pi^2} = \frac{9}{20}g_1^4\frac{1}{16\pi^2} . \tag{B.37}$$

Calculation of the $g_1^2 g_2^2$ factor

The calculation is similar to the caculation for the g_2^4 factor, except we take off the vertex factor ($\frac{3}{4}g_2^4$) in Eq. (B.36) and replace it by

$$\left(\frac{Y_\phi}{2} g_1^2 g_2^2 \frac{3}{5}\right) = \frac{1}{2}\frac{3}{5} g_1^2 g_2^2 \, .$$

Therefore the coefficient of $g_1^2 g_2^2$ is given by

$$\frac{15}{4} \times \frac{4}{3} \times \frac{1}{2} \times \frac{3}{5} \times g_1^2 g_2^2 \frac{1}{16\pi^2} = \frac{3}{2} g_1^2 g_2^2 \frac{1}{16\pi^2} \, . \tag{B.38}$$

Calculation of the $g_2^2 \lambda$ factor

The diagram in Fig. B.2 (c) has been calculated in the Yukawa couplings beta function. So

$$4 \times Fig.B.2(c) = -4 \times \frac{9}{4} g_2^2 \lambda \frac{1}{16\pi^2} = -9 g_2^2 \lambda \frac{1}{16\pi^2} \, . \tag{B.39}$$

Calculation of the $g_1^2 \lambda$ factor

The calculation is similar to the calculation for $g_2^2 \lambda$ factor, except we take off the vertex factor ($\frac{3}{4}g_2^4$) in Eq. (B.39) and replace it by

$$\left(\frac{Y_\phi}{2}\right)^2 g_1^2 \lambda \frac{3}{5} = \frac{1}{4}\frac{3}{5} g_1^2 \lambda \, .$$

Hence the coefficient of $g_1^2 \lambda$ is given by

$$-9 \times \frac{4}{3}\frac{1}{4} \times \frac{3}{5} g_1^2 \lambda \frac{1}{16\pi^2} = -\frac{9}{5} g_1^2 \lambda \frac{1}{16\pi^2} \, . \tag{B.40}$$

plugging all the ingredients in Eq. (4.3) yields the beta function of the Higgs quartic couplings given in Eq. (8.6).

Appendix C

The number of KK states in 2UED models

T^2 case

In the T^2 case the KK mass is $M_{j,k} = \frac{\sqrt{j^2+k^2}}{R}$, where by define $M_{KK} = \frac{1}{R}$ as the lightest KK mass, and the number of KK states originates from:

$$\sum_{j,k} \ln \frac{\mu}{\sqrt{j^2+k^2} M_{KK}} \qquad \text{for} \qquad 1 \leq j^2 + k^2 \leq \left(\frac{\mu}{M_{KK}}\right)^2 \tag{C.1}$$

$$\sum_{j,k} \ln \frac{\mu}{\sqrt{j^2+k^2} M_{KK}} = \sum_{j,k} \ln \frac{\mu}{M_{KK}} - \frac{1}{2} \ln(j^2+k^2) \, . \tag{C.2}$$

One can use polar coordinates and change the sum into an integral as

$$\sum_{j,k} \ln \frac{\mu}{M_{KK}} - \frac{1}{2} \ln(j^2+k^2) = \int_1^{\frac{\mu}{M_{KK}}} 2\pi r dr \left(\ln \frac{\mu}{M_{KK}} - \ln r \right) , \tag{C.3}$$

from which we obtain

$$\frac{\pi}{2} \left[\left(\frac{\mu}{M_{KK}}\right)^2 - 1 - 2 \ln \frac{\mu}{M_{KK}} \right] \, . \tag{C.4}$$

Therefore the gauge couplings running equation becomes

$$\frac{4\pi}{g_i^2(\mu)} = \frac{4\pi}{g_i^2(M_Z)} - \frac{b_i^{SM}}{2\pi} \ln \frac{\mu}{M_Z} + 2C \frac{b_i^{6D}}{2\pi} \ln \frac{\mu}{M_{KK}} - C \frac{b_i^{6D}}{2\pi} \left(\left(\frac{\mu}{M_{KK}}\right)^2 - 1 \right) \, , \tag{C.5}$$

where $C = \frac{\pi}{2}$, and in terms of the t parameter we have $\mu = M_Z e^t$. As such Eq.(C.5) becomes

$$\frac{4\pi}{g_i^2(\mu)} = \frac{4\pi}{g_i^2(M_Z)} - \frac{b_i^{SM}}{2\pi} \ln \frac{M_Z e^t}{M_Z} + 2C \frac{b_i^{6D}}{2\pi} \ln \frac{M_Z e^t}{M_{KK}} - C \frac{b_i^{6D}}{2\pi} \left(\left(\frac{M_Z e^t}{M_{KK}}\right)^2 - 1 \right) \, . \tag{C.6}$$

We take the derivative of Eq.(C.6) with respect to t to obtain

$$\begin{aligned} -2g_i^{-3}\frac{dg_i}{dt} &= -\frac{b_i^{SM}}{8\pi^2} + 2C\frac{b_i^{6D}}{8\pi^2}\left(1-\left(M_Z Re^t\right)^2\right) , \\ \frac{dg_i}{dt} &= \left[\frac{b_i^{SM}}{16\pi^2} + 2C\frac{b_i^{6D}}{16\pi^2}\left(S(t)^2-1\right)\right] g_i^3 , \end{aligned} \tag{C.7}$$

which is Eq.(6.12). Thus our KK number for the general 2UED model is $2C(S(t)^2-1)$, where our general model is this T^2 model, and where $S(t) = M_Z Re^t$, assuming that all modes contribute in the range of our energy scale.

S^2 case

In the S^2 case the KK mass is $M_{j,k} = \frac{\sqrt{j(j+1)}}{R}$, and we have $M_{KK} = \frac{\sqrt{2}}{R}$ being the lightest KK state in this model. Our KK number is then given by

$$\sum_{j,k}(2j+1)\ln\frac{\mu}{\sqrt{j^2+k^2}M_{KK}} \qquad \text{for} \quad 2 \le j(j+1) \le 2\left(\frac{\mu}{M_{KK}}\right)^2 , \tag{C.8}$$

where $2j+1$ is the number of degenerate states in each j-level.

Using $j(j+1) \approx j^2$ and defining $j_{max} = \sqrt{2}\frac{\mu}{M_{KK}}$ and $j_{min} = \sqrt{2}$,

$$\sum_{j,k}\ln\frac{\mu}{\sqrt{\frac{j(j+1)}{2}}M_{KK}} = \int_{\sqrt{2}}^{\sqrt{2}(\frac{\mu}{M_{KK}})} 2j dj \ln\frac{j_{max}}{j} , \tag{C.9}$$

and

$$\int_{\sqrt{2}}^{\sqrt{2}(\frac{\mu}{M_{KK}})} 2j dj \ln\frac{j_{max}}{j} \approx \left[\left(\frac{\mu}{M_{KK}}\right)^2 - 1 - 2\ln\frac{\mu}{M_{KK}}\right] . \tag{C.10}$$

Therefore our KK number, as a function of the t parameter, in this model, is given by $2(S(t)^2-1)$, assuming that all modes contribute in the range of our energy scale.

Model dependence of the RGE

Note that in specific realisations of the 2UED models, some of the states may not be present, therefore one needs to subtract those states which do not contribute from the total KK number. For instance the case of T^2 or S^2 compactifications, the states (0,2k) and (2k,0) for a given parity may not be present. Assuming that these states are not there, the number of KK states for such models becomes $2C(S^2-1)-2(S-1)$, where $C = \frac{\pi}{2}$ for the T^2 case or 1 for the S^2 case. We have numerically analysed such 2UED models to test the model dependence of the results obtained with the RGEs, and only minor changes in the plots were observed, with the major phenomenology discussed in section 6.4 remaining unaltered.

Appendix D

The action and conventions of the 5D MSSM

We will first introduce the conventions for writing the five dimensional SYM action in four dimensional superspace. This action corresponds to $\mathcal{N}=2$ from the 4D perspective. We compactify on an $S^1/\mathbb{Z}_2$ orbifold, such that the SYM becomes an $\mathcal{N}=1$ positive parity vector multiplet and negative parity chiral multiplet. These conventions are based on Refs. [53, 115, 153]. The maximal SYM case in five dimensions reduces to a 4D superspace, this may be found in Ref. [114].

The non-Abelian bulk action

The off-shell $\mathcal{N}=1$ pure SYM theory may be written in components:

$$S_{5D}^{SYM} = \int d^5x \, \mathrm{Tr}\left[-\frac{1}{2}(F_{MN})^2 - (D_M\Sigma)^2 - i\bar{\lambda}_i\gamma^M D_M\lambda^i + (X^a)^2 + g_5\,\bar{\lambda}_i[\Sigma,\lambda^i]\right], \tag{D.1}$$

where M,N run over $0,1,2,3,4$, while μ,ν run over $0,1,2,3$. The gauge group generators and the metric are $\mathrm{Tr}(T^{\mathcal{A}}T^{\mathcal{B}}) = \frac{1}{2}\delta^{\mathcal{A}\mathcal{B}}$ and $\eta_{MN} = \mathrm{diag}(-1,1,1,1,1)$. The coupling $1/g_5^2$ has been rescaled inside the covariant derivative, $D_M = \partial_M + ig_5A_M$, where A_M is a standard gauge vector field and F_{MN} its field strength. The other fields are a real scalar Σ, an $SU(2)_R$ triplet of real auxiliary fields X^a, $a=1,2,3$ and a symplectic Majorana spinor λ_i with $i=1,2$ which form an $SU(2)_R$ doublet. The reality condition is

$$\lambda^i = \epsilon^{ij}C\bar{\lambda}_j^T\,, \tag{D.2}$$

where $\epsilon^{12}=1$ and C is the 5D charge conjugation matrix $C\gamma^MC^{-1} = (\gamma^M)^T$. An explicit realisation of the Clifford algebra $\{\gamma^M,\gamma^N\} = -2\eta^{MN}$ is

$$\gamma^M = \left(\begin{pmatrix} 0 & \sigma^\mu_{\alpha\dot{\alpha}} \\ \bar{\sigma}^{\mu\dot{\alpha}\alpha} & 0 \end{pmatrix}, \begin{pmatrix} -i & 0 \\ 0 & i \end{pmatrix}\right), \quad \text{and} \quad C = \begin{pmatrix} -\epsilon_{\alpha\beta} & 0 \\ 0 & \epsilon^{\dot{\alpha}\dot{\beta}} \end{pmatrix}, \tag{D.3}$$

where $\sigma^{\mu}_{\alpha\dot{\alpha}} = (1, \vec{\sigma})$ and $\bar{\sigma}^{\mu\dot{\alpha}\alpha} = (1, -\vec{\sigma})$. $\alpha, \dot{\alpha}$ are spinor indices of SL$(2, C)$. For the $SU(2)_R$ indices we define

$$\epsilon_{ij} = \begin{pmatrix} 0 & -1 \\ 1 & 0 \end{pmatrix}, \quad \epsilon^{ij} = \begin{pmatrix} 0 & 1 \\ -1 & 0 \end{pmatrix}. \tag{D.4}$$

The superalgebra is given by

$$\{Q^i, \bar{Q}^j\} = 2\gamma^M P_M \delta^{i,j}. \tag{D.5}$$

The symplectic Majorana spinor SUSY parameter is $\bar{\epsilon}_i = \epsilon_i^\dagger \gamma^0$, which are also symplectic Majorana. To clarify notation we temporarily display all labels, writing the Dirac spinor in two component form $\psi^{i\,T} = (\psi^{Li}_{\alpha}, \bar{\psi}^{R\dot{\alpha}i})$ and $\bar{\psi}_i = (\psi_i^{R\alpha}, \bar{\psi}^L_{\dot{\alpha}i})$. The bar on the two component spinor denotes the complex conjugate representation of $SL(2, C)$. In particular, the reality condition (D.2) implies that

$$\lambda^1 = \begin{pmatrix} \lambda_{L\alpha} \\ \bar{\lambda}^{\dot{\alpha}}_R \end{pmatrix}, \quad \lambda^2 = \begin{pmatrix} \lambda_{R\alpha} \\ -\bar{\lambda}^{\dot{\alpha}}_L \end{pmatrix}, \quad (\bar{\lambda}_1)^T = \begin{pmatrix} \lambda^{\alpha}_R \\ \bar{\lambda}_{L\dot{\alpha}} \end{pmatrix}, \quad (\bar{\lambda}_2)^T = \begin{pmatrix} -\lambda^{\alpha}_L \\ \bar{\lambda}_{R\dot{\alpha}} \end{pmatrix}, \tag{D.6}$$

so the $SU(2)_R$ index on a two component spinor is a redundant label.

Next, using an $S^1/\mathbb{Z}_2$ orbifold the boundaries will preserve only half of the $\mathcal{N} = 2$ symmetries. We choose to preserve ϵ_L and set $\epsilon_R = 0$. The conjugate representations are constrained by the reality condition (D.2).

We may therefore write a $5D$ $\mathcal{N} = 1$ vector multiplet as a 4D vector multiplet and a chiral superfield:

$$V = -\theta\sigma^{\mu}\bar{\theta}A_{\mu} + i\bar{\theta}^2\theta\lambda - i\theta^2\bar{\theta}\bar{\lambda} + \frac{1}{2}\bar{\theta}^2\theta^2 D, \tag{D.7}$$

$$\Phi = \frac{1}{\sqrt{2}}(\Sigma + iA_5) + \sqrt{2}\theta\chi + \theta^2 F\,, \tag{D.8}$$

where the identifications between 5D and 4D fields are

$$D = (X^3 - D_5\Sigma) \quad F = (X^1 + iX^2)\,, \tag{D.9}$$

and we have used λ and χ to indicate λ_L and $-i\sqrt{2}\lambda_R$ respectively. The non-Abelian bulk action in $\mathcal{N} = 1$ 4D formalism is

$$\begin{aligned} S_5^{SYM} &= \int d^5x \left\{ \frac{1}{2}\mathrm{Tr}\left[\int d^2\theta W^{\alpha}W_{\alpha} + \int d^2\bar{\theta}\bar{W}_{\dot{\alpha}}\bar{W}^{\dot{\alpha}} \right] \right. \\ &\quad \left. + \frac{1}{2g_5^2}\int d^4\theta \mathrm{Tr}\left[e^{-2g_5V}\nabla_5 e^{2g_5V} \right]^2 \right\}. \end{aligned} \tag{D.10}$$

∇_5 is a "covariant" derivative with the respect to the field Φ [153]:

$$\nabla_5 e^{2g_5V} = \partial_5 e^{2g_5V} - g_5\Phi^\dagger e^{2g_5V} - g_5 e^{2g_5V}\Phi. \tag{D.11}$$

Let us now focus on 5D hypermultiplets. The bulk supersymmetric action is

$$S^H_{5D} = \int d^5x \Big[-(D_M H)^\dagger_i (D^M H^i) - i\bar{\psi}\gamma^M D_M \psi + F^{\dagger i} F_i + g_5 H^\dagger_i (\sigma^a X^a)^i_j H^j - g_5 \bar{\psi}\Sigma\psi + g_5^2 H^\dagger_i \Sigma^2 H^i + i g_5 \sqrt{2}\bar{\psi}\lambda^i \epsilon_{ij} H^j - i\sqrt{2} g_5 H^\dagger_i \epsilon^{ij} \bar{\lambda}_j \psi \Big] . \quad \text{(D.12)}$$

H_i are an $SU(2)_R$ doublet of scalars. ψ is a Dirac fermion and F_i are a doublet of scalars. With our conventions the dimensions of (H_i, ψ, F_i) are $(\frac{3}{2}, 2, \frac{5}{2})$. In general the hypermultiplet matter will be in a representation of the gauge group with Dynkin index defined by $d\delta^{ab} = \mathrm{Tr}[T^a T^b]$.

In the 4D superfield formulation, we again use the parity of the $P\psi_L = +\psi_L$ and $P\psi_R = -\psi_R$ to group the SUSY transformations into positive and negative parity chiral superfields, $PH = +H$ and $PH^c = -H^c$:

$$H = H^1 + \sqrt{2}\theta\psi_L + \theta^2(F_1 + D_5 H_2 - g_5 \Sigma H_2) \quad \text{(D.13)}$$

$$H^c = H_2^\dagger + \sqrt{2}\theta\psi_R + \theta^2(-F_2^\dagger - D_5 H_1^\dagger - g_5 H_1^\dagger \Sigma) . \quad \text{(D.14)}$$

The gauge transformations are $H \to e^{-\Lambda} H$ and $H^c \to H^c e^{\Lambda}$. The $\mathcal{N} = 1$ action in 4D language is

$$S^H_{5d} = \int d^5x \Big(\int d^4\theta [H^\dagger e^{2g_5 V} H + H^c e^{-2g_5 V} H^{c\dagger}] + \int d^2\theta H^c \nabla_5 H + \int d^2\bar{\theta} H^{c\dagger} \nabla_5 H^\dagger \Big) . \quad \text{(D.15)}$$

Appendix E

Input parameters used in our numerical calculations

Table E.1: *Initial values at M_Z scale used in our numerical calculations. Data is taken from Refs. [53, 74].*

Parameter	Value (90% CL)
$\alpha_1(M_Z)$	0.01696
$\alpha_2(M_Z)$	0.03377
$\alpha_3(M_Z)$	0.1184
$m_u(M_Z)$	1.27 MeV
$m_c(M_Z)$	0.619 GeV
$m_t(M_Z)$	171.7 GeV
$m_d(M_Z)$	2.90 MeV
$m_s(M_Z)$	55 MeV
$m_b(M_Z)$	2.83 GeV
$m_e(M_Z)$	0.48657 MeV
$m_\mu(M_Z)$	102.718 MeV
$m_\tau(M_Z)$	1746.24 MeV

Table E.2: *Present limits on neutrino masses and mixing parameters. Data is taken from Ref. [90] for $sin^2(2\theta_{13})$, and from Ref. [96].*

Parameter	Value (90% CL)
$\sin^2(2\theta_{12})$	$0.861(^{+0.026}_{-0.022})$
$\sin^2(2\theta_{23})$	> 0.92
$\sin^2(2\theta_{13})$	0.092 ± 0.017
Δm^2_{sol}	$(7.59 \pm 0.21) \times 10^{-5} eV^2$
Δm^2_{atm}	$(2.43 \pm 0.13) \times 10^{-3}\ eV^2$

Bibliography

[1] F. Abe *et al.* [CDF Collaboration], Phys. Rev. Lett. **73**, 225 (1994) [hep-ex/9405005]; F. Abe *et al.* [CDF Collaboration], Phys. Rev. D **50**, 2966 (1994); F. Abe *et al.* [CDF Collaboration], Phys. Rev. Lett. **74**, 2626 (1995) [hep-ex/9503002]; S. Abachi *et al.* [D0 Collaboration], Phys. Rev. Lett. **74**, 2632 (1995) [hep-ex/9503003]. H. D. Politzer, Phys. Rev. Lett. **30** (1973) 1346.

[2] M. L. Perl, G. S. Abrams, A. Boyarski, M. Breidenbach, D. Briggs, F. Bulos, W. Chinowsky and J. T. Dakin *et al.*, Phys. Rev. Lett. **35**, 1489 (1975); M. L. Perl, G. J. Feldman, G. S. Abrams, M. S. Alam, A. Boyarski, M. Breidenbach, J. Dorfan and W. Chinowsky *et al.*, Phys. Lett. B **70**, 487 (1977).

[3] G. Aad *et al.* [ATLAS collaboration], Phys. Lett. B716 (2012) 1 [arXiv:1207.7214].

[4] S. Chatrchyan *et al.* [CMS collaboration], Phys. Lett. B716 (2012) 30 [arXiv:1207.7235].

[5] H. Fritzsch and Z. -z. Xing, Prog. Part. Nucl. Phys. **45** (2000) 1 [hep-ph/9912358].

[6] M. C. Gonzalez-Garcia and Y. Nir, Rev. Mod. Phys. **75** (2003) 345 [hep-ph/0202058].

[7] G. Altarelli and F. Feruglio, New J. Phys. **6** (2004) 106 [hep-ph/0405048].

[8] T. Appelquist, H. -C. Cheng and B. A. Dobrescu, Phys. Rev. D **64** (2001) 035002 [hep-ph/0012100].

[9] T. Appelquist and H. -U. Yee, Phys. Rev. D **67**, 055002 (2003) [hep-ph/0211023].

[10] G. Aad *et al.* [ATLAS Collaboration], Phys. Rev. D **86**, 032003 (2012) [arXiv:1207.0319 [hep-ex]].

[11] E. Komatsu *et al.* [WMAP Collaboration], Astrophys. J. Suppl. **192**, 18 (2011) [arXiv:1001.4538 [astro-ph.CO]].

[12] B. A. Dobrescu and E. Poppitz, Phys. Rev. Lett. **87** (2001) 031801 [hep-ph/0102010].

[13] B. A. Dobrescu and E. Ponton, JHEP **0403** (2004) 071 [hep-th/0401032].

[14] G. Burdman, B. A. Dobrescu and E. Ponton, JHEP **0602** (2006) 033 [hep-ph/0506334].

[15] R. N. Mohapatra and A. Perez-Lorenzana, Phys. Rev. D **67** (2003) 075015 [hep-ph/0212254].

[16] N. Maru, T. Nomura, J. Sato and M. Yamanaka, Nucl. Phys. B **830** (2010) 414 [arXiv:0904.1909 [hep-ph]].

[17] G. Cacciapaglia, A. Deandrea and J. Llodra-Perez, JHEP **1003** (2010) 083 [arXiv:0907.4993 [hep-ph]].

[18] H. Dohi and K. -y. Oda, Phys. Lett. B **692** (2010) 114 [arXiv:1004.3722 [hep-ph]].

[19] T. P. Cheng and L. F. Li, Oxford, Uk: Clarendon (1984) 536 P. (Oxford Science Publications); F. Halzen and A. D. Martin, New York, Usa: Wiley (1984) 396p

[20] J. Iliopoulos, Contemp. Phys. **21**, 159 (1980); J. Iliopoulos, PTENS-74-4.

[21] D. J. Gross and F. Wilczek, Phys. Rev. Lett. **30**, 1343 (1973);

[22] S. L. Glashow, Nucl. Phys. **22**, 579 (1961); S. Weinberg, Phys. Rev. Lett. **19**, 1264 (1967); A. Salam in Elementary. 1968. Particle Physics (Nobel Symp. N 8), N. Svartholm (eds.) Almquist and Wiksells, Stockholm , p.367; A. Salam and J. C. Ward, Phys. Lett. **13**, 168 (1964).

[23] G. C. Branco and G. Senjanovic, Phys. Rev. D **18**, 1621 (1978).

[24] G. Senjanovic, Nucl. Phys. B **153**, 334 (1979).

[25] R. N. Mohapatra and G. Senjanovic, Phys. Rev. D **23**, 165 (1981).

[26] G. Arnison *et al.* [UA1 Collaboration], Phys. Lett. B **122**, 103 (1983); M. Banner *et al.* [UA2 Collaboration], Phys. Lett. B **122**, 476 (1983).

[27] P. W. Higgs, Phys. Rev. Lett. **13**, 508 (1964).

[28] P. W. Higgs, Phys. Lett. **12**, 132 (1964).

[29] F. Englert and R. Brout, Phys. Rev. Lett. **13**, 321 (1964).

[30] Y. Nambu, Phys. Rev. Lett. **4**, 380 (1960); J. Goldstone, Nuovo Cim. **19**, 154 (1961); J. Goldstone, A. Salam and S. Weinberg, Phys. Rev. **127**, 965 (1962).

[31] N. Cabibbo, Phys. Rev. Lett. **10**, 531 (1963); M. Kobayashi and T. Maskawa, Prog. Theor. Phys. **49**, 652 (1973).

[32] M. E. Peskin and D. V. Schroeder, Reading, USA: Addison-Wesley (1995) 842 p. C. Itzykson and J. B. Zuber, New York, Usa: Mcgraw-hill (1980) 705 P.(International Series In Pure and Applied Physics)

N. N. Bogolyubov and D. V. Shirkov, Intersci. Monogr. Phys. Astron. **3**, 1 (1959). S. Weinberg, Cambridge, UK: Univ. Pr. (1995) 609 p

[33] S. R. Coleman and J. Mandula, Phys. Rev. **159**, 1251 (1967).

[34] M. Drees, R. Godbole and P. Roy, Hackensack, USA: World Scientific (2004) 555 p;

[35] H. Baer and X. Tata, Cambridge, UK: Univ. Pr. (2006) 537 p

[36] R. Nevzorov, arXiv:1201.0115 [hep-ph].

[37] J. Wess and J. Bagger, Princeton, USA: Univ. Pr. (1992) 259 p.

[38] R. Haag, J. T. Lopuszanski and M. Sohnius, Nucl. Phys. B **88**, 257 (1975).

[39] J. Wess and B. Zumino, Nucl. Phys. B **70**, 39 (1974); J. Wess and B. Zumino, Phys. Rev. **163**, 1727 (1967); J. Wess and B. Zumino, Phys. Lett. B **49**, 52 (1974); J. Wess and B. Zumino, Nucl. Phys. B **78**, 1 (1974).

[40] A. Salam and J. A. Strathdee, Nucl. Phys. B **76**, 477 (1974).

[41] M. Dine and W. Fischler, Phys. Lett. B **110**, 227 (1982); C.R. Nappi and B.A. Ovrut, Phys. Lett. B **113**, 175 (1982); L. Alvarez-Gaumé, M. Claudson and M. B. Wise, Nucl. Phys. B **207**, 96 (1982).

[42] M. Dine, A. E. Nelson, Phys. Rev. D **48**, 1277 (1993) [hep-ph/9303230]; M. Dine, A.E. Nelson, Y. Shirman, Phys. Rev. D **51**, 1362 (1995) [hep-ph/9408384]; M. Dine, A.E. Nelson, Y. Nir, Y. Shirman, Phys. Rev. D **53**, 2658 (1996) [hep-ph/9507378].

[43] T. Kaluza, Sitzungsber. Preuss. Akad. Wiss. Berlin (Math. Phys.) **1921**, 966 (1921).

[44] O. Klein, Z. Phys. **37**, 895 (1926) [Surveys High Energ. Phys. **5**, 241 (1986)].

[45] G. Bhattacharyya, A. Datta, S. K. Majee and A. Raychaudhuri, Nucl. Phys. B **760** (2007) 117 [hep-ph/0608208].

[46] A. Cordero-Cid, H. Novales-Sanchez and J. J. Toscano, Pramana **80**, 369 (2013) [arXiv:1108.2926 [hep-ph]].

[47] N. Arkani-Hamed, H. C. Cheng, B. A. Dobrescu and L. J. Hall, Phys. Rev. D **62**, 096006 (2000) [hep-ph/0006238].

[48] A. Datta, K. Kong and K. T. Matchev, New J. Phys. **12**, 075017 (2010) [arXiv:1002.4624 [hep-ph]].

[49] B. A. Dobrescu, K. Kong, R. Mahbubani and , JHEP **0707**, 006 (2007) [hep-ph/0703231 [HEP-PH]].

[50] R. P. Feynman, Phys. Rev. **74**, 1430 (1948). J. S. Schwinger, Phys. Rev. **73**, 416 (1948). S. I. Tomonaga and J. R. Oppenheimer, Phys. Rev. **74**, 224 (1948).

[51] F. J. Dyson, Phys. Rev. **75**, 486 (1949).

[52] A. Deandrea, J. Welzel, P. Hosteins and M. Oertel, Phys. Rev. D **75** (2007) 113005 [hep-ph/0611172].

[53] A. S. Cornell, A. Deandrea, L. -X. Liu and A. Tarhini, Phys. Rev. D **85**, 056001 (2012) [arXiv:1110.1942 [hep-ph]].

[54] N. Arkani-Hamed, T. Gregoire and J. G. Wacker, JHEP **0203**, 055 (2002) [hep-th/0101233]; N. Marcus, A. Sagnotti and W. Siegel, Nucl. Phys. B **224**, 159 (1983); E. A. Mirabelli and M. E. Peskin, Phys. Rev. D **58**, 065002 (1998) [hep-th/9712214]; I. L. Buchbinder, S. J. Gates, Jr., H. -S. Goh, W. D. Linch, III, M. A. Luty, S. -P. Ng and J. Phillips, Phys. Rev. D **70**, 025008 (2004) [hep-th/0305169].

[55] M. Blennow, H. Melbeus, T. Ohlsson and H. Zhang, Phys. Lett. B **712**, 419 (2012) [arXiv:1112.5339 [hep-ph]].

[56] A. S. Cornell and L. -X. Liu, Phys. Rev. D **83** (2011) 033005 [arXiv:1010.5522 [hep-ph]].

[57] A. S. Cornell, A. Deandrea, L. -X. Liu and A. Tarhini, Eur. Phys. J. Plus **128** (2013) 6 [Eur. Phys. J. Plus **128** (2013) 6] [arXiv:1206.5988 [hep-ph]].

[58] A. S. Cornell and L. X. Liu, Phys. Rev. D **84**, 036002 (2011) [arXiv:1105.1132 [hep-ph]]. L. X. Liu and A. S. Cornell, Phys. Rev. D **86**, 056002 (2012) [arXiv:1204.0532 [hep-ph]].

[59] H. -C. Cheng, K. T. Matchev and M. Schmaltz, Phys. Rev. D **66**, 036005 (2002) [hep-ph/0204342]; H. -C. Cheng, J. L. Feng and K. T. Matchev, Phys. Rev. Lett. **89** (2002) 211301 [hep-ph/0207125].

[60] G. Bhattacharyya, A. Datta, S. K. Majee and A. Raychaudhuri, Nucl. Phys. B **821**, 48 (2009) [arXiv:0904.0937 [hep-ph]].

[61] C. Macesanu, C. D. McMullen and S. Nandi, Phys. Rev. D **66**, 015009 (2002) [hep-ph/0201300].

[62] L. X. Liu, Int. J. Mod. Phys. A **25**, 4975 (2010) [arXiv:0910.1326 [hep-ph]].

[63] L. X. Liu and A. S. Cornell, PoS KRUGER **2010**, 045 (2010) [arXiv:1103.1527 [hep-ph]].

[64] G. 't Hooft and M. J. G. Veltman, Nucl. Phys. B **44**, 189 (1972).

[65] G. 't Hooft, Nucl. Phys. B **61**, 455 (1973).

[66] D. M. Capper, D. R. T. Jones and P. van Nieuwenhuizen, Nucl. Phys. B **167**, 479 (1980).

[67] T. P. Cheng, E. Eichten and L. F. Li, Phys. Rev. D **9**, 2259 (1974). M. E. Machacek and M. T. Vaughn, Nucl. Phys. B **236**, 221 (1984).

[68] C. Jarlskog, Phys. Rev. Lett. **55**, 1039 (1985). C. Jarlskog, Z. Phys. C **29**, 491 (1985). I. Dunietz, O. W. Greenberg and D. d. Wu, Phys. Rev. Lett. **55**, 2935 (1985).

[69] H. D. Politzer, Phys. Rev. Lett. **30**, 1346 (1973).

[70] K. Inoue, A. Kakuto, H. Komatsu and S. Takeshita, Prog. Theor. Phys. **67**, 1889 (1982).

[71] D. Falcone, Int. J. Mod. Phys. A **17**, 3981 (2002) [hep-ph/0105124].

[72] A. S. Cornell, A. Deandrea, L. -X. Liu and A. Tarhini, Mod. Phys. Lett. A **28** (2013) 11, [arXiv:1209.6239 [hep-ph]]. A. S. Cornell, A. Deandrea, L. -X. Liu and A. Tarhini, arXiv:1206.5988 [hep-ph].

[73] K. S. Babu, Z. Phys. C **35**, 69 (1987).

[74] Z. -z. Xing, H. Zhang and S. Zhou, Phys. Rev. D **77**, 113016 (2008) [arXiv:0712.1419 [hep-ph]].

[75] T. Ohlsson, S. Riad and , Phys. Lett. B **718**, 1002 (2013) [arXiv:1208.6297 [hep-ph]].

[76] I. Antoniadis, Phys. Lett. B **246** (1990) 377.

[77] D. Choudhury, A. Datta, D. K. Ghosh and K. Ghosh, JHEP **1204** (2012) 057 [arXiv:1109.1400 [hep-ph]].

[78] G. Servant and T. M. P. Tait, Nucl. Phys. B **650** (2003) 391 [hep-ph/0206071].

[79] A. Arbey, G. Cacciapaglia, A. Deandrea and B. Kubik, JHEP **1301** (2013) 147 [arXiv:1210.0384 [hep-ph]].

[80] G. Cacciapaglia, A. Deandrea and J. Llodra-Perez, JHEP **1110** (2011) 146 [arXiv:1104.3800 [hep-ph]].

[81] G. Cacciapaglia and B. Kubik, JHEP **1302** (2013) 052 [arXiv:1209.6556 [hep-ph]].

[82] T. Kakuda, K. Nishiwaki, K. -y. Oda and R. Watanabe, arXiv:1305.1686 [hep-ph]; M. Blennow, H. Melbeus, T. Ohlsson and H. Zhang, Phys. Lett. B **712**, 419 (2012) [arXiv:1112.5339 [hep-ph]].

[83] K. Nishiwaki, K. -y. Oda, N. Okuda and R. Watanabe, Phys. Rev. D **85** (2012) 035026 [arXiv:1108.1765 [hep-ph]].

[84] C. Csaki, C. Grojean and H. Murayama, Phys. Rev. D **67** (2003) 085012 [hep-ph/0210133].

[85] [ATLAS Collaboration], Note ATLAS-CONF-2013-014.

[86] S. Chatrchyan *et al.* [CMS Collaboration], JHEP **06** (2013) 081 [arXiv:1303.4571 [hep-ex]].

[87] M. Sher, Phys. Rept. **179** (1989) 273.

[88] G. Degrassi, S. Di Vita, J. Elias-Miro, J. R. Espinosa, G. F. Giudice, G. Isidori and A. Strumia, JHEP **1208** (2012) 098 [arXiv:1205.6497 [hep-ph]].

[89] Y. Abe *et al.* [DOUBLE-CHOOZ Collaboration], Phys. Rev. Lett. **108** (2012) 131801 [arXiv:1112.6353 [hep-ex]].

[90] F. P. An *et al.* [DAYA-BAY Collaboration], Phys. Rev. Lett. **108** (2012) 171803 [arXiv:1203.1669 [hep-ex]].

[91] J. K. Ahn *et al.* [RENO Collaboration], Phys. Rev. Lett. **108**, 191802 (2012) [arXiv:1204.0626 [hep-ex]].

[92] G. Bhattacharyya, S. Goswami and A. Raychaudhuri, Phys. Rev. D **66**, 033008 (2002) [hep-ph/0202147].

[93] S. Weinberg, Phys. Rev. Lett. **43** (1979) 1566.

[94] Z. Maki, M. Nakagawa and S. Sakata, Prog. Theor. Phys. **28** (1962) 870.

[95] S. Antusch, J. Kersten, M. Lindner and M. Ratz, Nucl. Phys. B **674** (2003) 401 [hep-ph/0305273].

[96] J. Beringer *et al.* [Particle Data Group Collaboration], Phys. Rev. D **86**, 010001 (2012).

[97] K. Nakamura *et al.* [Particle Data Group Collaboration], J. Phys. G **37**, 075021 (2010).

[98] A. Bharucha, A. Goudelis and M. McGarrie, Eur. Phys. J. C **74**, 2858 (2014) [arXiv:1310.4500 [hep-ph]].

[99] F. Brummer, M. McGarrie and A. Weiler, JHEP **1404**, 078 (2014) [arXiv:1312.0935 [hep-ph]].

[100] S. Abel and M. McGarrie, JHEP **1407**, 145 (2014) [arXiv:1404.1318 [hep-ph]].

[101] G. Aad *et al.* [ATLAS Collaboration], JHEP **1310**, 189 (2013) [arXiv:1308.2631 [hep-ex]].

[102] S. Chatrchyan *et al.* [CMS Collaboration], Eur. Phys. J. C **73**, 2677 (2013) [arXiv:1308.1586 [hep-ex]].

[103] The ATLAS collaboration, ATLAS-CONF-2013-068.

[104] CMS Collaboration [CMS Collaboration], CMS-PAS-SUS-13-014.

[105] T. R. Taylor and G. Veneziano, Phys. Lett. B **212**, 147 (1988).

[106] G. Bhattacharyya and T. S. Ray, JHEP **1005**, 040 (2010) [arXiv:1003.1276 [hep-ph]].

[107] G. Bhattacharyya and T. S. Ray, Phys. Rev. D **87**, 015017 (2013) [arXiv:1210.0594 [hep-ph]].

[108] M. McGarrie and R. Russo, Phys. Rev. D **82**, 035001 (2010) [arXiv:1004.3305 [hep-ph]].

[109] M. McGarrie and D. C. Thompson, Phys. Rev. D **82**, 125034 (2010) [arXiv:1009.4696 [hep-th]].

[110] M. McGarrie, arXiv:1109.6245 [hep-ph].

[111] M. McGarrie, JHEP **1109**, 138 (2011) [arXiv:1101.5158 [hep-ph]].

[112] M. McGarrie, JHEP **1302**, 132 (2013) [arXiv:1210.4935 [hep-th]].

[113] M. McGarrie, JHEP **1303**, 093 (2013) [arXiv:1207.4484 [hep-ph]].

[114] M. McGarrie, JHEP **1304**, 161 (2013) [arXiv:1303.4534 [hep-th]].

[115] E. A. Mirabelli and M. E. Peskin, Phys. Rev. D **58**, 065002 (1998) [hep-th/9712214].

[116] Z. Chacko, M. A. Luty, A. E. Nelson and E. Ponton, JHEP **0001**, 003 (2000) [hep-ph/9911323].

[117] M. Schmaltz and W. Skiba, Phys. Rev. D **62**, 095005 (2000) [hep-ph/0001172].

[118] M. Schmaltz and W. Skiba, Phys. Rev. D **62**, 095004 (2000) [hep-ph/0004210].

[119] G. Aad *et al.* [ATLAS Collaboration], JHEP **1310**, 130 (2013) [arXiv:1308.1841 [hep-ex]].

[120] The ATLAS collaboration, ATLAS-CONF-2013-089.

[121] The ATLAS collaboration, ATLAS-CONF-2013-062.

[122] The ATLAS collaboration, ATLAS-CONF-2013-047.

[123] S. Chatrchyan *et al.* [CMS Collaboration], Eur. Phys. J. C **73**, 2568 (2013) [arXiv:1303.2985 [hep-ex]].

[124] CMS Collaboration [CMS Collaboration], and jets in pp collisions at 8 TeV," CMS-PAS-SUS-13-013.

[125] CMS Collaboration [CMS Collaboration], CMS-PAS-SUS-13-012.

[126] CMS Collaboration [CMS Collaboration], with b-jets in pp collisions at 8 TeV," CMS-PAS-SUS-13-004.

[127] D. J. Castano, E. J. Piard and P. Ramond, Phys. Rev. D **49**, 4882 (1994) [hep-ph/9308335].

[128] K. R. Dienes, E. Dudas and T. Gherghetta, Phys. Lett. B **436**, 55 (1998) [hep-ph/9803466].

[129] K. R. Dienes, E. Dudas and T. Gherghetta, Nucl. Phys. B **537**, 47 (1999) [hep-ph/9806292].

[130] A. Pomarol, Phys. Rev. Lett. **85**, 4004 (2000) [hep-ph/0005293].

[131] Y. Nomura and D. Poland, Phys. Rev. D **75**, 015005 (2007) [hep-ph/0608253].

[132] A. Abdalgabar and A. S. Cornell, J. Phys. Conf. Ser. **455**, 012050 (2013) [arXiv:1305.3729 [hep-ph]].

[133] A. Abdalgabar, A. S. Cornell, A. Deandrea and A. Tarhini, Phys. Rev. D **88**, 056006 (2013) [arXiv:1306.4852 [hep-ph]].

[134] A. Abdalgabar, A. S. Cornell, A. Deandrea and A. Tarhini, Eur. Phys. J. C **74**, 2893 (2014) [arXiv:1307.6401 [hep-ph]].

[135] A. Abdalgabar, A. S. Cornell, A. Deandrea and M. McGarrie, JHEP **1407**, 158 (2014) [arXiv:1405.1038 [hep-ph]].

[136] A. Abdalgabar and A. S. Cornell, Submitted to SAIP Proceeding (2014) to be appear in J. Phys. Conference Series.

[137] J. R. Ellis, G. Ridolfi and F. Zwirner, Phys. Lett. B **262**, 477 (1991).

[138] J. L. Lopez and D. V. Nanopoulos, Phys. Lett. B **266**, 397 (1991).

[139] M. S. Carena, J. R. Espinosa, M. Quiros and C. E. M. Wagner, Phys. Lett. B **355**, 209 (1995) [hep-ph/9504316].

[140] H. E. Haber, R. Hempfling and A. H. Hoang, Z. Phys. C **75**, 539 (1997) [hep-ph/9609331].

[141] G. Degrassi, S. Heinemeyer, W. Hollik, P. Slavich and G. Weiglein, Eur. Phys. J. C **28**, 133 (2003) [hep-ph/0212020].

[142] R. Rattazzi, C. A. Scrucca and A. Strumia, Nucl. Phys. B **674**, 171 (2003) [hep-th/0305184].

[143] T. Gregoire, R. Rattazzi, C. A. Scrucca, A. Strumia and E. Trincherini, Nucl. Phys. B **720**, 3 (2005) [hep-th/0411216].

[144] C. A. Scrucca, Mod. Phys. Lett. A **20**, 297 (2005) [hep-th/0412237].

[145] A. Falkowski, H. M. Lee and C. Ludeling, JHEP **0510**, 090 (2005) [hep-th/0504091].

[146] G. A. Diamandis, B. C. Georgalas, P. Kouroumalou and A. B. Lahanas, Phys. Rev. D **89**, 085007 (2014) [arXiv:1312.7410 [hep-th]].

[147] J. E. Camargo-Molina, B. O'Leary, W. Porod and F. Staub, JHEP **1312**, 103 (2013) [arXiv:1309.7212 [hep-ph]].

[148] C. Bouchart, A. Knochel and G. Moreau, Phys. Rev. D **84**, 015016 (2011) [arXiv:1101.0634 [hep-ph]].

[149] P. Batra, A. Delgado, D. E. Kaplan and T. M. P. Tait, JHEP **0402**, 043 (2004) [hep-ph/0309149].

[150] CMS Collaboration [CMS Collaboration], CMS-PAS-SUS-14-011; T. T. Yanagida and N. Yokozaki, JHEP **1410**, 133 (2014) [arXiv:1404.2025 [hep-ph]].

[151] P. Batra, A. Delgado, D. E. Kaplan and T. M. P. Tait, JHEP **0406**, 032 (2004) [hep-ph/0404251].

[152] A. Delgado, hep-ph/0409073.

[153] A. Hebecker, Nucl. Phys. B **632**, 101 (2002) [hep-ph/0112230].